

Macondo oil in northern Gulf of Mexico waters – Part 1: Assessments and forensic methods for *Deepwater Horizon* offshore water samples

James R. Payne^a and William B. Driskell^b

^aPayne Environmental Consultants, Inc., 1651 Linda Sue Lane, Encinitas, CA 92024
jrpayne@sbcglobal.net

^b6536 20th Ave NE, Seattle, WA 98115
bdriskell@comcast.net

Abstract

Forensic chemistry assessments documented the presence of Macondo (MC252) oil from the *Deepwater Horizon* (DWH) spill in offshore water samples collected under Natural Resource Damage Assessment (NRDA) protocols. In ocean depths, oiled water was sampled, observed, photographed, and tracked in dissolved oxygen (DO) and fluorometry profiles. Chemical analyses, sensor records, and observations confirmed the shifting, rising oil plume above the wellhead while smaller, less buoyant droplets were entrapped in a layer at ~1,000-1,400 m and advected up to 412 km southwest. Near-surface oil samples showed substantial dissolution weathering from oil droplets rising through the water column, as well as enhanced evaporative losses of lighter n-alkanes and aromatic hydrocarbons. Dispersant effects from surface applications and injected at the wellhead were seen in oil profiles as enhanced weathering patterns (increased dissolution), thus implying dispersants were a functionally effective mediation treatment. Forensic assessment methods are detailed in the supplemental information (SI).

Keywords

Deepwater Horizon, subsurface plume, chemical forensics, PAH, Natural Resource Damage Assessment, oil phase, dissolved phase.

Introduction

During the 2010 DWH blowout event, while surface slicks were plainly evident, widely spread, and of great concern, a less visible phenomenon was occurring. Early in the response, remotely-operated-vehicle (ROV) operators monitoring the wellhead reported encountering oil layers, primarily at ~1,000 m depth (pers comm, *Skandi Neptune* operators, 2010). Later Operational Science Advisory Team (OSAT), academic, and NRDA sampling efforts confirmed these observations, finding elevated polycyclic aromatic hydrocarbon (PAH) constituents, dispersant indicators, and selected monoaromatic components in the 900-1,400 m depth range (Camilli et al., 2010; Payne and Driskell, 2015a). Modelling efforts predicted droplets released from the well's collapsed drill pipe would be trapped at a depth between 1,280 and 1,310 m, whereas the (larger flow rate) release from the end of the riser would be trapped between 1,150 m and 1,220 m (Spaulding et al. 2015). While the chemical character of this layer was mostly predictable from similar earlier events (e.g., IXTOC I in 1979), understanding the formation of the deep plume and its protracted extension to the southwest required further observations and insights (Socolofsky et al., 2011; Spaulding et al., 2015; Payne and Driskell, 2015b, 2016).

When oil is released into seawater, its hydrocarbon components partition into dissolved and particulate (oil-droplet) phases (Payne et al., 1984, 1991a, 1991b, 2005; Payne and McNabb, Jr. 1984; NRC 1985,

1989, 2003, 2005; Wolfe et al., 1994; Payne and Driskell, 2003; Reddy et al., 2011; Camilli et al., 2010, 2011; Boehm et al., 2016). In a generally predictable manner, volatile aromatics such as benzene, toluene, ethylbenzene, and xylenes (BTEX) plus other alkylated monoaromatics and lower-molecular-weight PAH all appreciably dissolve in seawater (NRC 2003, 2005). During the DWH blowout (aka Macondo lease block or MC252), however, the partitioning activities were quite dynamic. Oil droplets and gas bubbles separated in the well's multiphasic, jetted flow resulted in an almost complete dissolution of lower-molecular-weight aromatics (alkylated benzenes) (Reddy et al., 2011) and aliphatics (at least through heptane, McAuliffe, 1987), plus a more limited dissolution of C₈-C₁₃ aliphatics and two- and three-ring aromatics (alkylated naphthalenes, fluorenes, phenanthrenes/anthracenes, and dibenzothiophenes). Similar behavior was observed during the 1979 IXTOC I blowout in the Bay of Campeche, GOM (Payne et al., 1980a, 1980b; Boehm and Fiest, 1982). During the DWH event, volatile gas bubbles were surfacing above the wellhead (pers obs) while evaporated BTEX and lighter PAH were captured in aerial fly-overs (Ryerson et al., 2011).

For traditional damage assessments (including to some extent, the DWH event), whole water total PAH (TPAH) values have been used to estimate toxicity and fate; essentially ignoring known oil-in-water partitioning processes. Partitioning has been reviewed in detail in several National Research Council reports (1985, 2003, 2005), and more recently by Faksness (2007); however, there have been only a few efforts to collect phase-discriminated data in actual oil-spill NRDA efforts. During the DWH event, portable field-filtration equipment built for this task (Payne et al., 1999) was deployed to process selected offshore NRDA water samples (Figure S- 2 and Figure S- 3). Filtering at the time of collection (vs. bench filtering days later), produces complementary dissolved- and particulate-oil phase samples that better reflect the actual environmental conditions. The filtering also uses larger sample volumes (3.5 L versus 1 L) to improve analytic method detection limits. These more detailed, phase-discriminated results dramatically expand the utility of data. From the DWH event, a limited data set from filtered samples provided partitioned source reference samples (Figure S- 4), which enabled a method to parse out phases in the other non-filtered whole water samples. Subsequent insights into oil fate and transport processes certainly improved forensic assessments but more importantly, provided dissolved-phase concentrations, the component more relevant for toxicological assessments.

Including independent BP and Response cruise efforts and pre- and post-impact, near-shore water samples, over 15,000 samples were collected by local, state, and federal agency representatives for the DWH NRDA. Other researchers utilizing the combined NRDA and BP data sets have reported on the distribution and attenuation of total PAH (TPAH aka TPAH₅₀ as a summation of 50 PAH components) in the water column (Spier et al., 2013, Boehm et al., 2016, Wade et al., 2016). Although admirably comprehensive, in the two more recent studies, the data were largely interpreted by estimating background concentrations and then comparing and delineating average TPAH as functions of time and distance from the wellhead. For both the Boehm and Wade studies, the scope of the spill was defined as the regions where TPAH concentrations exceeded 1 ppb (mostly within 15 to 20 km of the wellhead). Unfortunately, in Wade's comparative tabulation of pre-spill background estimates, many values were from early studies believed to be biased high due to sampling and procedural artifacts (de Lappe et al., 1983) or were constrained by median TPAH concentrations measured in non-representative DWH field blanks with unrelated PAH profiles (e.g., pre-contaminated rinse water with profiles unlike those from environmental samples). Post-spill field results from 2011 (Payne and Driskell, 2015a) suggest these to be overestimates for background (see below). Furthermore, both studies' focus on TPAH averages was biased by both the acknowledged *ad hoc* nature of the sampling design (implemented primarily for tracking and sampling subsurface oil with no utility as unbiased statistical estimates) and the complexity and heterogeneity of oil in the water column. Specifically, both studies averaged impacted and non-impacted water samples (tabulated by region, date, distance, etc.) and suggested an overall low level and range of impact, e.g., Wade's sample collection maps include efforts beyond the spill's impact region, off Texas and the east coast of Florida. Also, in our opinion, the traditional statistical parameter, TPAH,

poorly represents the multi-component, multi-phasic, non-linear nature of oil weathering and ignores current knowledge regarding oil's weathering conversion to unquantified polar compounds (discussed below). Together, the approach, the estimates, and TPAH index create a low-biased impression of the true scale and nature of the spill. Commendably, Spier's study looked at solubility-based groupings of analytes but then censored the data for detection limits, which led, in our opinion, to conclusions of attenuated oil distributions. Likewise, Boehm et al. (2016) acknowledged the multiphasic nature of oil-in-water mixtures but details for quantifying the separate phases were not addressed.

Our approach differs; rather than making generalized assumptions in culling and processing the data, we instead examined each sample's chemical profile and its supporting field data for evidence of MC252 oil (n=4,189). There are several approaches to oil-spill forensic assessments of individual samples using various chemistry parameters (PAH, SHC, biomarkers, volatiles, metals, and isotopes), diagnostic ratios, pattern matching, or multivariate analyses, to name a few (many of which are covered in Stout and Wang, 2016). For the DWH spill, only the traditional suite of PAH, SHC, and sometimes, biomarker data, were available for the Natural Resource Damage Assessment (NRDA). But the abundance of the data enabled developing some novel forensic methods (detailed in SI) and eventually, insights into the behavior and fate of the DWH oil. For this task, additional efforts were made to not only confirm a possible MC252 source but also to deconvolute each sample into its relative dissolved- and particulate-phase PAH components (Payne and Driskell 2015a, 2015b, 2015c). These forensic assessments were undertaken not to tabulate TPAH/phase levels but rather to create a dataset that could serve as confirmation for a parallel NRDA task, modelling oil's transport, fate, and effects wherein oil is treated as a multi-component material (French-McCay et al., 2015a, 2015b, 2018).

While the scope of this paper summarizes, in a somewhat narrative style, the methods, results and conclusions documenting the DWH exposure, forensic methods and enhanced-dissolution dispersant effects are detailed in the supplemental information (SI) and Part 2 of this series, Driskell and Payne (2018b).

Methods

Field Methods

The primary offshore sampling challenge for this event was in finding, tracking, and characterizing the entrapped deepwater oil plume (detailed in Payne and Driskell, 2015b, 2016, and White et al., 2016). Consequently, surface samples were a smaller component in the NRDA's offshore sampling (only ~18% of forensically reviewed water samples came from the upper 20 m depths). While surface slicks were of interest, they were forming and transporting in a mostly predictable manner, tracked by remote imaging, oceanographic models, and shoreline surveys. Other than initially documenting near-surface weathering and dissolution processes (Stout et al., 2016a), slicks did not require the effort relative to the oceanographic sampling methods necessary for tracking and sampling the deepwater plume.

Plume tracking at depth required innovative and adaptive efforts. Initially, water collection efforts were focused near the wellhead or within the basin of the blowout (loosely constrained by bathymetry of nearby salt dome features) but sampling moved further afield as knowledge of the deep plume's behavior developed. Field teams eventually evolved highly effective methods for finding and sampling the deepwater oil plume (Payne and Driskell, 2015b; 2016; French-McCay et al., 2015b) using a combination of live CTD, fluorescence, and dissolved oxygen tracking (Figure 1), and predictive modeling, plus at times, visuals from remotely operated vehicles (ROVs) equipped with a vast array of sensors and closed-circuit TV (Figure S- 1). The sensor records later provided additional lines of evidence in corroborating forensic chemistry results (Payne and Driskell, 2015c, 2016, 2017).

For the NRDA effort, over 15,000 discrete water samples (including nearshore and QC samples) were collected from numerous vessels-of-opportunity beginning near the wellhead in May 2010 during the initial weeks of the incident and then further afield during the subsequent months and with diminished efforts into fall of 2011. Water was mostly collected by conventional oceanographic methods using Go-Flo® or Niskin bottles (more method details are in SI), preserved in the field after collection by refrigeration or acidification, and later shipped and held refrigerated until extraction at the lab. Fast-runner boats were deployed from Port Fourchon, LA every two-to-three days to offload samples from the larger sampling vessels at sea and deliver them to onshore data/logistics centers where the collected samples were logged into a comprehensive chain-of-custody (COC) database and air-freighted in Blue-Ice® chilled coolers overnight (including Saturday deliveries) to the waiting analytical facilities. Throughout the massive scale of logistical and laboratory efforts, only 217 of 22,039 processed water samples (0.98%) were compromised by exceeding the 14-day maximum hold time specified by the project's Analytical Quality Assurance Plan (AQAP) (NOAA, 2014).

As mentioned above, for the purpose of assessing phase-partitioning (dissolved vs. particulate oil), on several cruise legs in 2010-11, whole-water samples were vacuumed through 0.7 μm glass-fiber filters immediately upon collection (Figure S- 2 and Figure S- 3) using a Portable Large Volume Water Sampling System (PLVWSS) (Payne et al., 1999). After filtration, the filters containing the particulate-phase oil were frozen in Certified-Clean glass jars and shipped to Alpha Analytical Laboratories (Mansfield, Massachusetts). The complement 3.5 L dissolved-phase samples were refrigerated in their original, Certified-Clean, one-gallon (3.8 L) amber-glass collection jugs from the PLVWSS and shipped refrigerated to the laboratory for the same analyses.

Analytical Laboratory Methods

Nearly all NOAA-NRDA water-column samples discussed in this paper were analyzed by Alpha Analytical Laboratory for detailed hydrocarbon composition in accordance with the AQAP (Stout 2015a, 2015b). The use of a single laboratory for this effort was critical for developing a quality dataset with known precision, comparability, accuracy, and completeness to support the multi-year forensics effort (Litman et al., 2018). Analyte lists, methods, and performance requirements were detailed in Stout et al. (2016a) and the AQAP but are also listed in the SI. Analytic methods briefly included:

- Total Extractable Hydrocarbons (TEH) and Saturated Hydrocarbon Compounds (SHC) measured by gas chromatography-flame ionization detector (GC-FID) using a modified EPA Method 8015B.
- PAH, Alkylated PAH, and Petroleum Biomarkers analyzed using Selected Ion Monitoring (SIM) gas chromatography/mass spectrometry (GC/MS) via a modified EPA Method 8270.
- Dispersant components including the surfactant, dioctyl-sulfosuccinate (DOSS), measured by liquid chromatography/mass spectrometry (LC/MS) (Gray et al., 2011, 2014 and Kujawinski et al., 2011) at ALS Kelso (previously CAS); while by standard GC/MS methods, Alpha Analytical reported the dispersant indicators, bis(2-ethylhexyl)fumerate, a DOSS-derived GC injection-port breakdown product associated with both Corexit 9527 and 9500, and glycol ethers (GE) common to both dispersants plus 2-butoxyethanol (a major solvent in Corexit 9527) (Stout, 2015a).
- Volatiles, primarily benzene, toluene, ethylbenzene and xylene(s) (BTEX) plus an expanded list, were analyzed by a purge-and-trap protocol under a modified EPA method 8260.

SHC and volatiles were reported in concentrations of $\mu\text{g/L}$ (parts per billion, ppb). PAH, biomarkers and dispersant indicators were reported in ng/L (parts per trillion, ppt). AQAP Target method detection limits (MDLs) for PAH, biomarkers, volatiles and SHC were 1-5 ng/L , 10 ng/L , 0.05 – 0.5 $\mu\text{g/L}$ and 0.8 $\mu\text{g/L}$, respectively (see SI tables). Total PAH values were reported as the sum of 50 PAH components (TPAH50), dropping retene (methyl isopropyl phenanthrene also measured as part of C4-phenanthrenes)

and perylene (often from background biogenic sources). Dispersant indicators were analyzed at Alpha Analytical without authentic standards and thus reported as semi-quantified estimates. From frozen lab storage, particulate (filter) samples were thawed, macerated, spiked with deuterated recovery standards, and extracted separately from the associated (dissolved) 3.5 L water portion but reported on the associated per-volume basis. Dissolved-phase sample volumes were measured during extraction and later used to calculate concentrations in both the dissolved and related particulate (filter) samples.

All chemistry data were independently validated by EcoChem (Seattle, WA) as third-party validators where anomalies were investigated, any errors emended, and/or exceedances qualified. Publicly available online data (NOAA ERMA) were reported as surrogate-recovery corrected; however, by preference and strictly for the purpose of forensic analysis, the raw data were used uncorrected for surrogates and uncensored for method detection limits (termed the “forensic dataset”). We are well aware of reviewers’ concern for this seemingly naïve practice but have found over years of oil profile analyses that the non-linear distortions in the profile patterns created by molecular-weight-based surrogate-recovery corrections introduce more variance than just using the raw data as generated. As a result, it has been standard practice to use non-surrogate-recovery data in oil-spill fingerprinting studies since the *Exxon Valdez* oil spill in 1989 (Stout and Wang, 2016). Likewise, below-detection-limit or below-reporting-limit data are often found to have profile pattern information useful to the forensic interpretations albeit, sometimes it’s just noise. If needed, public data users can recreate the forensic dataset using the surrogate recoveries to back-calculate the raw values.

Forensic Matching

For this assessment, only the offshore cruise samples collected in 2010 (5,332) were considered, and of those, a total of 4,189 were forensically characterized. Traditional ASTM (2000) methods use match, indeterminate, or no-match categories to describe forensic results. For water samples, similar categories were assigned; however, for further understanding the oil’s behavior and supporting the needs of fate and transport modelling (French-McCay et al., 2015b), the match category was further subdivided into three phase assignments, i.e., dissolved, particulate, or unresolvable (the last being unparseable phase[s] but matching MC252 oil) (Payne and Driskell, 2015c; 2016). The forensic objective was to assess whether the sample contained MC252 oil and, if possible, to parse out the phase components. Thus, for DWH water samples, seven categories were relevant (Table 1). The first three were considered positive matches, consistent with MC-252 oil but differentiated by phase profiles. The remaining four were non-matching, either another oil, inconclusive, or clean.

The forensic fingerprinting methods are fully described in the supplemental information (SI) but briefly, the approach for DWH data evolved from our earlier *Cosco Busan* mixing model (Driskell et al., 2010; Driskell and Payne, 2018a). For that event, we developed a parsing, mixing-model approach whereby the reference oil sample (normalized to hopane, chrysene or naphthobenzothiophene) was graphically overlaid on a given field sample profile and then rescaled to tease out any potential source-oil portion and decide whether and how much of the released oil was present in the sample. For this task, the source oil could be statistically weathered to best compare to the stage of weathering seen in the field sample. The weathering model was based upon multiple-regression analyses of each analyte. Multiple lines of evidence were used prior to confirming a match to the source oil. This approach was accepted by both spill Trustees and the Responsible Party (RP) for legal settlement. For the DWH event, rather than statistically weathering the source oil for comparisons, actual weathered-particulate-oil profiles from the field-filtered samples were used for the comparative reference oil (the weathered reference series is posted in Figure S- 4). Secondly, because most of the deeper offshore water samples were exposed only to simplified weathering factors (i.e., dissolution and biodegradation; no evaporation or photo-oxidation occurred at depth) and not an amalgam of diverse weathered states (typical of surface slicks), it also

became possible to parse particulate- and dissolved-phase portions from the remaining majority of the cruise samples, the 1 L unfiltered whole-water samples. The final dataset, including extra details regarding phase state and weathering and sampling metadata, suggested patterns and trends that led to further insights into transport and weathering processes. For example, when first encountered, enhanced dissolution patterns were enigmatic until a correlation with dispersant indicators was noted (See part 2 of this series, Driskell and Payne, 2018b).

Results

The results for forensic-evaluation end users primarily comprise the spatial distribution of the various phase-characterized categories from MC252 matched samples; cursory map plots are presented to depict a few relevant features. From the profile patterns, trends in dissolution and weathering are discussed along with their context in the DWH scenario; results are noted and interpreted to illustrate transport and fate processes.

BTEX components appeared near the wellhead in gas bubbles, hydrates, and as a mixture of oil-droplet-associated and purely dissolved constituents in the deep samples (Figure 2 and Socolofsky et al., 2011). Rapid dissolution at depth and resulting loss of buoyancy caused most BTEX to appear with order-of-magnitude higher concentrations than corresponding TPAH at depth in the nearfield. However, benzene, the most volatile and water-soluble BTEX constituent, was largely absent both in the near-surface waters and further from the wellhead (Figure 2 and Figure 3). In surface samples, detected BTEX constituents generally appeared within 20 km of the wellhead, thereby suggesting continued dissolution from rising oil droplets as they collected and advected near the surface (Figure 2 and Figure 3). During the 1979 IXTOC I oil well blowout in Mexico, similar rapid and selective benzene removal (dissolution) from the rising oil plume was reported from a much shallower 60 m ascent (Payne et al., 1980b) (DWH wellhead at 1,528 m). Surfacing DWH oil was subject to additional evaporative losses (Stout et al., 2016a) as directly evidenced in surface oil-sample profiles and the BTEX captured in air samples from above the spill (Ryerson et al., 2011). At depth, benzene could be observed at elevated concentrations (~20-40 µg/L) out to 15 km, while in comparison, the more persistent toluene occurred at elevated concentrations (10-80 µg/L) out to 20 km. Remarkably, in the deepwater plume, lower levels of toluene and xylenes were detected associated with forensically matched oil droplets out to 183 km SW of the wellhead (Figure 3).

Looking at the less volatile hydrocarbons, from 45 cruises, 4,189 water samples examined for PAH, SHC, and biomarkers produced 1,766 consistent with MC252 profiles (matching categories 1-3) (Table S- 1). Most matching samples had low values of TPAH, < 1,000 ng/L (ppt), with category medians at 875, 177 and 30 ppt, for particulate-, dissolved-, and unresolved-phase categories (1-3) respectively (Figure 4). Here, solely for the sake of comparing to other studies, our assessments found DWH BTEX and PAH distributions occurred on a vast spatial and temporal scale where numerous PAH signatures could be sourced to MC252 oil out to 100 km from the wellhead at concentrations up to 1.0 ppb (Wade and Boehm studies suggest 20-25 km) and out to 267 km with at least 0.1 ppb. Again, we emphasize that these values only represent the range of encounters from non-random biased collections, i.e., monitoring near the wellhead combined with plume-tracking efforts rather than using a pre-designed, non-biased sampling scheme.

Because impacts in the near-surface zone of high biological productivity were of significant concern, the shallow water results (0-20 m depth, Figure 5) are displayed separately from deeper samples showing, within this data set, the extent and distribution of just near-surface matches. The data depict four cruises specifically planned for off-shore, near-surface sampling plus numerous surface and near-surface samples taken during deeper casts on the other NRDA cruises. From 691 forensically assessed, shallow-depth samples, 360 were confirmed as containing MC252 oil. Half of these contained particulate oil droplets,

most with extra dissolved components. Dispersant-mediated effects were apparent in about one-sixth of the profiles, i.e., they showed the diagnostics of enhanced dissolution discussed in Driskell and Payne (2018b). A few anomalously high-concentration samples in the NRDA dataset suggested the inclusion of surface-slick oil. Although cited in other studies as maxima, these were considered to be diluted oil rather than oil suspended in water and thus, as sampling artifacts, they are excluded from results (Figure 5 depicts water matrices only).

At the entrapped plume depth (~1,000-1,400 m), field collections followed a sensor trail of particulate-phase (category 1) samples out to 155 km from the wellhead, while dissolved-profile (category 2) samples, typically with dispersant indicators, ranged to 267 km SW from the wellhead, and unresolved-phase (category 3) samples to 412 km from the wellhead (Figure 6, Figure 7, Figure 8, and Figure S- 5). Dispersant-mediated samples with dispersant-modified, accelerated-dissolution profiles (described in Driskell and Payne, 2018b) extended out to 184 km SW within the deepwater plume and up to 148 km NE in surface waters (< 20 m) atop the shelf (Figure 9). Non-matching samples were collected out to 530 km along the continental shelf break and 437 km near but outside of the plume track from the wellhead (Figure S- 6). These indeterminate and non-matching category samples (category 5-7) were expected, even desired, as they help to define the plume boundaries (see white-coded samples in Figure S- 5AFigure S- 5. Four 3D spatial views of samples colored by forensic categories. A) oblique view of all samples looking north (column of blue is rising plume near wellhead, and white dots represent non-matching category 4-7 samples) B) view A with only matched samples displayed, C) at plume depth looking NE from beyond plume's end (500 km), D) top view from above wellhead.) and confirm that sampling/procedural artifacts (e.g., equipment contamination, category 4) were not a major problem during the field effort.

In 2011, the year following the blowout, offshore sampling efforts were focused on benthic sampling (unlike the earlier focus on the water column), presuming that most waterborne hydrocarbons would have traveled far afield or settled to the seafloor as marine snow (Payne and Driskell, 2015a; Stout and Payne, 2016, Stout et al., 2016b). At that time, absent the extensive surface oil slicks, the modest number of midwater samples that were acquired (n=55 from 10 sites within the event basin and ranging from 100 km west to 135 km east of the wellhead) showed no evidence of the deep plume layer. There were no DO anomalies or fluorescent spikes noted; midwater TPAH concentrations were 0-30 ppt and showed only noisy trace patterns with most analytes below method blanks. For aliphatics, TPH ranged from 0-1 ppb with patterns dominated by biogenic plant waxes. Dispersant indicators were principally absent or ambiguously close to detection limits.

Forensic Interpretations

Knowledge of the initial formation and transport processes of the oil droplets released from the wellhead was critical for understanding the dissolution/weathering behavior of the oil. Conceptually, the blowout was initially envisioned as vertically cone-shaped in the water column forming from the ever-broadening, rising plume of gases and particulate oil droplets jetting from the wellhead. But forensic data suggested there was no semblance of a cone pattern in matched-sample distributions (see depiction of Socolofsky et al., 2011). Rather, in the dynamic environment of ever-shifting currents, the rising plume created a diverse mix of whole-oil particulate droplets each weathered by dissolution processes relative to their size (Spaulding et al., 2015, Payne and Driskell, 2015a) and displaced by the water parcel motions during ascent. Acoustic doppler current profiler (ADCP) data from three locations around the wellhead in May and June 2010 (available at <http://www.ndbc.noaa.gov/>) showed low, time-varying currents (<5-15 cm/sec) in different directions (changing by as much as 180° in less than 48 hours) between 80 and 1,500 m (Kim et al., 2012; French-McCay et al., 2018).

After separation from their buoyant ascending droplets, dissolved hydrocarbons lingered behind in the water column. But rather than being directly advected away from the wellhead, some were instead transported back and forth through the continuously rising droplet plume (Valentine et al., 2012). Specifically, as these dissolved phases' water parcels passed back over the wellhead's rising oil droplets, additional dissolution from the freshly rising droplets plus the original dissolved components created an enriched profile (Payne and Driskell, 2015a, 2016). In the forensic data, these profiles appear as particulate oil with extra dissolved portions (Figure S- 7 lower and Figure S- 12). Eventually, cumulative advective transport carried all the residual waterborne components to the southwest with the droplets and dissolved-phase water parcels further subjected to differential diffusion, internal waves, turbulence, basin circulation and tidal currents (Payne and Driskell, 2015a; French-McCay et al., 2015b; 2016; 2018).

Dissolution in oiled-water signatures was evidenced by the weathering of lower-molecular-weight PAH, aliphatics (<C₁₃), and BTEX that universally occurred as oil droplets ascended to the surface (Stout et al., 2016a). There was also evidence of photo-degradation and re-entrainment of surfaced oil in near-surface water samples as specifically reflected by the hopane-normalized losses of higher-alkylated (C3- and C4-) chrysenes, fluoranthenes/pyrenes, benz(a)anthracene, and also, the triaromatic steranes (Andersson, 1993; Garrett et al., 1998; Prince et al., 2003; Plata et al., 2008; Aeppli et al., 2014; Radovic et al., 2014, Bacossa et al., 2015; Stout et al., 2016a).

From forensic data, surfacing droplets typically became part of a surface slick's amalgam of DWH oil in various weathered states plus any background contamination from vessels' exhaust, deck washes, bilge dumps, dispersant drops, and/or *in situ* burn operations. Many surface profiles were irresolvably complex in PAH signature but relying more on biomarkers and other lines of evidence, MC252 oil was confirmed in 359 out of 690 near-surface (< 20 m) water samples for at least 100 km in most directions from the wellhead (Figure 5).

With the requisite amount of wave energy or impacting rainfall (Murphy et al. 2015), surface slicks and sheens can be mechanically broken up and droplets re-entrained in the upper depths (to some degree, down to 10-20 m but more commonly 0-2 m). Data from Special Monitoring of Applied Response Technologies (SMART) fluorescence monitoring (during workable sea states) and surface-focused cruises confirmed enhanced near-surface concentrations. While use of dispersants is still contentious in the spill-response community for other reasons, these findings again demonstrated that surface-applied dispersants were generally effective at creating micro-droplets that would facilitate the dissolution, weathering, and re-entrainment processes (Bejarano et al. 2013, Brandvik et.al, 2013, 2014, Davis and Loomis, 2014, Payne and Driskell, 2015d, Boehm et al., 2016, Li et al. 2016, Spaulding et al. 2015, 2017).

In contrast, direct dispersant application at the wellhead was unique; it had not been attempted prior to the *Deepwater Horizon* oil spill, and thus no data existed on the efficacy or fate of dispersants released in the deep subsurface. From early NRDA and Response data, dispersants were initially observed in plume-depth, whole-water samples but it couldn't be confirmed whether they were simply dissolved in the water or truly associated with the oil droplets (Payne and Beegle-Krause, 2011 and Kujawinski et al., 2011). Later reports of plume-depth, filtered-water NRDA samples having dispersant indicators still associated with the oil-phase droplets (Payne and Driskell, 2015d) finally confirmed their oil-associated functionality in the field. Analyses also showed that dispersants applied directly at the wellhead were active in creating atypical oil-droplet signatures with accelerated loss of the more soluble, lesser alkylated PAH and perhaps delayed biodegradation of SHC (Payne and Driskell, 2015d; Driskell and Payne, 2018b). These mechanistic results showing persisting dispersant attachment to oil droplets and accelerated loss of PAH, together suggest direct wellhead injection was effective for reducing oil-droplet sizes and thus, limiting oil rising to the surface and potentially being transported to shorelines. Others

arrive at similar conclusions based on their own approach and evidence (Kujawinski et al., 2011, Spier et al., 2013, and Nagamine, 2014).

Completing the inventory of miscellaneous sample categories, 96 (2.3%) water samples contained an oil that was not matched to MC252 (Table S- 1, Category 4). Of these, 67 were due to hydraulic oil leaked from the ROVs. Fortunately, hydraulic oil reference samples were taken and thus, the contamination was easily spotted (generally from elevated hopane and norhopane levels – see Figure S- 8). Due to hydraulic oil's refined nature, it often contributed very little to PAH and thus, could usually be confidently deconvoluted or ignored. The remaining 29 non-match samples represented either other obviously-anomalous-but-unidentified contaminants or were from unknown petrogenic sources.

Unknown sources could include seeps, which were often suggested as potentially major sources of oil contamination in the Gulf (Boehm et al., 2016, Wade et al., 2016). Based on satellite work of MacDonald et al. (2002), the US Geological Survey estimated approximately 350 sheen-forming seeps occur perennially in the northern Gulf of Mexico region (Kvenholden and Cooper, 2003). More recent work by Garcia-Pineda et al. (2015) suggested 1,000 geophysical anomalies (potential seep formations) but far fewer active oil seeps. Survey work in just the 50 x 50 km Macondo prospect region showed 562 gas plumes detected with 52 various sized slicks appearing over time in synthetic aperture radar (SAR) imagery (Garcia-Pineda et al., 2015). The slicks were intermittent and modest, averaging a total of perhaps 0.14 m³ of oil/day (0.91 barrels) with high evaporation rates yielding a proposed 24 hr residence/turnover of the sheen hydrocarbons. Following the spill, BP dispatched multiple vessels in 2010 and 2011 to document various aspects of seep chemistry and dynamics. Beneath seep sheens, shallow depth (0-3 m), oiled-water concentrations were within the range of concentrations seen during the spill (excluding the actual surface-slick oil) and were also similar to shallow samples collected at the nearby chronic Taylor Energy sheen site in 2012 (BP, 2014). But seep-oiled water samples from deeper depths, below any surface reinfusion effects, (25-2,200m) were very sparse (only 3 of 296 samples collected on the seep-focused visits by BP cruises) and of low concentration (average 0.24 ppb; 4-10x post-spill background reported by Adhikari et al., 2015). Based solely on these non-extraordinary concentrations from seep-focused sampling plus the sparse detections, we conclude that, despite the impressive tally of documented seeps, the chronic, low-level, sheen-forming, seep inputs to the Gulf of Mexico are dwarfed in comparison to the prolonged, high-volume (55-60K bbl/day) release from the 2010 DWH event (McNutt et al., 2011; Spaulding et al., 2015; French-McCay et al., 2016).

The limited 2011 water column data suggest that turnover in the midwater column was complete with a return to absent-to-trace hydrocarbon concentrations without petrogenic signatures. These results helped to further confirm the very low non-spill-impacted “background” concentrations during 2010. From the more extensive sampling of near bottom waters in 2011, there was still an obvious DWH signal present either from floc re-suspension or dissolution processes from oil-contaminated sediments (Stout and Payne 2016, Stout et al., 2016b, Zier vogel et al., 2016).

TPAH Limitations

Total PAH (TPAH), oil's traditional statistical parameter, is oft quoted but poorly represents the multi-component, multi-phasic, non-linear nature of oil weathering when used as a summary proxy for the amount of oil in a sample. In nature, multiple biotic and abiotic processes are constantly and selectively modifying hydrocarbon signatures; a weathered oil droplet, ravaged by dissolution, photooxidation and microbial attacks, undergoes vast transformations in composition, physical properties and toxicology (Hall et al., 2013; Bacosa et al., 2015). And yet, simply summing the residual PAH components is often the only comparative value presented and thereafter used to evaluate exposures and toxicological effects. For NRDA modelers, tracking individual “pseudo-components” of the oil (BTEX, alkanes and PAH

groupings by similar solubilities and vapor pressures) has been a more effective method of assessing transport, fate, and impacts (French-McCay et al., 2015a, 2015b, 2018). Providing forensic phase-discrimination data represents even further progress towards a more realistic depiction of oil fate and behavior.

TPAH values are also biased in the sense that they only represent the detectable GC/MS target analytes, the “quantifiable PAH,” which itself may only represent 1.3-4% of the fresh oil’s mass (Camilli et al., 2010; Stout, 2015b). Recent work has shown that the GC/MS view of hydrocarbons in oil, while reliable and prodigiously productive, has constrained our ability to document that weathering processes don’t obliterate the oil; it just becomes “transformatively” less visible through our instrumental lens. GC/FID and GC/MS quantification and profiling of aliphatics and PAH only reflect the non-polar target analytes amenable to our instruments and methods (typically reporting ~50 PAH, 55 biomarkers and 34 SHC). Using as alternative method, Fourier transform ion cyclotron resonance (FT-ICR) mass spectrometry, McKenna et al. (2013) identified more than 30,000 hydrocarbon compounds in Macondo oil, while Aeppli et al. (2012), Ruddy et al. (2014) and Radovic et al. (2014), among others, documented advanced oxidation states in slicks and stranded tarballs due to photooxidation and shoreline weathering. Although the 2010 NRDA water-column samples have not yet been analyzed using these methods, it is highly likely that some large fraction of the residual deep-plume constituents was microbially converted into similar polar products (Gutierrez et al., 2013a, 2013b; Hall et al., 2013; Gros et al., 2014; Huba and Gardinali, 2016). For example, unquantified polar derivatives would be a logical explanation for the most distant category 3 sample collected 412 km from the wellhead, which held barely a trace of a primarily dissolved-PAH profile but possessed all other indicators of the deepwater plume (fluorescence spike, DO sag, and dispersant indicators) (Figure 10). Supporting this finding, Du and Kessler (2012) reported a DO anomaly attributed to mass respiration of MC252 oil by microbes extending 505 km SW of the wellhead. Although reported and evaluated only by their low level TPAH values, samples with these trace contaminants (and their unquantified cohorts) probably deserve closer attention and reporting. Beginning with the *Exxon Valdez* oil spill, studies have suggested enhanced low-level toxicity for weathered oil products (Carls et al., 1999; French-McCay, 2015a; Morris et al., 2015; Incardona et al., 2004, 2005, 2013, 2015); research regarding toxicity of these polar compounds is ongoing (Overholt et al., 2016, Fingas and Banta, 2016).

Conclusions

After forensically examining 4,189 offshore water samples from the 2010 NRDA field collections, MC252 oil was detected at depth, further phase- and weathering-state discriminated, and characterized for dispersant effects. Benzene was largely removed by dissolution from rising droplets during ascent but remained at depth out to 15 km while other BTEX components (toluene and xylenes) were detected at depth up to 183 km from the wellhead. Typical of surface oil dynamics, near-surface increases in dissolved and particulate-oil fractions were observed as a result of wind-induced entrainment of surface films and dispersant effects. MC252 oil was identified in deeper water samples as higher-molecular-weight particulate-phase hydrocarbons up to 155 km from the wellhead, and as dissolved-phase as far as 267 km from the wellhead. Furthermore, based primarily on dispersant indicators, fluorescence and DO features, the presence of the plume was detected 412 km SW from the wellhead.

Acknowledgments

Funding for this effort was provided by the National Oceanic and Atmospheric Administration (NOAA) through subcontract with Industrial Economics, Incorporated (IEc). The findings and conclusions in this paper are those of the authors and do not necessarily represent the views of NOAA, IEc, or other natural resource Trustees for the *Deepwater Horizon* NRDA.

References

Adhikari, P.L., K. Maiti, E.B. Overton. 2015. Vertical fluxes of polycyclic aromatic hydrocarbons in the Northern Gulf of Mexico. *Mar. Chem.* 168, 60–68. dx.doi.org/10.1016/j.envpol.2016.01.064.

Aeppli, C., C.A. Carmichael, R.K. Nelson, K.L. Lemkau, W.M. Graham, M.C. Redmond, D.L. Valentine, and C.M. Reddy. 2012. Oil weathering after the *Deepwater Horizon* disaster led to the formation of oxygenated residues. *Environ. Sci. Technol.* 46: 8799-8807.

Aeppli, C., R.K. Nelson, J.R. Radovic, C.A. Carmichael, D.L. Valentine, and C.M. Reddy. 2014. Recalcitrance and degradation of petroleum biomarkers upon abiotic and biotic natural weathering of *Deepwater Horizon* oil. *Environ. Sci. Technol.*, 48: 6726-6734.

Andersson, J.T. 1993. Polycyclic aromatic sulfur heterocycles III. Photochemical stability of the potential oil pollution markers phenanthrenes and dibenzothiophenes. *Chemosphere* 27: 2097-2102.

ASTM D 5739-00. 2000. Standard practice for Oil Spill Source Identification by gas chromatography and positive ion electron impact low resolution mass spectrometry. ASTM International, 100 Barr Harbor Drive, P.O. Box C700, West Conshohocken, PA 19428-2959.

Bacosa, H.P., D.L. Erdner, Z. Liu. 2015. Differentiating the roles of photooxidation and biodegradation in the weathering of Light Louisiana Sweet crude oil in surface water from the *Deepwater Horizon* site. *Mar. Pollut. Bull.* 95 (1):265-272.

Bejarano, A.C., E. Levine, and A.J. Mearns. 2013. Effectiveness and potential ecological effects of offshore surface dispersant use during the *Deepwater Horizon* oil spill: a retrospective analysis of monitoring data. *Environ Monit Assess* 185:10281. doi:10.1007/s10661-013-3332-y.

Boehm, P.D. and D.L. Fiest. 1982. Subsurface distributions of petroleum from an offshore well blowout: The IXTOC 1 blowout, Bay of Campeche. *Environ. Sci. Technol.* 16: 67-74.

Boehm P.D., K.J. Murray, L.L. Cook. 2016. Distribution and attenuation of polycyclic aromatic hydrocarbons in Gulf of Mexico seawater from the *Deepwater Horizon* oil accident. *Environ. Sci. Technol.* 50 (2), 584–592.

British Petroleum (BP). 2014. Gulf Science Data Water Chemistry Data File. Reference No. W-01v01-01. Last modified November 12, 2013 <http://gulfsciencedata.bp.com/go/doc/6145/1942326/>.

Brandyvik, P.J., Ø. Johansen, F. Leirvik, U. Farooq and P.S. Daling. 2013. Droplet breakup in subsurface oil releases – Part 1: Experimental study of droplet breakup and effectiveness of dispersant injection. *Mar. Pollut. Bull.* 73:319-326.

Brandvik, P.J., Ø. Johansen, U. Farooq, G. Angell and F. Leirvik. 2014. Sub-surface oil releases – Experimental study of droplet distributions and different dispersant injection techniques- version 2. A scaled experimental approach using the SINTEF Tower basin. SINTEF report no: A26122. Trondheim Norway 2014. ISBN: 9788214057393.

Camilli, R., C.M. Reddy, D.R. Yoerger, B.A.S. VanMooy, M.V. Jakuba, J.C. Linsey, C.P. McIntyre, S.P. Sylva, and J.V. Maloney. 2010. Tracking hydrocarbon plume transport and biodegradation at the *Deepwater Horizon*. *Science* 330:201-204.

Camilli R, D. Di Iorio, A. Bowen, C.M. Reddy, A.H. Techet, D.R. Yoerger, L.L. Whitcomb, J.S. Seewald, S.P. Sylva, and J. Fenwick. 2011. Acoustic measurement of the *Deepwater Horizon* Macondo well flow rate. *Proceedings of the National Academy of Sciences*. doi: 10.1073/pnas.110038108.

Carls, M.G., S.D. Rice, J.E. Hose. 1999. Sensitivity of fish embryos to weathered crude oil: Part I. Low-level exposure during incubation causes malformations, genetic damage, and mortality in larval Pacific herring (*Clupea pallasi*). *Environ. Toxicol. Chem.* 18, 481-493.

Davis, C. S. and N. C. Loomis. 2014. *Deepwater Horizon* Oil Spill (DWHOS) Water Column Technical Working Group, Image Data Processing Plan: Holocam description of data processing methods used to determine oil droplet size distributions from in situ holographic imaging during June 2010 on cruise *M/V Jack Fitz* 3. Woods Hole Oceanographic Institution and MIT/WHOI Joint Program in Oceanography. 15 pages + Appendices.

de Lappe, B.W., R.W. Risebrough, and W. Walker II. 1983. A large-volume sampling assembly for the determination of synthetic organic and petroleum compounds in the dissolved and particulate phases of seawater. *Canadian J. of Fish. and Aquatic Sci.*; 40(2), 322-336.

Driskell, W.B., J.R. Payne and G.S. Douglas. 2010. Forensic fingerprinting of *Cosco Busan* samples containing mixed-oil sources. Presentation at the Society of Environmental Toxicology and Chemistry, Special session on the *Cosco Busan* Spill. SEATAC 31st Annual Meeting, November 7-10, 2010. Portland, OR.

Driskell, W.B. and J.R. Payne. 2018a. Development and application of phase-specific methods in oiled-water forensic studies. *Oil Spill Environmental Forensics – Case Studies*, S.A. Stout and Z. Wang (eds.), Elsevier/Academic Press. Pp. 289-321.

Driskell, W.B. and J.R. Payne. Submitted. 2018b. Macondo oil in northern Gulf of Mexico waters – Part 2: Dispersant-accelerated PAH dissolution in the *Deepwater Horizon* plume. *Mar. Pollut. Bull.*

Du, M. and J.D. Kessler. 2012. Assessment of the spatial and temporal variability of bulk hydrocarbon respiration following the *Deepwater Horizon* Oil Spill. *Environ. Sci. Technol.* 46, 10499-10507. dx.doi.org/10.1021/es301363k

Faksness, L-G. 2007. Weathering of oil under Arctic conditions: Distribution and toxicity of water soluble oil components dissolving in seawater and migrating through sea ice. A combined laboratory and field study. Ph.D. Dissertation at the University of Bergen & the University Centre in Svalbard. 152 pp.

Fingas, M.F. and J. Banta. 2016. Polar compounds in oils and their aquatic toxicity. Proceedings of the Thirty-ninth AMOP Technical Seminar, Environment and Climate Change Canada, Ottawa, ON, pp. 197-259.

French-McCay, D., J. Rowe, R. Balouskus, A. Morandi, and M.C. McManus. 2015a. Technical Reports for *Deepwater Horizon* Water Column Injury Assessment. WC-TR.28: Injury quantification for planktonic fish and invertebrates in estuarine, shelf and offshore waters. U.S. Dept. of Interior, *Deepwater Horizon Response & Restoration*, Admin. Record, www.doi.gov/deepwaterhorizon/adminrecord. DWH-AR0172019. 41 p. DWH NRDA Water Column Technical Working Group Report, September 30, 2015.

French-McCay, D.P., K. Jayko, Z. Li, M. Horn, Y. Kim, T. Isaji, D. Crowley, M. Spaulding, S. Zamorski, J. Fontenault, R. Shmookler, and J.J. Rowe. 2015b. Technical Reports for *Deepwater Horizon* Water Column Injury Assessment – WC_TR.14: Modeling oil fate and exposure concentrations in the deepwater plume and rising oil resulting from the *Deepwater Horizon* oil spill. RPS ASA, South Kingstown, RI, USA, August 2015.

French-McCay, D., M. Horn, Z. Li, D. Crowley, M. Spaulding, D. Mendelsohn, K. Jayko, Y. Kim, T. Isaji, J. Fontenault, R. Shmookler, and J. Rowe. 2016. Simulation modeling of ocean circulation and oil spills in the Gulf of Mexico – Appendix VI data collection, analysis and model validation. Prepared by RPS ASA for the US Department of the Interior, Bureau of Ocean Energy Management, Gulf of Mexico OCS Region, New Orleans, LA.

French-McCay, D., M. Horn, Z. Li, K. Jayko, M. Spaulding, D. Crowley, D. Mendelsohn. 2018. Modeling distribution, fate, and concentrations of *Deepwater Horizon* oil in subsurface waters of the Gulf of Mexico. *Oil Spill Environmental Forensics – Case Studies*, S.A. Stout and Z. Wang (eds.), Elsevier/Academic Press. Pp. 683-735.

Garcia-Pineda, O., I. MacDonald, W. Shedd, M. Silva, and B. Shumaker. 2015. Transience and persistence of natural hydrocarbon seepage in Mississippi Canyon, Gulf of Mexico. *Deep-Sea Res. II*, 119-129. <http://dx.doi.org/10.1016/j.dsr2.2015.05.011i>

Garrett, R.M., I.J. Pickering, C.E. Haith, and R.C. Prince. 1998. Photooxidation of crude oils. *Environ. Sci. Technol.* 32(23): 3719-3723.

Gray, J.L., L.K. Kanagy, E.T. Furlong, J.W. McCoy, and C.J. Kanagy. 2011. Determination of the anionic surfactant di(ethylhexyl)sodium sulfosuccinate in water samples collected from Gulf of Mexico coastal waters before and after landfall of oil from the *Deepwater Horizon* oil spill, May to October, 2010. U.S. Geological Survey Open-File Report 2010-1318, 15 p. [www.pubs.usgs.gov/of/2010/1318/](http://pubs.usgs.gov/of/2010/1318/).

Gray, J.L., L.K. Kanagy, E.T. Furlong, C.J. Kanagy, J.W. McCoy, A. Mason, and G. Lauenstein. 2014. Presence of the Corexit component dioctyl sodium sulfosuccinate in Gulf of Mexico waters after the 2010 *Deepwater Horizon* oil spill. *Chemosphere* 95: 124-130.

Gros, J., C.M. Reddy, C. Aeppli, R.K. Nelson, C.A. Carmichael, and J.S. Arey. 2014. Hydrocarbons in weathered oil samples from the *Deepwater Horizon* disaster. *Environ. Sci. Technol.* 48: 1628-1637.

Gutierrez, T., D. Berry, T. Yang, S. Mishamandani, L. McCKay, A. Teske, and M.D. Aitken. 2013a. Role of bacterial exopolysaccharides (EPS) in the fate of the oil released during the *Deepwater Horizon* oil spill. *PLOS ONE* 8(6): e67717.

Gutierrez, T., D.R. Singleton, D. Berry, T. Yang, M.D. Aitken, and A. Teske. 2013b. Hydrocarbon-degrading bacteria enriched by the *Deepwater Horizon* oil spill identified by cultivation and DNA-AIP. *ISME Journal*, 7, 2091-2104. doi: 10.1038/ismej. 2013.98.

Hall, G.J., G.S. Frysinger, C. Aeppli, C.A. Carmichael, J. Gros, K.L. Lemkau, R.K. Nelson, C.M. Reddy. 2013. Oxygenated weathering products of *Deepwater Horizon* oil come from surprising precursors, *Mar. Pollut. Bull.*, 75 (1-2): 140-149.

Huba, A.K. and P.R. Gardinali. 2016. Characterization of a crude oil weathering series by ultrahigh-resolution mass spectrometry using multiple ionization modes. *Sci. Total Environ.*; 563-564: 600-610.

Incardona, J.P., T.K. Collier, N.L. Scholz. 2004. Defects in cardiac function precede morphological abnormalities in fish embryos exposed to polycyclic aromatic hydrocarbons. *Toxicol. Appl. Pharmacol.* 196, 191-205.

Incardona, J.P., M.G. Carls, H. Teraoka, C.A. Sloan, T.K. Collier, N.L. Scholz. 2005. Aryl hydrocarbon receptor-independent toxicity of weathered crude oil during fish development. *Environ. Health Perspect.* 113, 1755-1762.

Incardona, J.P., T.L. Swarts, R.C. Edmunds, T.L. Linbo, A. Aquilina-Beck, C.A. Sloan, L.D. Gardner, B.A. Block, N.L. Scholz. 2013. *Exxon Valdez to Deepwater Horizon: Comparable toxicity of both crude oils to fish early life stages, Aquatic Toxicology* Vol. 142–143: 303-316.

Incardona, J.P., M.G. Carls, L. Holland, T.L. Linbo, D.H. Baldwin, M.S. Myers, K.A. Peck, M. Tagal, S.D. Rice and N.L. Scholz. 2015. Very low embryonic crude oil exposures cause lasting cardiac defects in salmon and herring. *Scientific Reports* 5:13499, DOI: 10.1038/srep13499.

Kvenholden, K.A and C.K. Cooper. 2003. Natural seepage of crude oil into the marine environment. *Geo-Mar. Lett.* 23, 140-146.

Kim, Y.H., T. Isaji, L. Decker, M. Spaulding. 2012. Draft technical reports for *Deepwater Horizon* Water Column Trustees: Meteorology and oceanography of the Gulf of Mexico. Project No. 2011-144. RPS ASA, 55 Village Square Drive, South Kingstown, RI 02879. 58 pp plus appendices.

Kujawinski, E.B., M.C.K. Soule, D.L. Valentine, A.K. Boysen, K. Longnecker, and M.C. Redmond. 2011. Fate of dispersants associated with the *Deepwater Horizon* oil spill. *Environ. Sci. Technol.* 45(5): 1298-1306.

Li, Z., M. L. Spaulding, D. French McCay, D. Crowley, and J.R. Payne. 2016. Development of a unified oil droplet size distribution model with application to surface breaking waves and subsea blowout releases considering dispersant effects. *Mar. Pollut. Bull.* 114 (1): 247–257.

Litman, E., S. Emsbo-Mattingly, and W. Wong. 2018. Critical review of an interlaboratory forensic dataset: Effects on data interpretation in oil spill studies. *Oil Spill Environmental Forensics – Case Studies*, S.A. Stout and Z. Wang (eds.), Elsevier/Academic Press. Pp. 1-23.

MacDonald, I.R., I. Leifer, R. Sassen, P. Stine, R. Mitchell, and N. Guinasso, Jr. 2002. Transfer of hydrocarbons from natural seeps to the water column and atmosphere. *Geofluids* 2(2): 95-107.

McAuliffe, C.D. 1987. Organism exposure to volatile/soluble hydrocarbons from crude oil spills – a field and laboratory comparison. *Proceedings of the 1987 International Oil Spill Conference*, American Petroleum Institute, Washington, D.C., pp. 275-288.

McKenna, A.M., R.K. Nelson, C.M. Reddy, J.J. Savory, N.K. Kaiser, J.E. Fitzsimmons, A.G. Marshall, and R.P. Rodgers. 2013. Expansion of the analytical window for oil spill characterization by ultrahigh resolution mass spectrometry: Beyond gas chromatography. *Environ. Sci. Technol.* 47: 7530-7539.

McNutt M., R. Camilli, G. Guthrie, P. Hsieh, V. Labson, B. Lehr, D. Maclay, A. Ratzel, M. Sogge. 2011. Assessment of flow rate estimates for the *Deepwater Horizon*/Macondo well oil spill. Flow Rate Technical Group report to the National Incident Command, Interagency Solutions Group, March 10, 2011.

Morris, J.M., M.O. Krasnec, M.W. Carney, H.P. Forth, C.R. Lay, I. Lipton, A.K. McFadden, R. Takeshita, D. Cacela, J.V. Holmes, J. Lipton. 2015. *Deepwater Horizon* oil spill Natural Resource Damage Assessment comprehensive toxicity testing program: overview, methods, and results. U.S. Dept. of Interior, *Deepwater Horizon Response & Restoration*, Admin. Record, www.doi.gov/deepwaterhorizon/adminrecord. DWH-AR0293761, 805 p. DWH NRDA Toxicity Technical Working Group Report, August 31, 2015.

Murphy, D. W., C. Li, V. d'Albignac, D. Morra, and J. Katz. 2015. Splash behaviour and oily marine aerosol production by raindrops impacting oil slicks, *J. Fluid Mech.* 780, 536–577.

Nagamine, S. I. 2014. The effects of chemical dispersants on buoyant oil droplets. Master Thesis, University of Hawaii at Manoa, May 2014. 122 p.

National Research Council (NRC). 1985. Oil in the Sea: Inputs, Rates, and Effects. National Academy Press, Washington, D.C.

National Research Council (NRC). 1989. Using Oil Spill Dispersants on the Sea. National Academy Press, Washington, D.C.

National Research Council (NRC). 2003. Oil in the Sea III: Inputs, Rates, and Effects. National Academy Press, Washington, D.C.

National Research Council (NRC). 2005. Oil Spill Dispersants: Efficacy and Effects. National Academy Press, Washington D.C., 377 pp.

NOAA. 2014. Analytical quality assurance plan, Mississippi Canyon 252 (*Deepwater Horizon*) natural resource damage assessment, Version 4.0. May 30, 2014.

Overholt, W.A., K.P. Marks, I.C. Romero, D.J. Hollander, T.W. Snell, and J.E. Kostra. 2016. Hydrocarbon-degrading bacteria exhibit a species-specific response to dispersed oil while moderating ecotoxicity. *Applied and Environmental Microbiology*, 82(2), 518-527.

Payne, J.R., G.S. Smith, P.J. Mankiewicz, R.F. Shokes, N.W. Flynn, W. Moreno and J. Altamirano. 1980a. Horizontal and vertical transport of dissolved and particulate-bound higher-molecular-weight hydrocarbons from the IXTOC I blowout. Proceedings: Symposium on Preliminary Results from the September 1979 Researcher/Pierce IXTOC I Cruise. June 9-10, 1980, Key Biscayne, Florida. pp. 119-166. NTIS Accession Number PB81-246068.

Payne, J.R., N.W. Flynn, P.J. Mankiewicz, and G.S. Smith. 1980b. Surface evaporation/dissolution partitioning of lower-molecular-weight aromatic hydrocarbons in a down-plume transect from the IXTOC

I wellhead. Proceedings: Symposium on Preliminary Results from the September 1979 Researcher/Pierce IXTOC I Cruise. June 9-10, 1980, Key Biscayne, Florida. pp. 239-263. NTIS Accession Number PB81-246068.

Payne, J.R. and G.D. McNabb, Jr. 1984. Weathering of petroleum in the marine environment, *Mar. Technol. Soc. J.* 18(3): 24-42.

Payne, J.R., B.E. Kirstein, G.D. McNabb, Jr., J.L. Lambach, R. Redding, R.E. Jordan, W. Hom, C. de Oliveira, G.S. Smith, D.M. Baxter, and R. Geagel. 1984. Multivariate analysis of petroleum weathering in the marine environment - subarctic. Volume I, Technical Results; Volume II, Appendices. In: Final Reports of Principal Investigators, Vol. 21 and 22. February 1984, U.S. Department of Commerce, National Oceanic and Atmospheric Administration, Ocean Assessment Division, Juneau, Alaska. 690 pp. Volume 21 NTIS Accession Number PB85-215796; Volume 22 NTIS Accession Number PB85-215739.

Payne, J.R., J.R. Clayton, Jr., G.D. McNabb, Jr., and B.E. Kirstein. 1991a. *Exxon Valdez* oil weathering fate and behavior: Model predictions and field observations. *Proceedings of the 1991 Oil Spill Conference*, American Petroleum Institute, Washington, D.C., pp 641-654.

Payne, J.R., L.E. Hachmeister, G.D. McNabb, Jr., H.E. Sharpe, G.S. Smith, and C.A. Manen. 1991b. Brine-induced advection of dissolved aromatic hydrocarbons to arctic bottom waters. *Environ. Sci. Technol.* 25(5): 940-951

Payne, J.R., T.J. Reilly, and D.P. French. 1999. Fabrication of a portable large-volume water sampling system to support oil spill NRDA efforts. *Proceedings of the 1999 Oil Spill Conference*, American Petroleum Institute, Washington, D.C., 1179-1184.

Payne, J.R. and W.B. Driskell. 2003. The importance of distinguishing dissolved- versus oil-droplet phases in assessing the fate, transport, and toxic effects of marine oil pollution. *Proceedings of the 2003 Oil Spill Conference*, American Petroleum Institute, Washington, D.C., pp 771-778.

Payne, J.R., W.B. Driskell, J.F. Braddock, J. Bailey, J.W. Short, L. Ka'ahue, T.H. Kuckertz. 2005. From tankers to tissues – Tracking the degradation and fate of oil discharges in Port Valdez, Alaska. *Proceedings of Arctic Marine Oil Spill Conference 2005*, Calgary, Alberta, Canada. pp 959-991.

Payne, J.R. and C.J. Beegle-Krause. 2011. Physical transport and chemical behavior of dispersed oil. White paper commissioned for the CRRC Workshop: The Future of Dispersant Use in Spill Response. September 20-22, 2011. NOAA Disaster Response Center, Mobile, Alabama. Available at: http://www.crrc.unh.edu/workshops/dispersant_future_11/Dispersant_Initiative_FINALREPORT.pdf.

Payne, J.R. and W.B. Driskell. 2015a. 2010 DWH offshore water column samples—Forensic assessments and oil exposures. U.S. Dept. of Interior, *Deepwater Horizon Response & Restoration*, Admin. Record, www.doi.gov/deepwaterhorizon/adminrecord. DWH-AR0039118, 37 p. DWH NRDA Chemistry Technical Working Group Report, September 1, 2015.

Payne, J.R. and W.B. Driskell. 2015b. Offshore adaptive sampling strategies. U.S. Dept. of Interior, *Deepwater Horizon Response & Restoration*, Admin. Record, www.doi.gov/deepwaterhorizon/adminrecord. DWH-AR0023786, 75 p. DWH NRDA Chemistry Technical Working Group Report, August 30, 2015.

Payne, J.R. and W.B. Driskell. 2015c. Forensic fingerprinting methods and classification of *Deepwater Horizon* oil spill offshore water samples. U.S. Dept. of Interior, *Deepwater Horizon Response & Restoration, Admin. Record*, www.doi.gov/deepwaterhorizon/adminrecord. DWH-AR0039170, 31 p. DWH NRDA Chemistry Technical Working Group Report, September 1, 2015.

Payne, J.R. and W.B. Driskell. 2015d. Dispersant effects on waterborne oil profiles and behavior during the *Deepwater Horizon* Oil Spill. U.S. Dept. of Interior, *Deepwater Horizon Response & Restoration, Admin. Record*, www.doi.gov/deepwaterhorizon/adminrecord. DWH-AR0039201, 22 p. DWH NRDA Chemistry Technical Working Group Report, August 30, 2015.

Payne, J.R. and W.B. Driskell. 2016. Water column sampling for forensics. In Standard Handbook Oil Spill Environmental Forensics – Fingerprinting and Source Identification (2nd Edition), S. Stout and Z. Wang (eds.) Elsevier/Academic Press, 2016: 983-1014.

Payne, J.R. and W.B. Driskell. 2017. Water-column measurements and observations from the *Deepwater Horizon* oil spill Natural Resource Damage Assessment. *Proceedings of the 2017 International Oil Spill Conference*, American Petroleum Institute, Washington, D.C.

Plata, D.L., C. Sharpless, C.M. Reddy. 2008. Photochemical degradation of polycyclic aromatic hydrocarbons in oil films. *Environ. Sci. Technol.* 24: 2432-2438.

Prince, R.C., R.M. Garrett, R.E. Bare, M.J. Grossman, T. Townsend, J.M. Suflita, K. Lees, E.H. Owens, G.A. Sergy, J.F. Braddock, J.E. Lindstrom, R.R. Lessard. 2003. The roles of photooxidation and biodegradation in long-term weathering of crude and heavy fuel oils. *Spill Sci. Technol. Bull.* 8(2): 145-156.

Radović, J.R., C. Aeppli, R.K. Nelson, N. Jimenez, C.M. Reddy, J.M. Bayona, and J. Albaigés. 2014. Assessment of photochemical processes in marine oil spill fingerprinting. *Mar. Pollut. Bull.* 79(1-2):268–277, <http://dx.doi.org/10.1016/j.marpolbul.2013.11.029>.

Reddy, C.M., J.S. Arey, J.S. Seewald, S.P. Sylva, K.L. Lemkau, R.K. Nelson, C.A. Carmichael, C.P. McIntyre, J. Fenwick, G.T. Ventura, B.A.S. Van Mooy, and R. Camilli. 2011. Composition and fate of gas and oil released to the water column during the *Deepwater Horizon* oil spill. *Proceedings of the National Academy of Sciences* 109(50): 20229-20234. www.pnas.org/cgi/doi/10.1073/pnas.1101242108

Ruddy, B.M., M. Huettel, J.E. Kostka, V.V. Lobodin, B.J. Bythell, A.M. McKenna, C. Aeppli, C.M. Reddy, R.K. Nelson, A.G. Marshall, and R.P. Rodgers. 2014. Targeted petroleomics: Analytical investigation of Macondo well oil oxidation products from Pensacola Beach. *Energy & Fuels* 2014 28 (6): 4043-4050 doi: 10.1021/ef500427n

Ryerson, T.B., K.C. Aikin, W.M. Angevine, E.L. Atlas, D.R. Blake, C.A. Brock, F.C. Fehsenfeld, R.-S. Gao, J.A. de Gouw, D.W. Fahey, J.S. Holloway, D.A. Lack, R.A. Lueb, S. Meinardi, A.M. Middlebrook, D.M. Murphy, J.A. Neuman, J.B. Nowak, D.D. Parrish, J. Peischl, A.E. Perring, I.B. Pollack, A.R. Ravishankara, J.M. Roberts, J.P. Schwarz, J.R. Spackman, H. Stark, C. Warneke, L.A. Watts. 2011. Atmospheric emissions from the *Deepwater Horizon* spill constrain air-water partitioning, hydrocarbon fate, and leak rate. *Geophys. Res. Lett.*, 38, L07803, doi:10.1029/2011GL046726.

Socolofsky, S.A., E.E. Adams, and C.R. Sherwood. 2011. Formation dynamics of subsurface hydrocarbon intrusions following the *Deepwater Horizon* blowout. *Geophys. Res. Lett.* 38: L09602.

Spaulding, M.S., D. Mendelsohn, D. Crowley, Z. Li and A. Bird. 2015. Technical Reports for *Deepwater Horizon* Water Column Injury Assessment-WC_TR 13. Application of OILMAP DEEP to the *Deepwater Horizon* blowout. RPS ASA, 55 Village Square Drive, South Kingstown, RI 02879. August 2015. U.S. Dept. of Interior, *Deepwater Horizon* Response & Restoration, Admin. Record, www.doi.gov/deepwaterhorizon/adminrecord. DWH-AR0285366.pdf

Spaulding, M.Z. Li, D. Mendelsohn, D. Crowley, D. French-McCay, and A. Bird, 2017. Application of an Integrated Blowout Model System, OILMAP DEEP, to the *Deepwater Horizon* (DWH) Spill. *Mar. Pollut. Bull.* 120(1): 37-50.

Spier, C., W.T. Stringfellow, T.C. Hazen, M. Conrad. 2013. Distribution of hydrocarbons released during the 2010 MC252 oil spill in deep offshore waters. *Environmental Pollution* 173: 224-230.

Stout, S.A. 2015a. Review of dispersants used in response to the *Deepwater Horizon* oil spill. U.S. Dept. of Interior, *Deepwater Horizon* Response & Restoration, Admin. Record, www.doi.gov/deepwaterhorizon/adminrecord. DWH-AR0038542, 25 p. DWH NRDA Chemistry Technical Working Group Report, September 1, 2015.

Stout, S.A. 2015b. Chemical composition of fresh Macondo crude oil. U.S. Dept. of Interior, *Deepwater Horizon* Response & Restoration, Admin. Record, www.doi.gov/deepwaterhorizon/adminrecord. DWH-AR0038495, 21 p. DWH NRDA Chemistry Technical Working Group Report, August 2015.

Stout, S.A. and J.R. Payne. 2016. Macondo Oil in deep-sea sediments: Part 1 Sub-sea weathering of oil deposited on the seafloor. *Mar. Pollut. Bull.* 111: 365-380.

Stout, S.A. and Z. Wang. 2016. Standard Handbook Oil Spill Environmental Forensics – Fingerprinting and Source Identification. Second Edition. Elsevier/Academic Press. London, UK. 1107 pp.

Stout, S.A., J.R. Payne, S. Emsbo-Mattingly, and G. Baker. 2016a. Weathering of field-collected floating and stranded Macondo oils during the shortly after the *Deepwater Horizon* oil spill. *Mar. Pollut. Bull.* 105: 7-22.

Stout, S.A., J.R. Payne, R.W. Ricker, G. Baker, and C. Lewis. 2016b. Macondo oil in deep-sea sediments: Part 2 – Distribution and distinction from background and natural oil seeps. *Mar. Pollut. Bull.* 111: 381-401.

Valentine, D.L., I. Mezic, S. Macesic, N. Crnjarc-Zic, S. Ivic, P.J. Hogan, V.A. Fonoberov, and S. Loire. 2012. Dynamic autoinoculation and the microbial ecology of a deepwater hydrocarbon irruption. *Proceedings of the National Academy of Sciences* 109(50):20286-20291; doi:10.1073/pnas.1108820109.

Wade, T. L., J. L. Sericano, S.T. Sweet, A.H. Knap, N.L. Guinasso. 2016. Spatial and temporal distribution of water column total polycyclic aromatic hydrocarbons (PAH) and total petroleum hydrocarbons (TPH) from the *Deepwater Horizon* (Macondo) incident. *Mar. Pollut. Bull.* 103(1-2):286-93. doi: 10.1016/j.marpolbul.2015.12.002.

White, H.K., R.N. Conmy, I.R. MacDonald, and C.M. Reddy. 2016. Methods of oil detection in response to the *Deepwater Horizon* oil spill. *Oceanography* 29(3): 76-87. <http://dx.doi.org/10.5670/oceanog.2016.72>.

Wolfe, D.A., M.J. Hameedi, J.A. Galt, G. Watabayashi, J. Short, C. O’Claire, S. Rice, J. Michel, J.R. Payne, J. Braddock, S. Hanna, and D. Sale. 1994. The fate of the oil spilled from the *Exxon Valdez*. *Environ. Sci. Technol.* 28(13): 561-56

Ziervogel K., Dike C., Asper V., Montoya J., Battles J., D’Souza N., U. Passow, A. Diercks, M. Esch, S. Joye, C. Dewald, C. Arnosti. 2016. Enhanced particle flux and heterotrophic bacterial activities in Gulf of Mexico bottom waters following storm-induced sediment resuspension. *Deep Sea Res. Part II Top. Stud. Oceanogr.* 129 77–88. 10.1016/j.dsr2.2015.06.017.

Table 1. Forensic Matching Categories for Water Samples

	Category Code	Comparable Category*	Description
Match	1	A	MC252—containing particulate phase oil (with or without extra dissolved)
	2		MC252—dissolved phase only
	3		MC252— phase uncertain, (unresolvablely complex)
No Match	4	E	other oil or obvious ship-board contaminants (e.g., hydraulic fluid)
Indeterminate or clean	5	C	possible MC252 – oil-like profile but insufficient to link to MC252
	6	D	indeterminate—trace PAH detected but no oil-like profile
	7		no PAH detected or apparent noise (clean)

*Non-numeric categories used in other reports for DWH NRDA forensics assessments of oil, tissues and sediment matrices (Stout et al., 2016b).

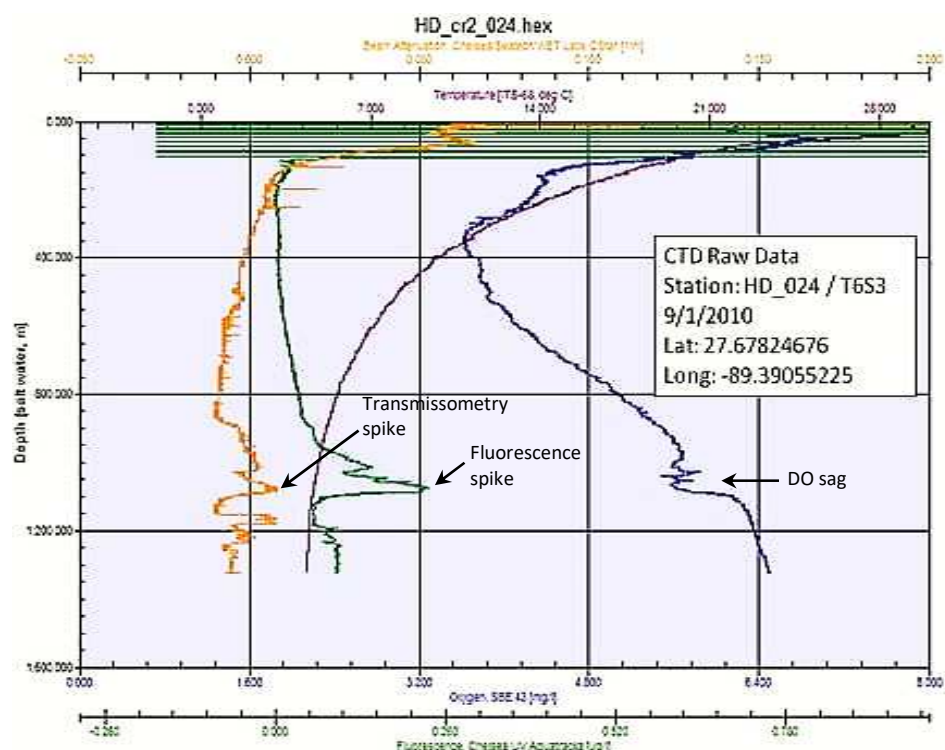


Figure 1. Field plot showing strong anomalies in dissolved oxygen (blue), fluorescence (green), and transmissometry (orange) live sensor data highlighted the deep subsurface oil plume at 1060 m depth. Samples would ideally be collected at the plume depth and +/- 200 m to capture the oil lens and the surrounding water above and below (from Payne and Driskell, 2015b).

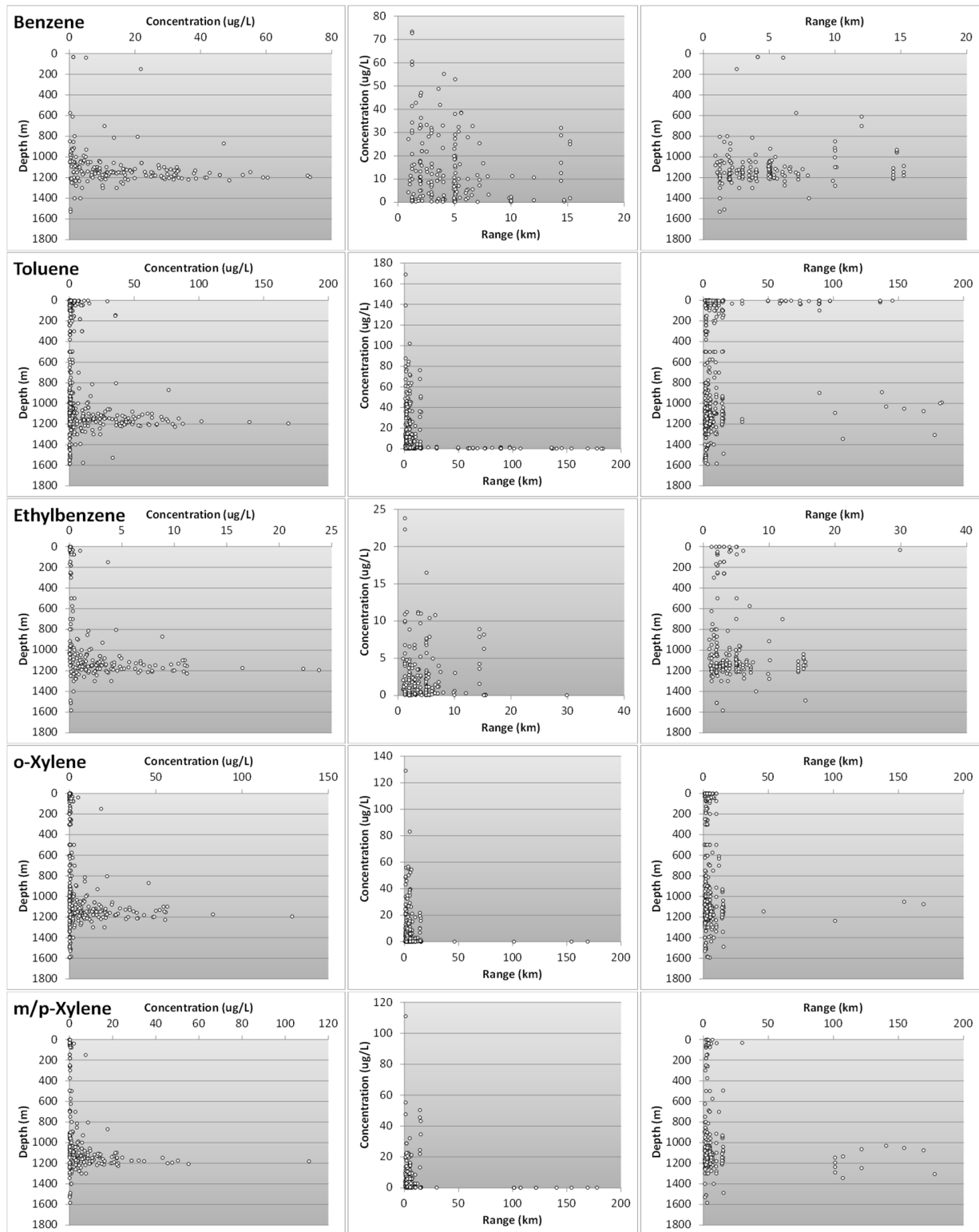


Figure 2. Distribution of BTEX in forensic-matched (category 1-3) samples by concentration ($\mu\text{g/L}$), depth (m) and range (km) from wellhead.

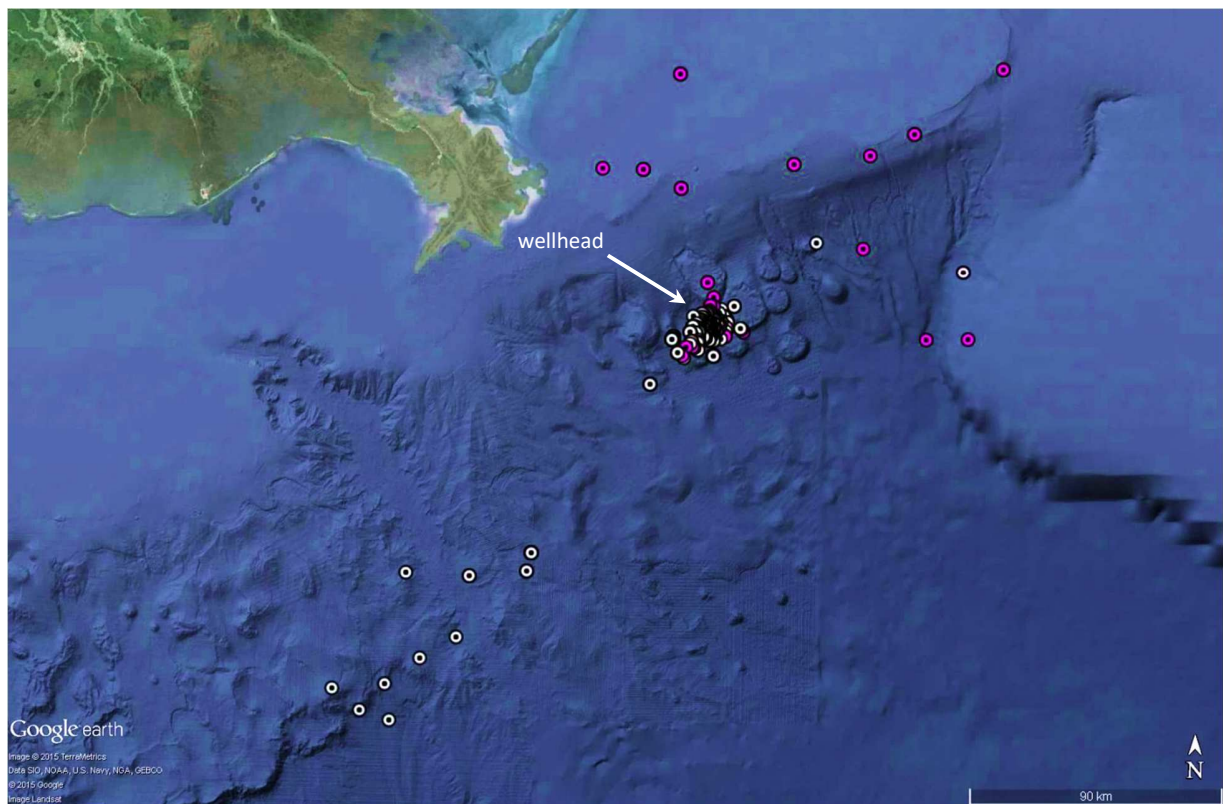


Figure 3. Distribution of BTEX-containing forensically-matched samples. Red dots are 0-20 m depth, white dots from greater than 800 m. Farthest surface sample NE at 145 km, deep plume sample SW at 183 km (also see Figure 2).

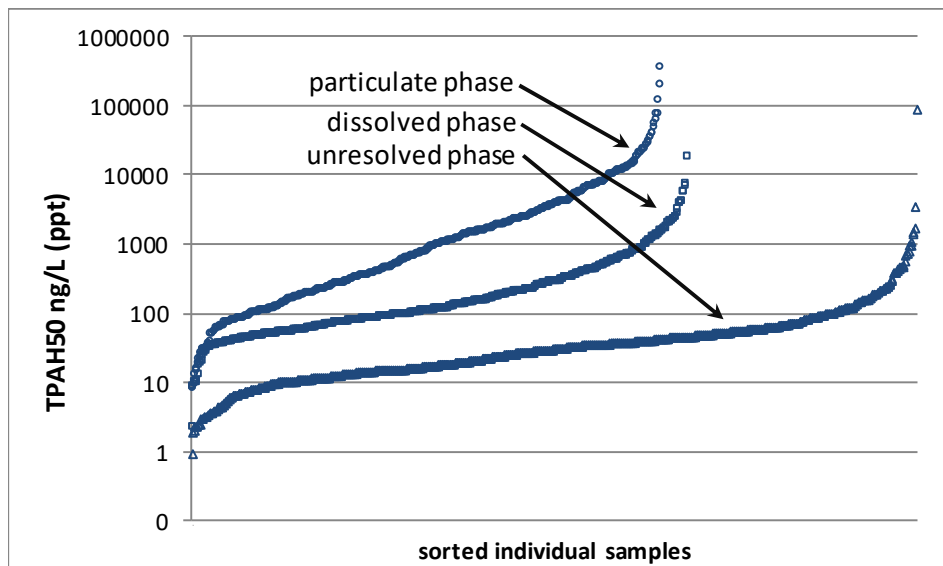


Figure 4. Sorted TPAH distributions of all MC-252 matched samples (Categories 1-3), all depths showing relative range of concentrations.

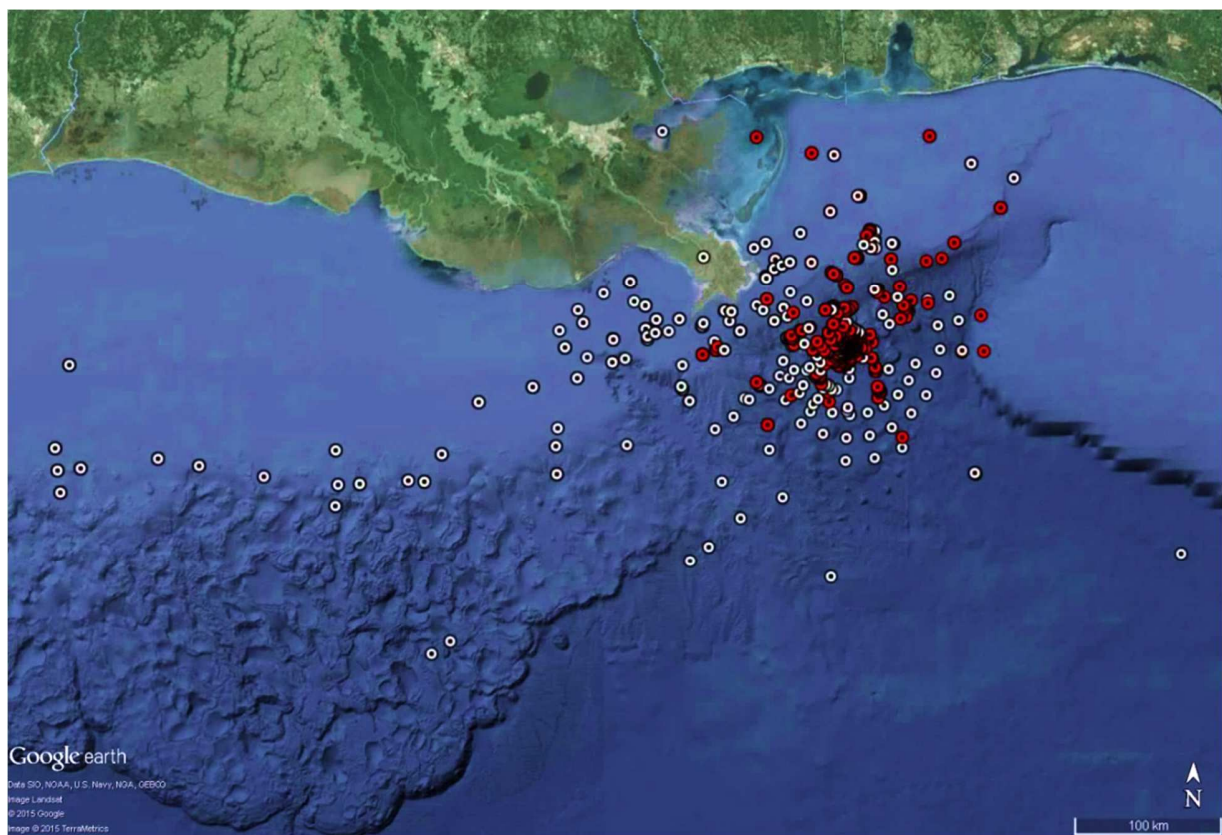


Figure 5. Near-surface (0-20m depth) forensic matches (dark) and non-matches (light) (n=359 and 331, respectively).

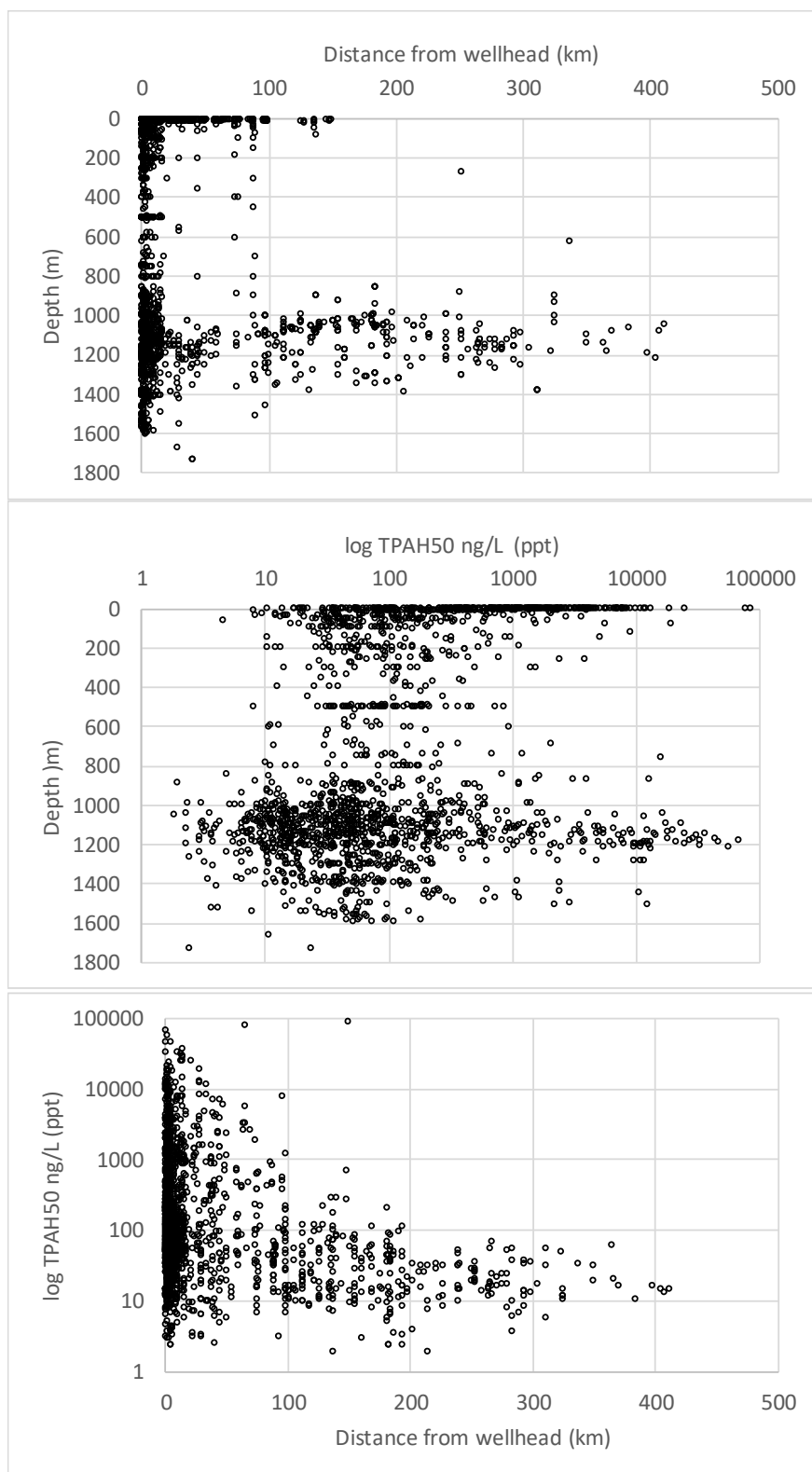


Figure 6. Distribution and concentration (TPAH50) of water samples forensically matched to MC252 oil (category 1-3, n=1,766).

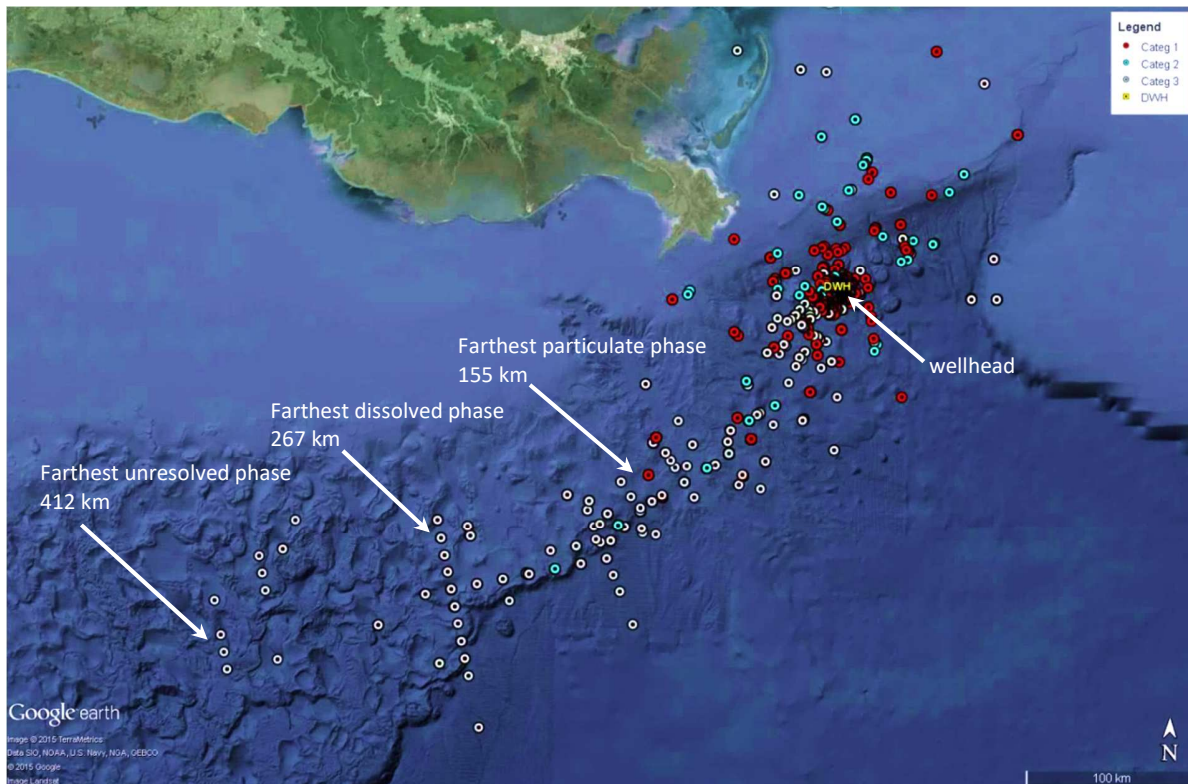


Figure 7. Distribution of offshore water samples matching MC252 source oil. Matched particulate (Cat. 1; dark), dissolved (Cat. 2; gray), and unresolved phase (Cat. 3; white) samples range to 155, 267, and 412 km from wellhead, respectively. Each location may have collocated samples at multiple depths (see Figure 6). n=1,766 matches.

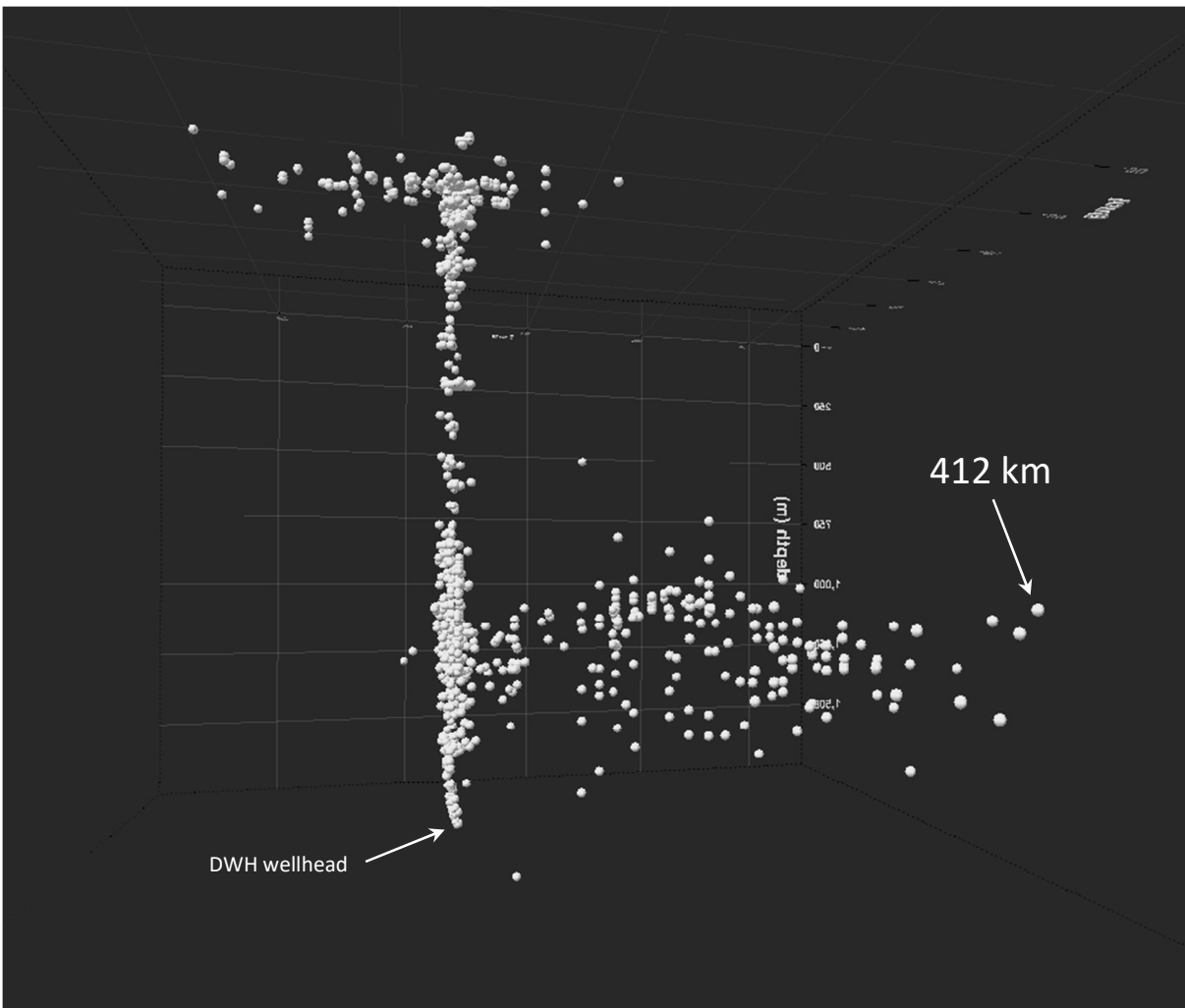


Figure 8. MC252 matched samples in 3D spatial view at 1,000-1,400 m plume depth looking east from beyond plume's distal end (also see Figure S- 5).

(note to editor: this version may be more suitable for printed journal. The color version below is intended for the on-line version)

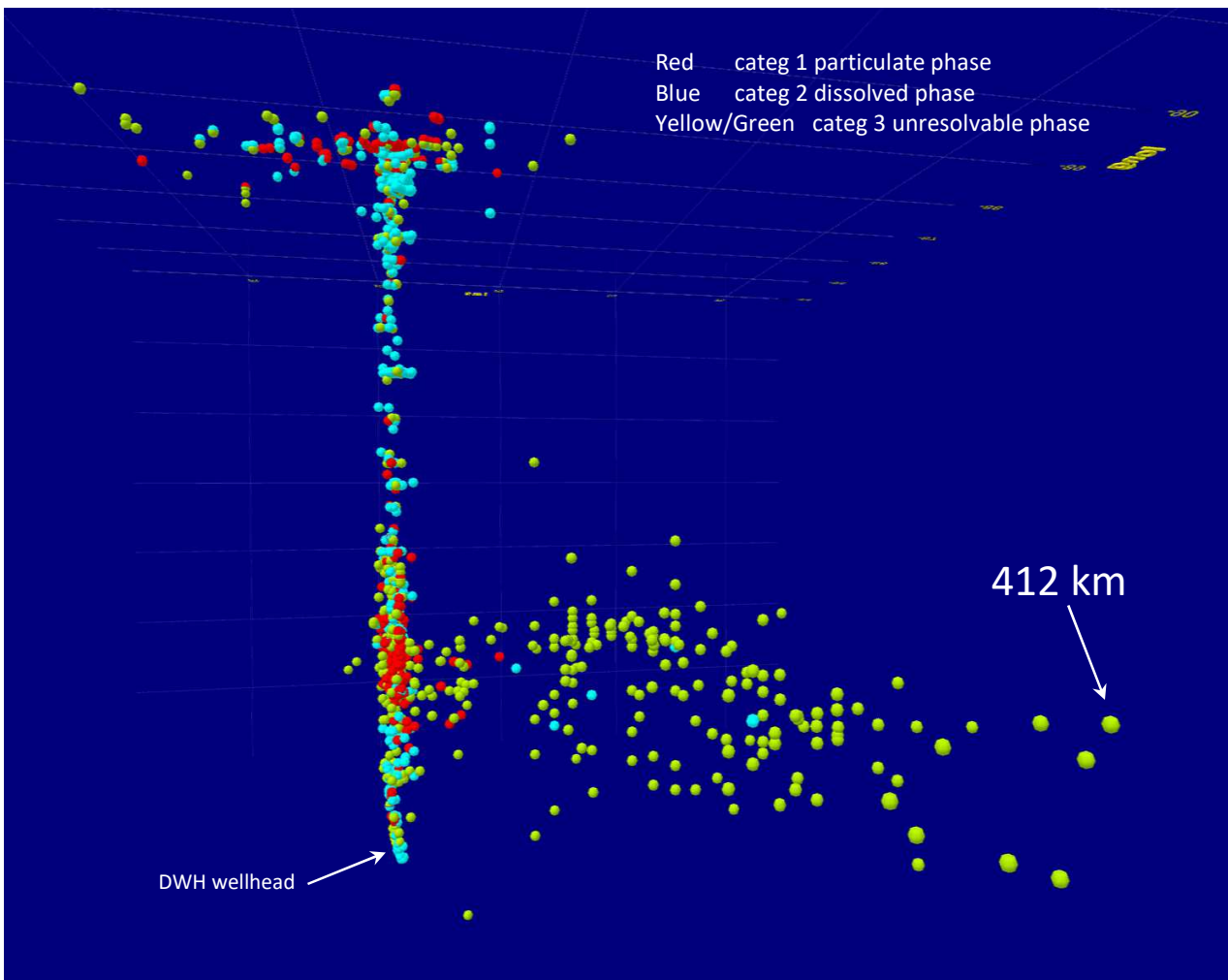


Figure 8. MC252 matched samples in 3D spatial view at 1,000-1,400 m plume depth looking east from beyond plume's distal end (also see Figure S- 5).

Note to editor – alternative colored image

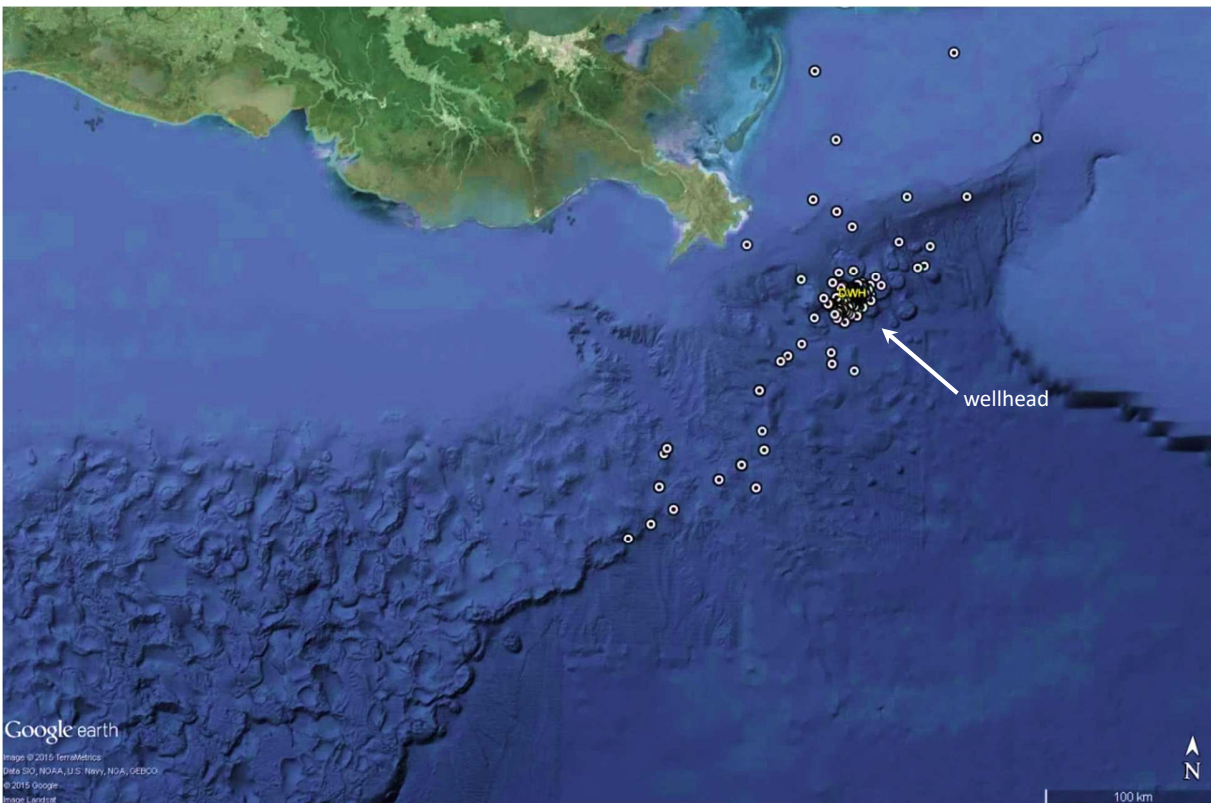


Figure 9. Distribution of dispersant-mediated samples matching MC252 source oil. Samples southwest of the wellhead were at deep plume depth. Samples on shelf northeast of the wellhead were from <20m depth.

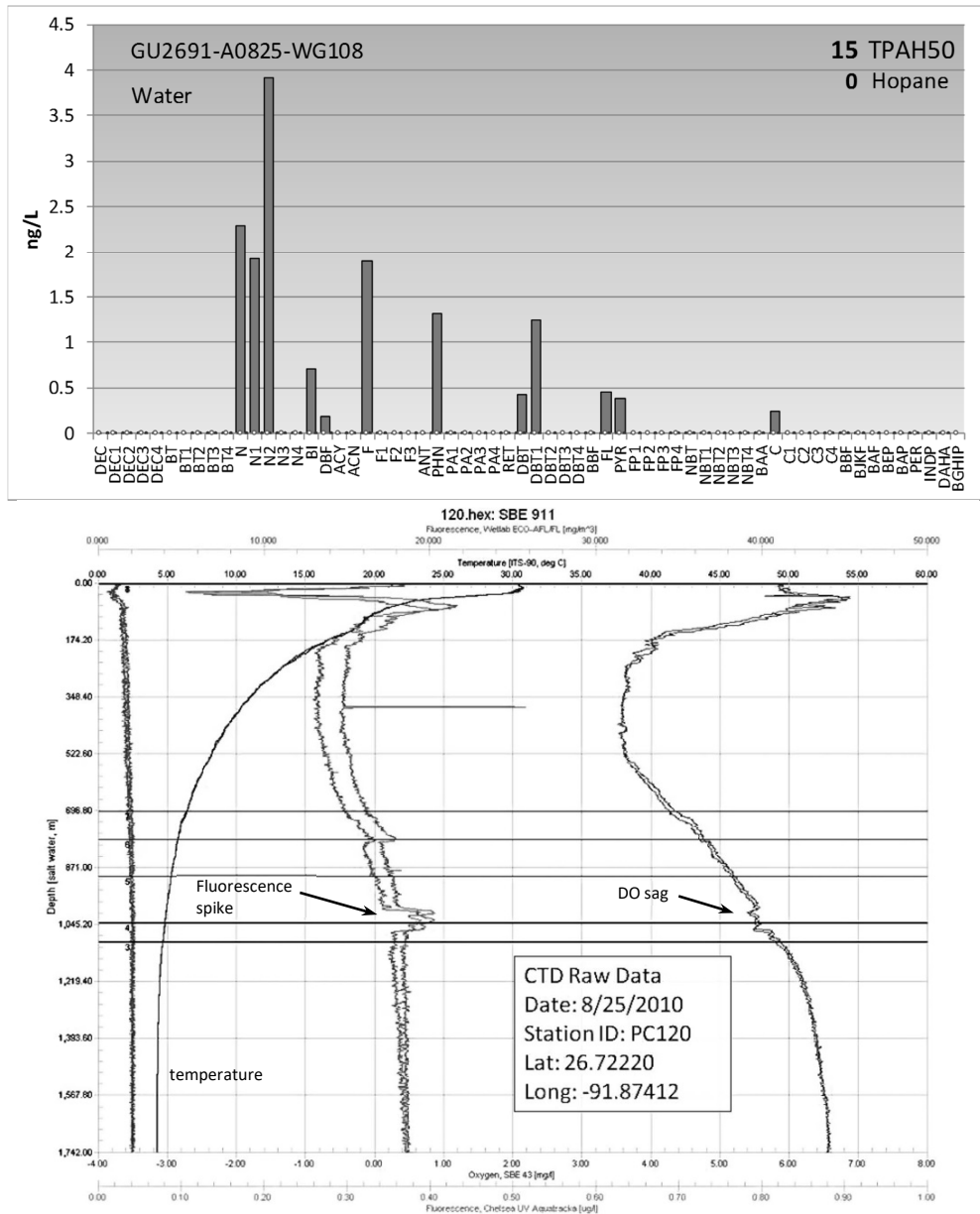


Figure 10. Trace dissolved PAH pattern (upper plot) from 1,000m depth with fluorescence spike, DO sag (lower plot) and a trace of dispersant indicators (22.5 ng/L, not shown) suggesting the presence of the deepwater plume 412 km from wellhead but without detectable residual PAH components. These data suggest the alkanes and PAH may have been biotically converted to polar components not amenable to GC/FID and SIM GC/MS resolution.

Supplemental Information for:

Macondo oil in northern Gulf of Mexico waters – Part 1: Assessments and forensic methods for *Deepwater Horizon* offshore water samples

James R. Payne^a and William B. Driskell^b

^aPayne Environmental Consultants, Inc., 1651 Linda Sue Lane, Encinitas, CA 92024
jrpayne@sbcglobal.net

^b6536 20th Ave NE, Seattle, WA 98115
bdriskell@comcast.net

List of Hydrocarbon Analytes from MC252 Analytical Quality Assurance Plan (NOAA, 2014)

AQAP TABLE 1.1a
Extended PAH (Parent and Alkyl Homologs) and Related Compounds

	Compound	RF Source		Compound	RF Source		Compound	RF Source
D0	cis/trans-Decalin		PA4	C4-Phenanthrenes/Anthracenes	P0	BEP	Benzo[e]pyrene	
D1	C1-Decalins	D0	RET	Retene		BAP	Benzo[a]pyrene	
D2	C2-Decalins	D0	DBT0	Dibenzothiophene		PER	Perylene	
D3	C3-Decalins	D0	DBT1	C1-Dibenzothiophenes	DBT0	IND	Indeno[1,2,3-cd]pyrene	
D4	C4-Decalins	D0	DBT2	C2-Dibenzothiophenes	DBT0	DA	Dibenz[a,h]anthracene	
BT0	Benzothiophene		DBT3	C3-Dibenzothiophenes	DBT0	GHI	Benzo[g,h,i]perylene	
BT1	C1-Benzo(b)thiophenes	BT0	DBT4	C4-Dibenzothiophenes	DBT0	4MDT	4-Methyldibenzothiophene	DBT0
BT2	C2-Benzo(b)thiophenes	BT0	BF	Benzo(b)fluorene		2/3- 2MDT	2-Methyldibenzothiophene	DBT0
BT3	C3-Benzo(b)thiophenes	BT0	FL0	Fluoranthene		1MDT	1-Methyldibenzothiophene	DBT0
BT4	C4-Benzo(b)thiophenes	BT0	PY0	Pyrene		3MP	3-Methylphenanthrene	P0
N0	Naphthalene		FP1	C1-Fluoranthenes/Pyrenes	FL0	2MP	2/4-Methylphenanthrene	P0
N1	C1-Naphthalenes	N0	FP2	C2-Fluoranthenes/Pyrenes	FL0	2MA	2-Methylnaphthalene	A0
N2	C2-Naphthalenes	N0	FP3	C3-Fluoranthenes/Pyrenes	FL0	9MP	9-Methylphenanthrene	P0
N3	C3-Naphthalenes	N0	FP4	C4-Fluoranthenes/Pyrenes	FL0	1MP	1-Methylphenanthrene	P0
N4	C4-Naphthalenes	N0	NBT0	Naphthobenzothiophenes		2-Methylnaphthalene		
B	Biphenyl		NBT1	C1-Naphthobenzothiophenes	NBT0	1-Methylnaphthalene		
DF	Dibenzofuran		NBT2	C2-Naphthobenzothiophenes	NBT0	2,6-Dimethylnaphthalene		
AY	Acenaphthylene		NBT3	C3-Naphthobenzothiophenes	NBT0	1,6,7-Trimethylnaphthalene		
AE	Acenaphthene		NBT4	C4-Naphthobenzothiophenes	NBT0			
F0	Fluorene		BA0	Benz[a]anthracene				
F1	C1-Fluorenes	F0	C0	Chrysene/Triphenylene		Other		
F2	C2-Fluorenes	F0	BC1	C1-Chrysenes	C0	Carbazole		
F3	C3-Fluorenes	F0	BC2	C2-Chrysenes	C0			
A0	Anthracene		BC3	C3-Chrysenes	C0			
P0	Phenanthrene		BC4	C4-Chrysenes	C0			
PA1	C1-Phenanthrenes/Anthracenes	P0	BBF	Benzo[b]fluoranthene				
PA2	C2-Phenanthrenes/Anthracenes	P0	BJKF	Benzo[k]fluoranthene				
PA3	C3-Phenanthrenes/Anthracenes	P0	BAF	Benzo[a]fluoranthene				

Response factor (RF) to be used for quantitation. If blank, compound is included in the calibration mix.

Target Method Detection Limit Range	
Sediment/Soil =	0.1 – 0.5 ng/g dry weight
Tissue =	0.2 – 1.0 ng/g wet weight
Water =	1 – 5 ng/L
Target Reporting Limit	
Oil =	2.0 mg/kg

¹ Quantitative concentrations of C29-hopane and 18 α -oleanane may be provided if laboratories are calibrated to do so; the C30-hopane is a minimum requirement.

AQAP TABLE 1.1b
Alkanes/Isoprenoids Compounds and Total Extractable Hydrocarbons

Abbr.	Analyte	Abbr.	Analyte
nC9	n-Nonane	nC24	n-Tetracosane
nC10	n-Decane	nC25	n-Pentacosane
nC11	n-Undecane	nC26	n-Hexacosane
nC12	n-Dodecane	nC27	n-Heptacosane
nC13	n-Tridecane	nC28	n-Octacosane
1380	2,6,10 Trimethyldodecane	nC29	n-Nonacosane
nC14	n-Tetradecane	nC30	n-Triacontane
1470	2,6,10 Trimethyltridecane	nC31	n-Hentriacontane
nC15	n-Pentadecane	nC32	n-Dotriacontane
nC16	n-Hexadecane	nC33	n-Tritriacontane
nPr	Norpristane	nC34	n-Tetratriacontane
nC17	n-Heptadecane	nC35	n-Pentatriacontane
Pr	Pristane	nC36	n-Hexatriacontane
nC18	n-Octadecane	nC37	n-Heptatriacontane
Ph	Phytane	nC38	n-Octatriacontane
nC19	n-Nonadecane	nC39	n-Nonatriacontane
nC20	n-Eicosane	nC40	n-Tetracontane
nC21	n-Heneicosane		
nC22	n-Docosane	TEH	$\Sigma(C_9-C_{40})$ Integration of the FID signal over the entire hydrocarbon range from n-C9 to n-C44 after silica gel cleanup.
nC23	n-Tricosane	TEM	$\Sigma(C_9-C_{40})$ Integration of the FID signal over the entire hydrocarbon range from n-C9 to n-C44 no silica gel cleanup.

Target Method Detection Limit

Sediment (Alkanes) = 0.01 µg/g dry weight

Sediment (TEH) = 1 µg/g dry weight

Water (Alkanes) = 0.8 µg/L

Water (TEH) = 10 µg/L

Target Reporting Limit

Oil (Alkanes) = 200 mg/kg

Oil (TEH) = 200 mg/kg

TEH = Total Extractable Hydrocarbons with silica gel "clean-up"

TEM = Total Extractable Matter with no extract "clean-up"

AQAP TABLE 1.1c
Standard Volatile Organic Compounds

Analyte
1,2,4-Trimethylbenzene
1,3,5-Trimethylbenzene
4-Isopropyltoluene
Benzene
Ethylbenzene
Isopropylbenzene
m,p-Xylenes
Naphthalene ²
n-Butylbenzene
n-Propylbenzene
o-Xylene
sec-Butylbenzene
Styrene
tert-Butylbenzene
Toluene

	Target Method Detection Limit Range
Sediment/Soil =	0.1 – 1 ng/g
Water =	0.05 – 0.5 µg/L
	Target Reporting Limit
Oil =	2 mg/kg

² Naphthalene is also included on the Table 1.1a target analyte list of PAH compounds. The PAH analysis is the preferred method, rather than this volatile method. Thus, if a sample location is analyzed for both PAH and VOC the result from the PAH analysis will be noted in the database as the preferred result.

AQAP TABLE 1.1e
Petroleum Biomarkers for Quantitative Analysis

Compound ¹	Quant ion m/z	Compound	Quant ion m/z
C23 Tricyclic Terpane (T4)	191	Tetrakishomohopane-22S (T32)	191
C24 Tricyclic Terpane (T5)	191	Tetrakishomohopane-22R (T33)	191
C25 Tricyclic Terpane (T6)	191	Pentakishomohopane-22S (T34)	191
C24 Tetracyclic Terpane (T6a)	191	Pentakishomohopane-22R (T35)	191
C26 Tricyclic Terpane-22S (T6b)	191	13b(H),17a(H)-20S-Diacholestane (S4)	217
C26 Tricyclic Terpane-22R (T6c)	191	13b(H),17a(H)-20R-Diacholestane (S5)	217
C28 Tricyclic Terpane-22S (T7)	191	13b,17a-20S-Methyldiacholestane (S8)	217
C28 Tricyclic Terpane-22R (T8)	191	14a(H),17a(H)-20S-Cholestane (S12)	217
C29 Tricyclic Terpane-22S (T9)	191	14a(H),17a(H)-20R-Cholestane (S17)	217
C29 Tricyclic Terpane-22R (T10)	191	13b,17a-20R-Ethyldiacholestane (S18)	217
18a-22,29,30-Trisnorhopane-Ts (T11)	191	13a,17b-20S-Ethyldiacholestane (S19)	217
C30 Tricyclic Terpane-22S (T11a)	191	14a,17a-20S-Methylcholestane (S20)	217
C30 Tricyclic Terpane-22R (T11b)	191	14a,17a-20R-Methylcholestane (S24)	217
17a(H)-22,29,30-Trisnorhopane-Tm (T12)	191	14a(H),17a(H)-20S-Ethylcholestane (S25)	217
17a/b,21b/a 28,30-Bisnorhopane (T14a)	191	14a(H),17a(H)-20R-Ethylcholestane (S28)	217
17a(H),21b(H)-25-Norhopane (T14b)	191	14b(H),17b(H)-20R-Cholestane (S14)	217
30-Norhopane (T15)	191	14b(H),17b(H)-20S-Cholestane (S15)	217
18a(H)-30-Norneohopane-C29Ts (T16)	191	14b,17b-20R-Methylcholestane (S22)	217
17a(H)-Diahopane (X)	191	14b,17b-20S-Methylcholestane (S23)	217
30-Normoretane (T17)	191	14b(H),17b(H)-20R-Ethylcholestane (S26)	217
18a(H)&18b(H)-Oleananes (T18)	191	14b(H),17b(H)-20S-Ethylcholestane (S27)	217
Hopane (T19)	191	C26,20R- +C27,20S- triaromatic steroid	231
Moretane (T20)	191	C28,20S-triaromatic steroid	231
30-Homohopane-22S (T21)	191	C27,20R-triaromatic steroid	231
30-Homohopane-22R (T22)	191	C28,20R-triaromatic steroid	231
30,31-Bishomohopane-22S (T26)	191		
30,31-Bishomohopane-22R (T27)	191		
30,31-Trishomohopane-22S (T30)	191		
30,31-Trishomohopane-22R (T31)	191		

¹ Peak identification provided in parentheses.

Target Detection Limit
 Sediments/Soil = 2 ug/Kg dry weight
 Waters = 10 ng/L

Target Reporting Limit
 Oil = 2 mg/Kg

Forensic assessment methods for *Deepwater Horizon* water samples

Weathered Reference Series of filtered particulate samples

The weathered reference series comprises the particulate (filtered) portions of field samples forensically matched to MC252 source oil. Field samples were collected during the release event at depth on cruises in the vicinity of the wellhead (2-8 km), filtered aboard the vessel into particulate (filter) and dissolved (filtrate) portions and later biomarker-confirmed as MC252 oil.

Sampling approaches included commonly used rosette samplers and later, remotely-operated-vehicles (ROVs) instrumented with real-time dissolved oxygen (DO), fluorometry, and conductivity/temperature/depth (CTD) sensors (Figure S- 1) to detect, track, and sample above, within, and below the deep plume rather than collecting samples randomly or systematically at pre-assigned depths (Figure 1). Filtered, phase-separated water samples were collected in the field (Payne et al., 1999; Payne and Driskell 2015a, 2015b, 2015c) to use in later parsing out phase information (dissolved versus particulate) in the routinely collected, unfiltered whole-water samples (Figure S- 2 and Figure S- 3).

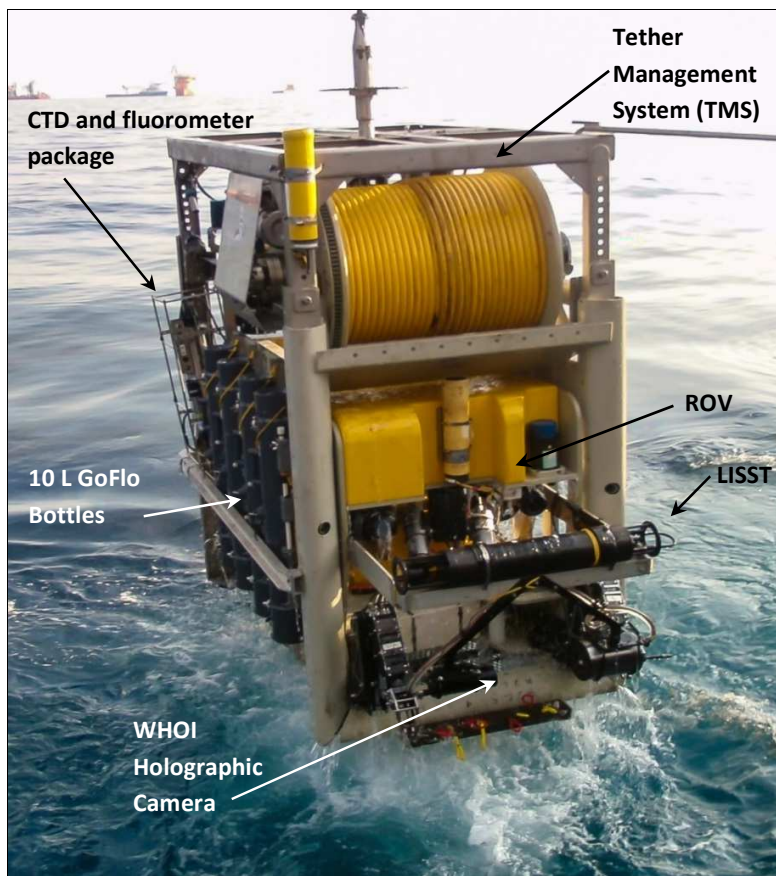


Figure S- 1. Remotely Operated Vehicle (ROV) equipped with CTD package for temperature, salinity, dissolved oxygen and pH; fluorometers for in situ oil/PAH measurements; 670 kHz and 300 kHz forward-looking sonar systems (internal to the ROV) for detecting oil droplet clouds at depth; 10 L GoFlo® bottles; video camera with visible and UV/black-light; Laser In Situ Scattering and Transmissometry (LISST®) instrument; and WHOI holographic camera for recording oil-droplet-size distributions.



Figure S- 2. Vacuum filtration of dissolved and particulate fractions from a 5 L GoFlo® Bottle soon after collection. The water sample passes from the bottom sampling valve on the GoFlo® Bottle (here secured to deck steps) through a 0.7 μm glass fiber filter housed in the stainless steel filtration unit and then into the amber-glass collection jug in the pump box upstream of a Gast oil-less vacuum pump.

Validating field-filtration separation of dissolved- vs. particulate (oil)-phase samples is sometimes a concern of those unfamiliar with the method. Effective filtration is confirmed by the analytical results:

- 1) the PAH profiles (i.e., left-hand plots in Figure S- 3) showing significant concentrations of non-water-soluble, higher-molecular-weight oil components (dibenzothiophenes, fluoranthenes/pyrenes, naphthobenzothiophenes, and chrysenes) only in the particulate phase (filter) while the water-soluble, lower-molecular-weight naphthalenes, fluorenes, and phenanthrenes/anthracenes (all parent-PAH dominated) appear only in the dissolved phase (filtrate);
- 2) high concentrations (157 $\mu\text{g/L}$ TPH) of non-water-soluble n-alkanes ($n\text{-C}_{10}$ to $n\text{-C}_{38}$) in the particulate phase vs. < 1 $\mu\text{g/L}$ TPH in the dissolved phase (note the different SHC concentration scales for the two phases; also, $n\text{-C}_{25}$ and $n\text{-C}_{28}$ in the bottom right plot are laboratory artifacts below 0.14 $\mu\text{g/L}$); and
- 3) the complete absence of insoluble hopane in the dissolved phase.

The final selected particulate weathered reference series (filters only) suggests the patterns and relative rates of dissolution losses in the water column as the larger droplets rose to the water surface (Figure S- 4). Note that unlike other accidental spill events, fresh DWH oil was continuously released for 87 days and, prior to being sampled, subjected to unknown horizontal and vertical mitigation paths during the release (Valentine et al., 2012). Therefore, DWH weathering effects were not “time” sequential from the initial blowout. The weathering references are instead ordered empirically by their weathering states, i.e., general relative losses of the naphthalene through dibenzothiophene groups as expected per their known dissolution behavior in seawater plus various other diagnostic ratios. The SHC weathering patterns (far right column of Figure S- 4) depict dissolution and degradation of the lower-molecular-weight n-alkanes ($<\text{C}_{13}$) relative to fresh oil.

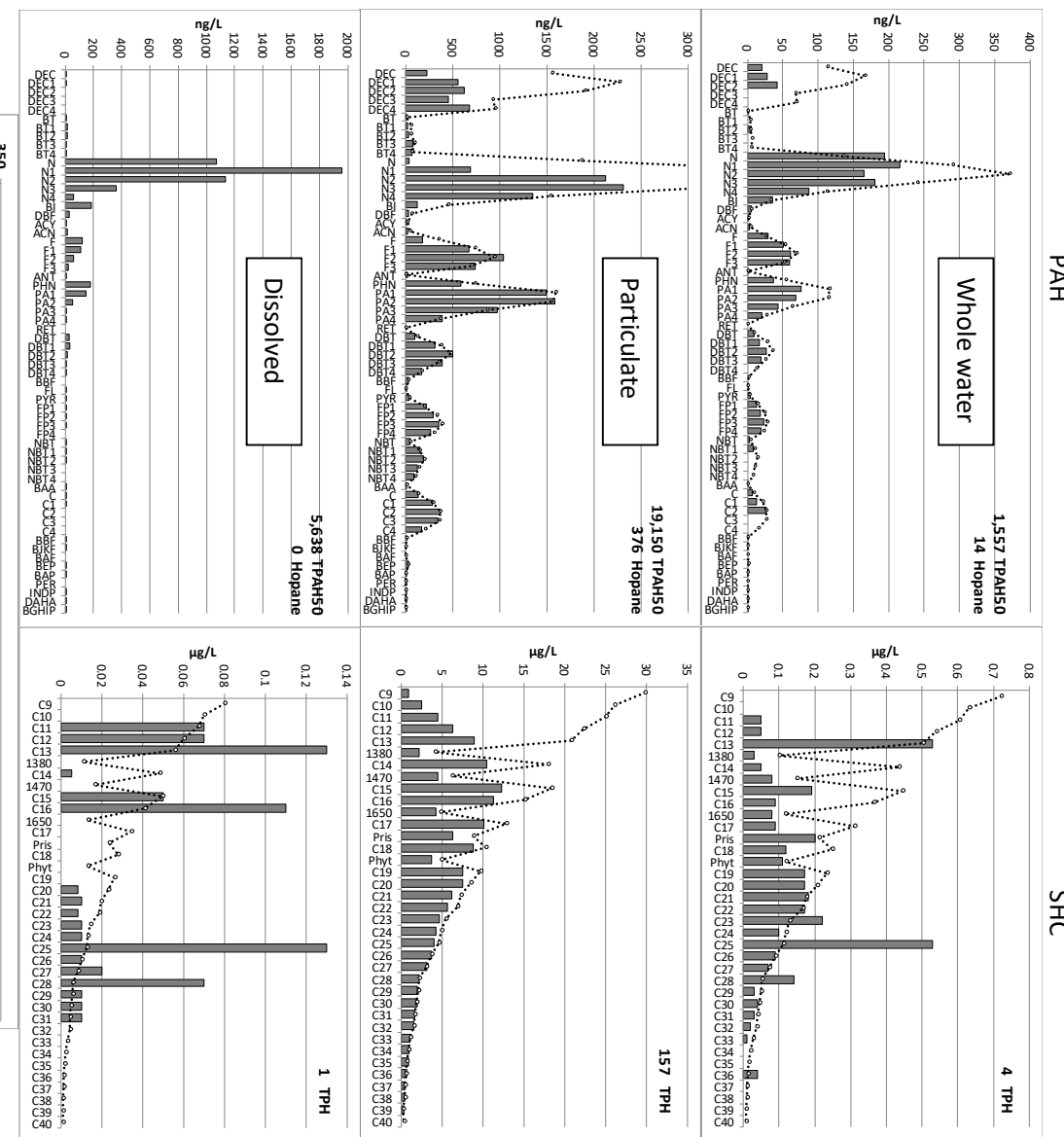


Figure S-3. Example of PAH and SHC from whole water (upper), particulate-filter fraction (upper mid), and dissolved (i.e., filtered) fraction (lower mid) from a single water sample 16 June 2010, 252 ft (77 m) depth. Example biomarkers (bottom) from particulate fraction in separate sample. Dotted line represents fresh MC252 oil scaled to the sample's C2-chrysene (none in dissolved fraction). The 1L whole-water sample was subsampled from the Go-Flo® Bottle prior to the 3.5L filtered/dissolved sample. Note the different concentrations scale for the SHC in the particulate- versus dissolved-phase fractions, 0-35 and 0-0.14 $\mu\text{g/L}$, respectively.

The heavily weathered samples at the end of the series are more variable, in lower concentrations, and are missing the full suite of biomarkers. At these lower concentrations (e.g., reference samples 10 and 11), many biomarkers are below detection, and the triaromatic steranes (TAS) show dissolution losses (Stout and Payne, 2016; and Stout et al., 2016a, 2016b). The samples do, however, fit the PAH trend for the series, have corroborating evidence, and are used with confidence. In references 8 and 11, the slightly elevated T15 (norhopane), spiking to the left of hopane, suggests the minor presence of ROV-sourced hydraulic oil contamination that here doesn't affect the PAH profiles (discussed further below).

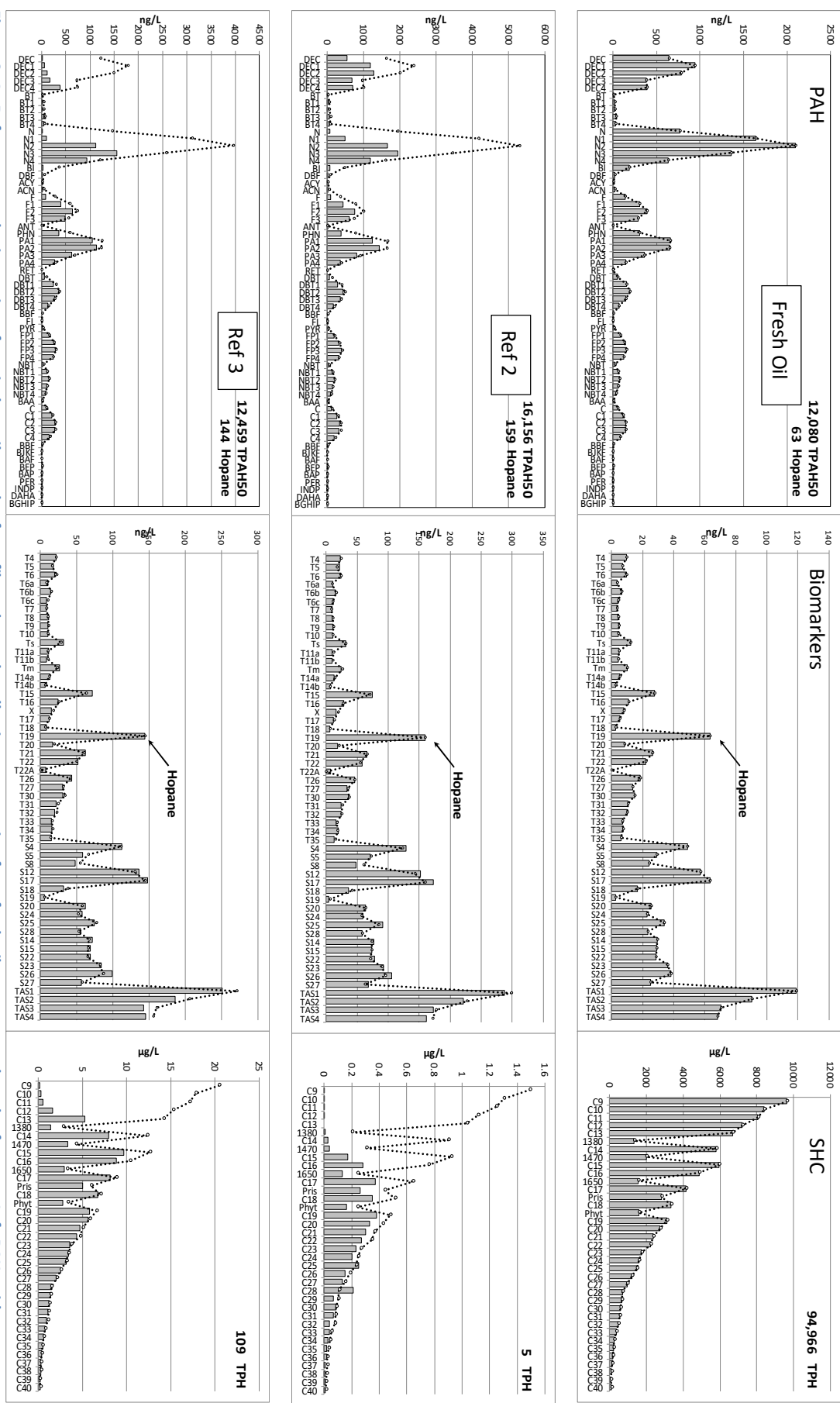
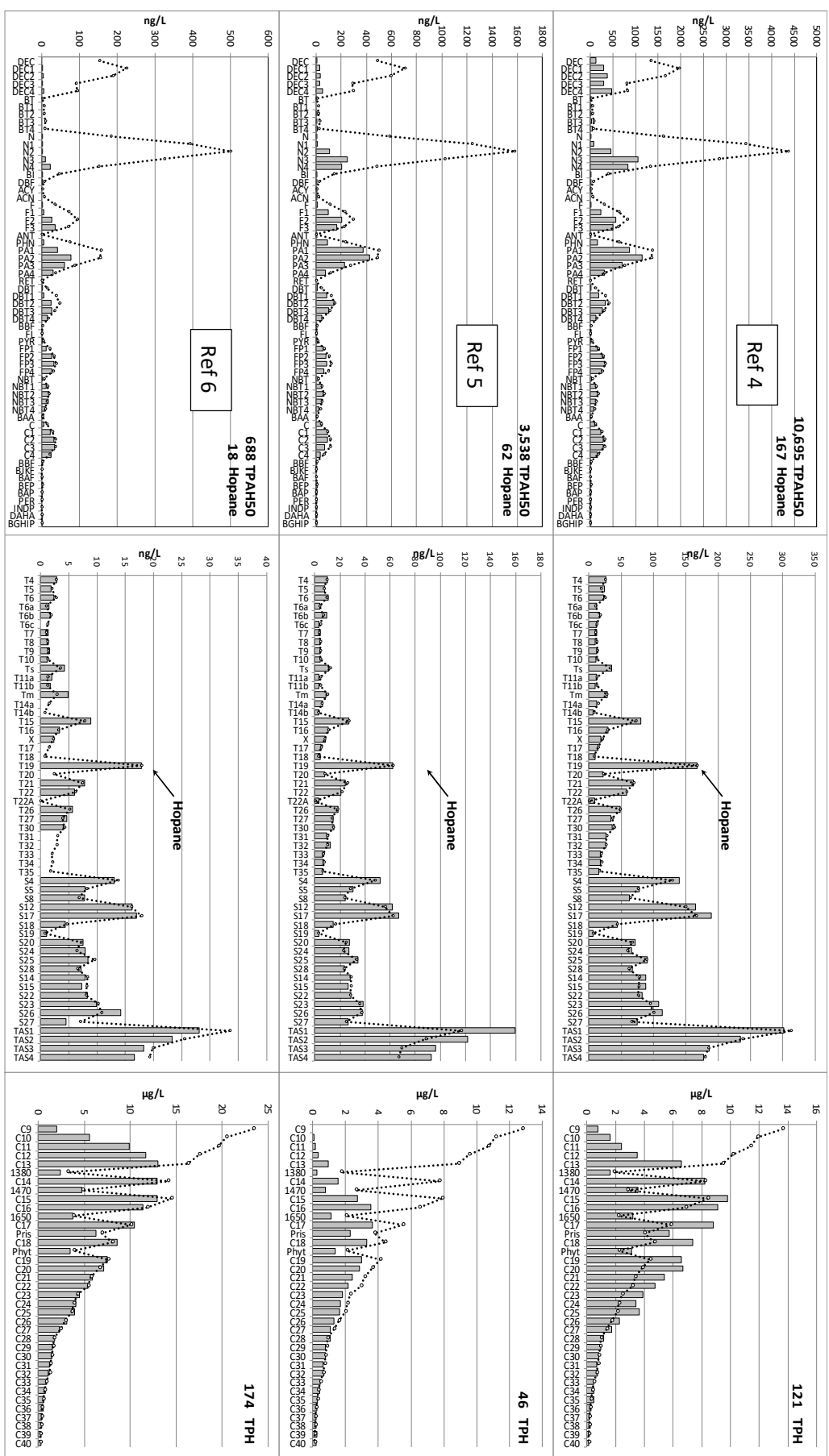
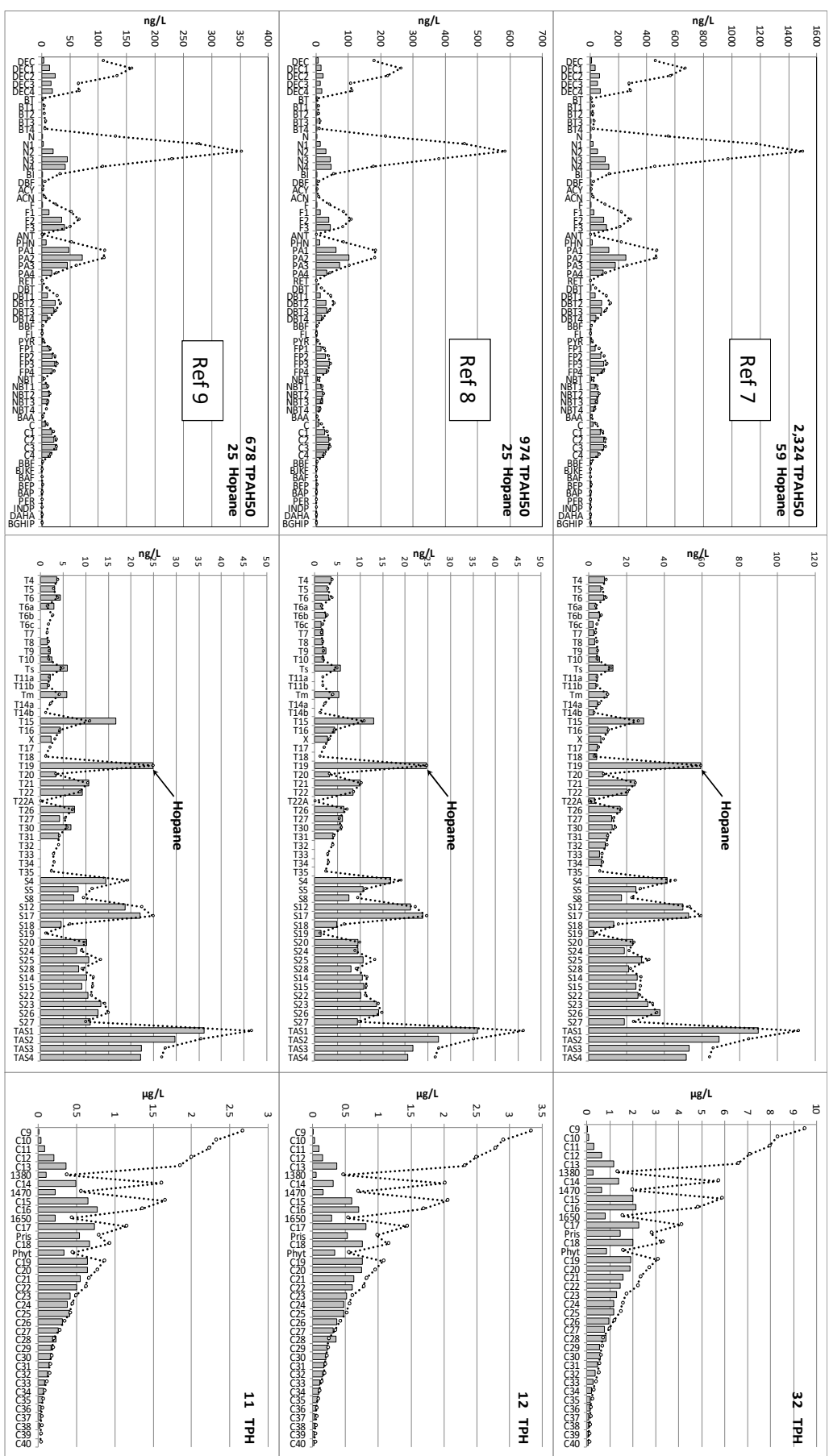


Figure S-4. Reference weathering series of particulate-oil samples from filtered-sample collections progressing from fresh oil to most weathered reference. Left-PAH, mid- biomarkers, right-SHC. Reference-source oil (dotted line) normalized to NBT2 in all PAH plots, hopane (T19) in biomarkers, and n-C₂₆ in SHC. All samples except Reference 5 were collected at depth and not subject to evaporation or photooxidation weathering.





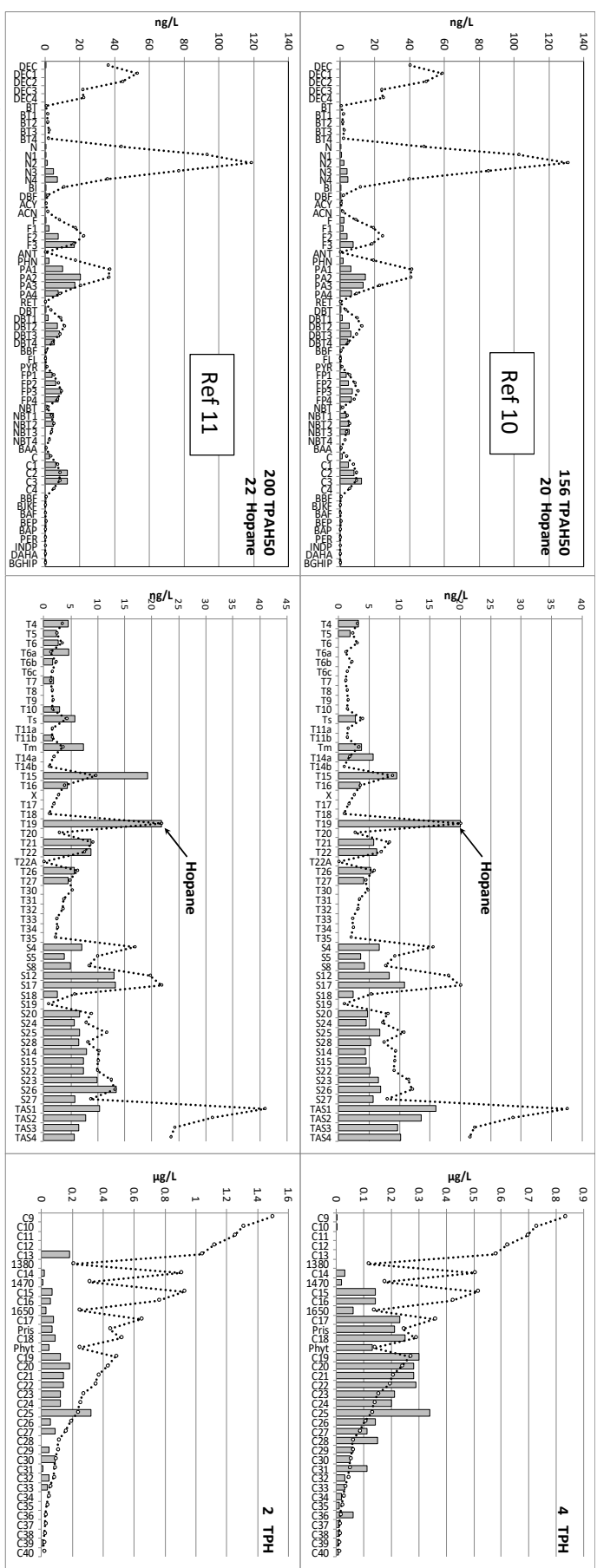


Figure S-4 (cont) Reference weathering series of particulate-oil samples from filtered-sample collections progressing from fresh oil to most weathered reference. **Left-PAH, mid-biomarkers, right-SHC.** Reference-source oil (dotted line) normalized to NBT2. In all PAH plots, hopane (T19) in biomarkers, and n-C₂₆ in SHC. All samples except Reference 5 were collected at depth and not subject to evaporation or photooxidation weathering.

Summary of Forensics Approach

This portion of the supplement information details methods used in forensically examining 4,189 water samples from early NRDA offshore field collections whereby MC252 oil was detected at depth, matched, weathering-state discriminated, and characterized for dispersant effects (Payne and Driskell, 2015a, 2015b, 2015c, 2015d, 2016, and 2017, and Driskell and Payne 2018b). Obtaining a reference series of weathered oils based on known MC-252 samples, field-filtered into dissolved and particulate fractions, was critical to implementing and validating this effort. Using a weight-of-evidence forensic approach combining mixing-model and hopane-confirmation methods in conjunction with CTD, fluorescence and DO profiles plus spatial and temporal data, it was possible to detect MC-252 oil against a background of uncontaminated GOM waters and parse particulate- and dissolved-phase portions over space and time in mixed profiles from unfiltered, whole-water samples (Figure S- 5, Figure S- 6, and Table S- 1). The fingerprinting methods discussed in detail below were also adapted to assess dispersed samples using a weathering reference series of dispersed samples (see Part 2 of this submission – Driskell and Payne 2018b). Evidenced for the first time were dispersant-mediated effects on PAH profiles (accelerated dissolution) and field documentation that *in situ* dispersant injection at depth actually aided in breaking up the oil droplets (Payne and Driskell, 2015d; Driskell and Payne, 2018b).

Assessment Methods

Briefly, our approach looks for predictably familiar, traditional weathering patterns with the loss of both lighter-molecular-weight PAH and, within each PAH homologue group by degree of alkylation. This task is rather straightforward unless there is a mixture of phases or different weathering states present. Consider three examples. In water, dissolution is one of the dominant oil weathering processes but, unlike in solid matrices (oil, tarballs, sediments or tissues), the weathered dissolved-phase components remain within the water matrix along with the oil droplets to create the first example, a typical mixed-phase signature. When examining results from a whole-water sample, normally one could not differentiate the dissolved phase from the particulate oil phase. With the methods presented herein, however, it becomes possible. In the second example, the dissolved components can become separated from their particulate oil source and thus appear as just a dissolved-phase profile (e.g., as DWH droplets rise to the surface, dissolved components are separated and remain behind) or, third example, in meandering currents at depth, the dissolved components in a previously-exposed water parcel may be advected back through the rising oil droplets (Valentine et al., 2012) and thus, create an enriched dissolved phase. Again, these mixtures may be parsed by the methods presented herein.

In their appearance, dissolved-phase components are essentially the complement of the weathered droplet source, the “missing” portion from the initial fresh droplet’s profile. Driven by a kinetically-controlled approach to equilibrium as reflected by each analyte’s octanol-water partitioning constant (K_{ow}), pure dissolved-phase profiles generally lack the insoluble or low-solubility components typically used in fingerprinting oil, i.e., biomarkers, SHC or the more recalcitrant, higher-molecular-weight PAH (Figure S- 3 third profile on left). By themselves, dissolved-phase profiles alone cannot be confidently attributed to a source; additional lines of evidence must be used to support a “matching” forensic call.

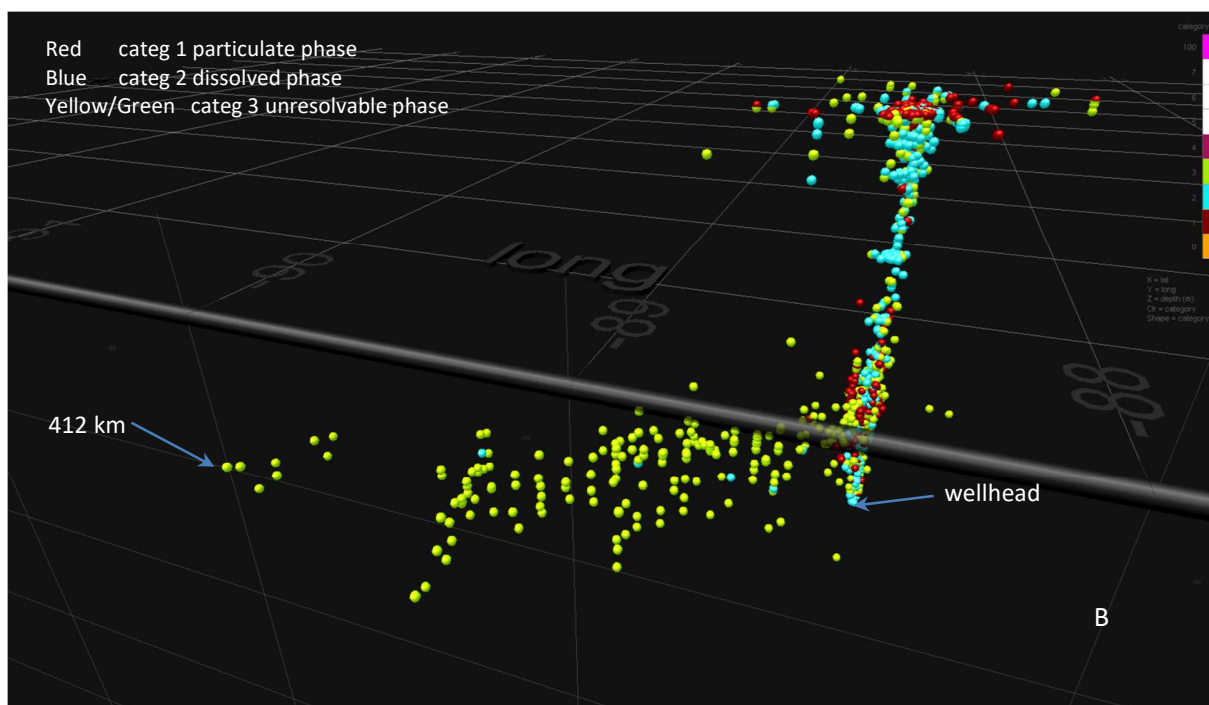
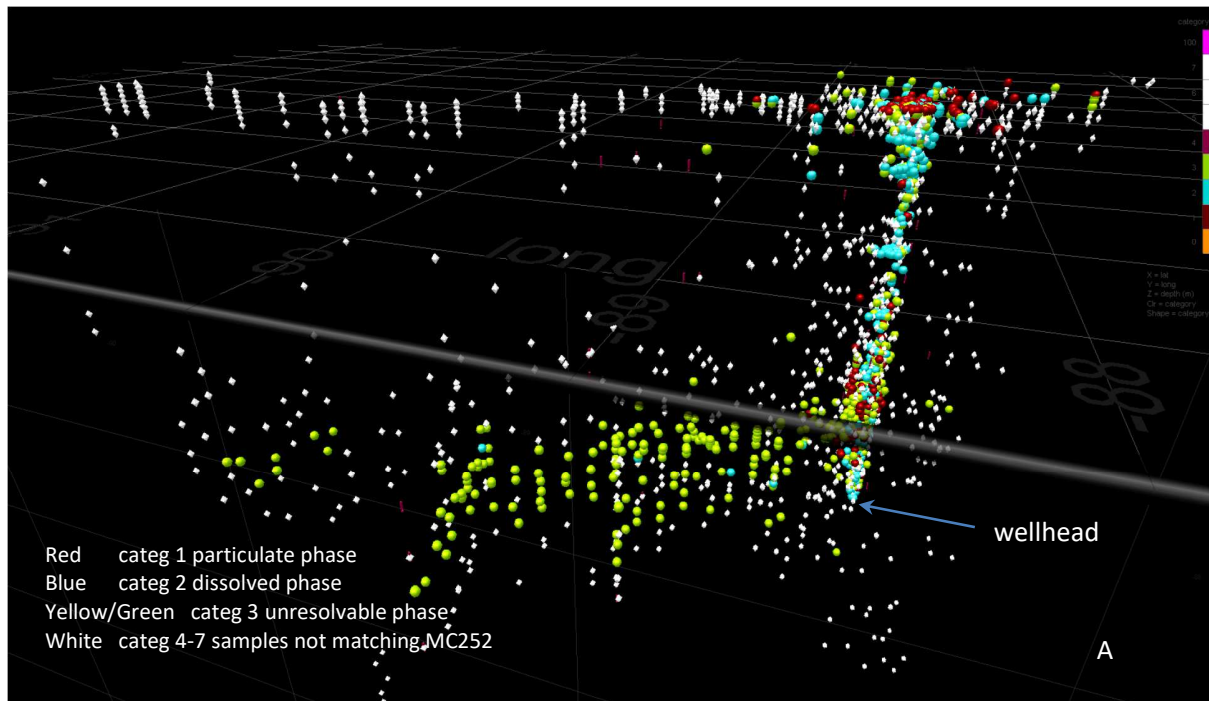


Figure S- 5. Four 3D spatial views of samples colored by forensic categories. A) oblique view of all samples looking north (column of blue is rising plume near wellhead, and white dots represent non-matching category 4-7 samples) B) view A with only matched samples displayed, C) at plume depth looking NE from beyond plume's end (500 km), D) top view from above wellhead.

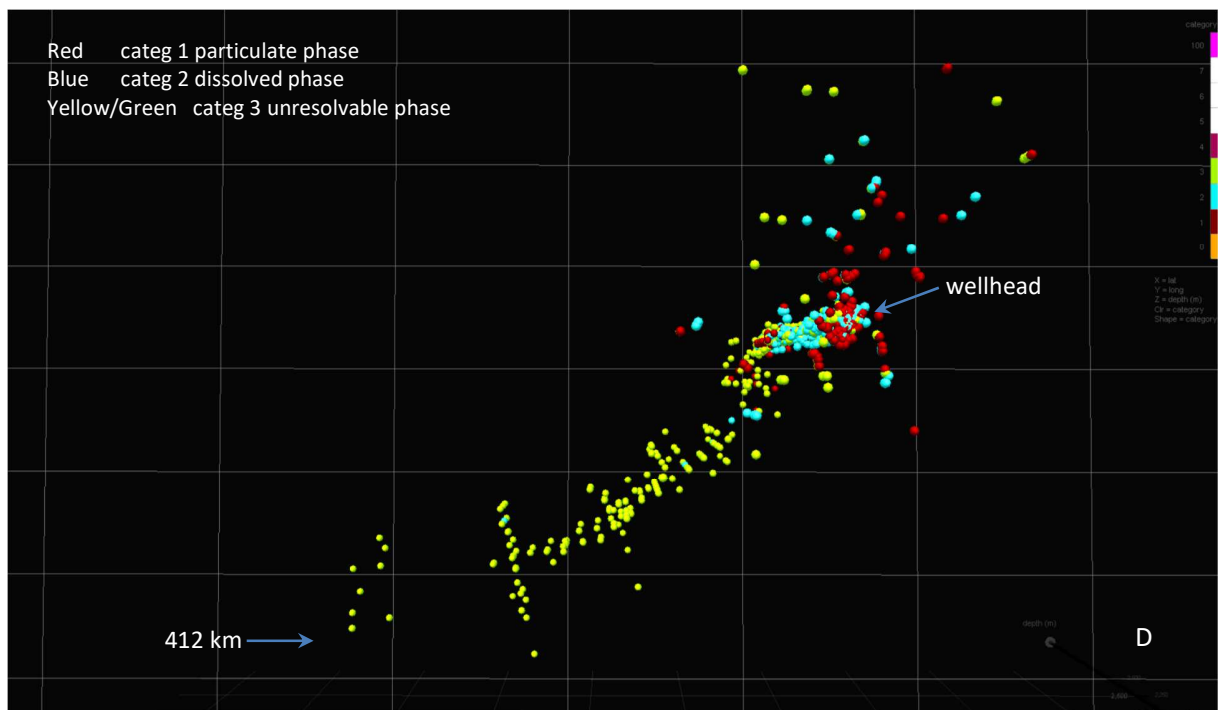
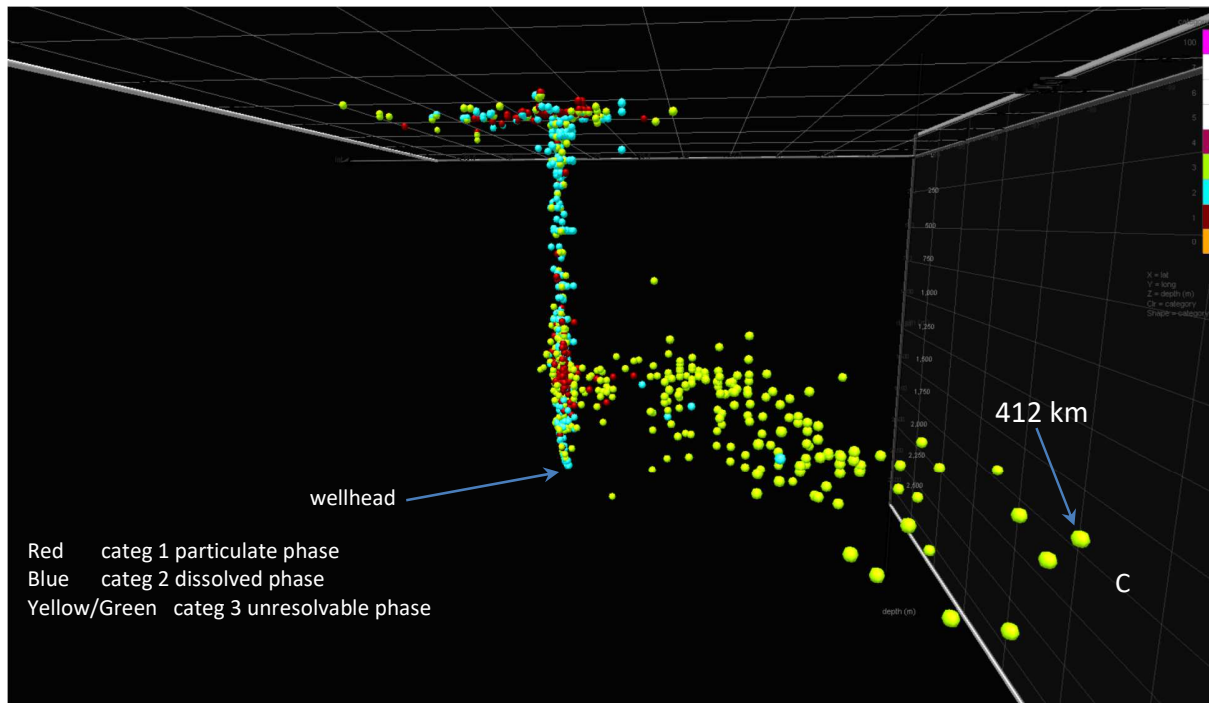


Figure S- 5 (cont.). Four 3D spatial views of samples colored by forensic categories. A) oblique view of all samples looking north (column of blue is rising plume near wellhead, and white dots represent non-matching category 4-7 samples) B) view A with only matched samples displayed, C) at plume depth looking NE from beyond plume's end (500 km), D) top view from above wellhead.

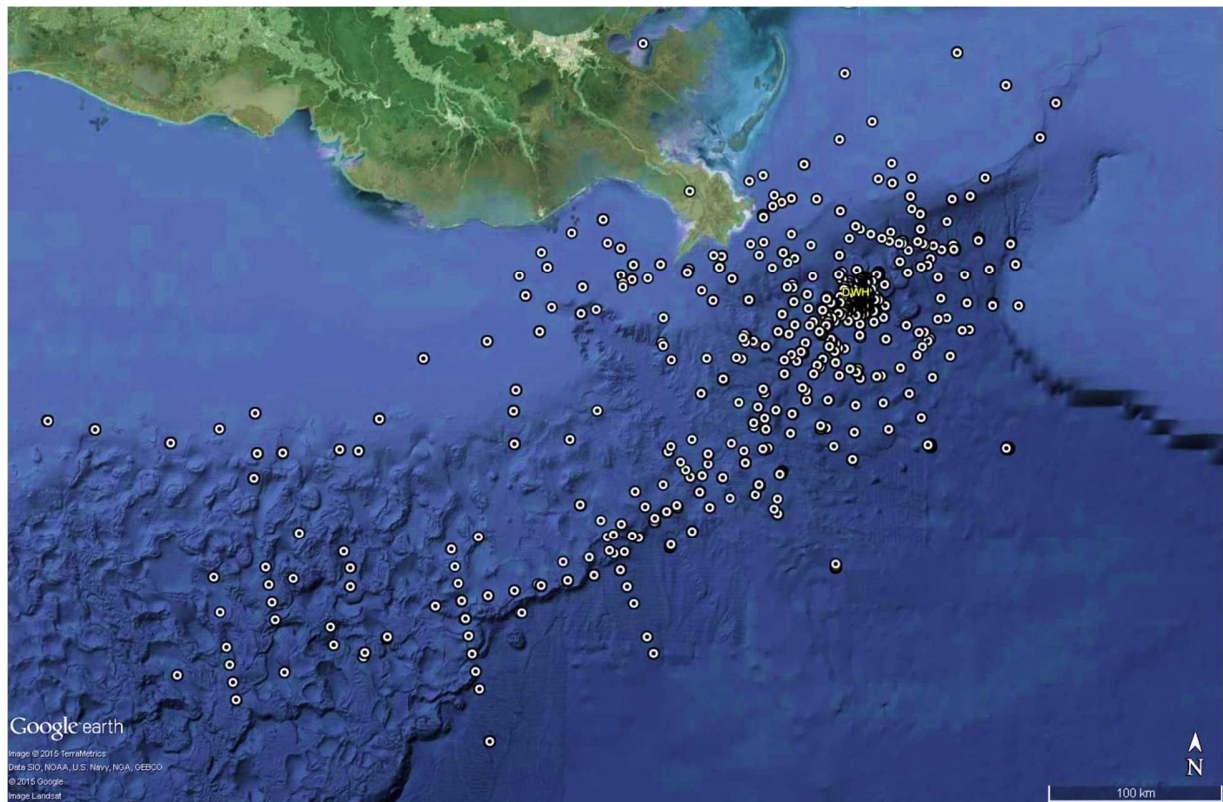


Figure S- 6. Distribution of samples not detecting MC-252 (categories 4-7) ranging to 530 km from wellhead. Multiple depths are overlaid (see white dot symbols in Figure S- 5A). n=2,443.

Table S-1 Summary of the numbers of samples that were classified into each of the 7 categories, by cruise.

Study Name	Categories						
	MC252 Match			No Match	Indeterminate		
	weathered source (cat 1)	dissolved only (cat 2)	unresolved phase (cat 3)	other oil (cat 4)	Possible (cat 5)	Indeterminate (cat 6)	no PAH or noise (cat 7)
Brooks-McCall Cruise 02 MAY 15-17 2010	14	30	2		7	2	
Brooks-McCall Cruise 03 MAY 19-21 2010	8	22	1		3	13	
Brooks-McCall Cruise 04 MAY 23-25 2010	24	21	2		1		
Brooks-McCall Cruise 05 MAY 30-JUN 1 2010	32	29	3		2		3
Brooks-McCall Cruise 06 JUN 5-7 2010	32	15	13		9		6
Brooks-McCall Cruise 07 JUN 11-13 2010	33	21	23	2	2	11	4
Brooks-McCall Cruise 08 JUN 17-19 2010	11	17	18	6		36	7
Brooks-McCall Cruise 09 JUN 22-26 2010	13	46	12			8	9
Brooks-McCall Cruise 11 JUL 4-8 2010	12	11	12		5	7	9
Brooks-McCall Cruise 12 JUL 10-14 2010	23	20	11			23	20
Bunny Bordelon Cruise 01 MAY 30-JUN 2 2010	9	2	3		3	4	13
Endeavor Cruise 01 JUN 2010	10	7	24	4	10	4	44
Gordon Gunter Cruise 01 MAY 27-JUN 4 2010	29	20	9		3	43	42
Gordon Gunter Cruise 06 AUG 2-8 2010			5	1		1	53
Henry Bigelow Cruise 01 JUL 28-AUG 11 2010			7			23	36
Henry Bigelow Cruise 02 AUG 12-23 2010	1	2	71	2	29	4	282
HOS Davis Cruise 01 AUG 10-22 2010	7	9	16			4	17
HOS Davis Cruise 02 AUG 25-SEP 5 2010	1	10	31	2	4	15	1
HOS Davis Cruise 03 SEP 8-28 2010		1	74	40	2	29	48
HOS Davis Cruise 04 NOV 1-17 2010			37		15	50	45
HOS Davis Cruise 05 DEC 4-18 2010		10	8	7	1	4	15
Jack Fitz Cruise 01 MAY 9-14 2010	5	13	5	17	2	1	
Jack Fitz Cruise 02 MAY 21-31 2010	52	61	7	1	10	13	1
Jack Fitz Cruise 03 JUN 11-20 2010	12	38	15	2	7	23	1
Ocean Veritas Cruise 01 MAY 26-30 2010	8	1				10	1
Ocean Veritas Cruise 04 JUN 13-17 2010	23	9	24			13	
Ocean Veritas Cruise 05 JUN 19-23 2010		1	5				
Ocean Veritas Cruise 06 JUN 25-29 2010	5	3	20		2	46	4
Ocean Veritas Cruise 07 JUN 29-JUL 5 2010	18	14	25			31	34
Ocean Veritas Cruise 09 JUL 13-17 2010	8	6	34			32	22
Ocean Veritas Cruise 11 JUL 26-29 2010	5		18			47	11
Pisces Cruise 03 AUG 5-14 2010	1		7	1	6	4	107
Pisces Cruise 04 AUG 18-SEP 2 2010		1	88	2	2	34	122
Pisces Cruise 05 SEP 8-17 2010			19			2	27
Pisces Cruise 06 SEP 25-OCT 4 2010			5		1	2	7
Sarah Bordelon Cruise 07 DEC 4-19 2010			31	1		17	15
Seward Johnson Cruise 01 JUL 09-AUG 7 2010				1		1	72
Thomas Jefferson Cruise 02 JUN 3-10 2010	31	19	24	3	5	43	64

Thomas Jefferson Cruise 03 JUN 15-JUL 2 2010	8	18	13	1	3	38	212
Walton Smith Cruise 01 SEP 06-17 2010			21	1	1	4	13
Walton Smith Cruise 03 SEP 25-OCT 3 2010			12		9	6	67
Walton Smith Cruise 04 APR 19-MAY 27 2011						7	48
Water Sampling (R/V Intl Peace) 05-07/2010	45	38	29	1	13	1	47
Weatherbird II Cruise 01 MAY 06-15 2010		13					
Weatherbird II Cruise 02 MAY 23-26 2010	1	1		3	3	14	5
totals	494	515	784	98	160	670	1534
	11.61%	12.10%	18.42%	2.30%	3.76%	15.74%	36.04%

For DWH offshore waters, additional lines of evidence might include the presence of dispersant indicators, BTEX volatiles, depth, location and date of the sample collection. For the entrained deep oil plume, unique features in conductivity/temperature/depth (CTD), dissolved oxygen (DO), and fluorometry sensor data were strong corroborating evidence (Figure 1). Specifically, in the field, a simultaneous fluorescence spike and DO sag between 1,000-1,400 m meant the sampler had found the plume. Thus, the typical forensic workflow and hierarchy for evaluating each sample became:

1. PAH weathering patterns and diagnostics (e.g., dibenzothiophene/phenanthrene ratios, hopane matching described further below)
2. Biomarker patterns (if available) and diagnostic ratios
3. Dispersant indicators
4. CTD, DO and fluorometry signals
5. Volatiles (BTEX only)
6. SHC patterns
7. Sampling date and proximity to wellhead
8. Nearby sample trends and patterns

Our primary forensic approach, pattern recognition of the signatures, relies heavily on graphic displays to compare samples to reference sources and highlight any anomalies. To visualize and assimilate the multiple lines of evidence, an Excel dashboard utility was developed to bring together, for two samples, all relevant data in a single display of multiple graphics, maps and diagnostic values, superimposed with a scaled reference oil sample for comparison (Payne and Driskell, 2015c). These data are retrieved as needed from a data table within the application, diagnostic ratios calculated, and results plotted in the interactive displays.

Reference Weathering Series

For comparisons, the most relevant DWH reference was, of course, the original “fresh” crude oil (aka MC252) as represented by oil collected on May 21, 2010 through the riser insertion tube on the *Discoverer Enterprise*. This particular oil sample was collected in large volume and eventually became a NIST-certified, Standard Reference Material oil (SRM 2797) that, per the project’s Analytic Quality Assurance Plan (AQAP) requirements (NOAA, 2014), was run by the laboratory as a performance validation check with each analytic batch of NRDA samples. The average analyte values from 620 repeated SIM GC/MS analytic runs at Alpha Analytical Laboratories was used as the PAH and biomarker forensic reference profiles. Reference TPH values (n-alkanes and isoprenoids) derive from similar multiple, routine GC/FID analyses (n=1,100) of the SRM.

Because oil profiles change as they weather, comparing a sample to just a single fresh reference source is not sufficient to fully implement this method; a series of weathered reference samples is required. To create the series, field samples were collected at depth during cruises in the vicinity of the wellhead (2-8 km) during the release, filtered aboard the vessel into particulate (filter) and dissolved (filtrate) portions (Payne et al., 1999) and later biomarker-confirmed as MC252 oil (Payne and Driskell, 2015c). The final selected particulate series from all Category 1 matches, filters only (Figure S- 4), suggests the patterns and relative rates of dissolution losses in the water column as the larger droplets rose to the water surface.

Knowing that weathering is a variable effect from physical and biological processes, initially selecting the few “reference” samples from among the available dataset to represent the generic DWH oil weathering process was slightly subjective. From the three-dimensional scatter cloud of available candidates

plotted by DBT2/PA2 and DBT3/PA3 double-ratio values (Douglas et al., 1996) and TPAH/hopane ratios, mid-trending samples were selected. From the scatter cloud of just these MC252-confirmed filtered samples, we knew early on that we would encounter some interesting variants in weathered particulate profiles. Note that these final selections were not considered as “gold standards” but rather as representatives of the weathering progression against which to assess (fit) a similarly aged sample. As the assessment task progressed and insights grew (recall, $n = 4,189$), it was infrequently necessary to add or eliminate individual references, or at least acknowledge an anomalous component in the reference series. Additional references, not in the weathering series, included samples of hydraulic oil used on ROV samplers and various hydrocarbon anomalies (e.g., persistent field blank contaminants with PAH profiles that were drastically different from MC252 oil).

In traditional forensic wisdom, as an oil mass weathers, the SHC are preferentially consumed by microbes, often disappearing entirely while the PAH profile diminishes at a slower rate. In the weathered reference series (Figure S- 4), up until reference sample 8 of 11, there is remarkably little evidence of microbial degradation of intermediate-molecular-weight aliphatic components close to the wellhead (generally < 5-8 km). Likewise, remarkably persistent SHC occurred in many of the submerged oil plume samples collected at depth and within 5 km of the wellhead, particularly in the early stages of dispersant-mediated weathering (Payne and Driskell, 2015d). Delayed microbial activity may reflect possible toxicity from the high BTEX and hydrocarbon concentrations, dispersants, limited nutrients, or some other factor(s). This effect was particularly evident in the early stages of dispersant-mediated weathering and is discussed further in Payne and Driskell (2015d) and Part 2 of this series, Driskell and Payne (2018b).

Biomarkers (Figure S- 3 bottom and Figure S- 4 middle column plots) from the reference series show the persistent, non-degraded patterns (general absence of weathering albeit with some excepted slight variance) but most importantly, confirm the standard practice of using the most recalcitrant and insoluble C30 hopane biomarker ($17\alpha(H),21\beta(H)$ -hopane) as a quantitation standard against which to observe and quantify particulate-oil depletion (Prince et al. 1994). Recent work by Bagby et al. (2016) looking at biodegradation in DWH sediments suggests that n-C₃₈, octatriacontane, is perhaps even more recalcitrant than hopane.

Mixing Models

Having empirically established a reference particulate oil weathering series, a graphical “reference-template,” mixing method could be implemented. This mixing-model approach was first developed and used on the *Cosco Busan* oil spill (San Francisco Bay, 2007) for matching and mixing patterns to evaluate field samples (Driskell et al., 2010; Driskell and Payne, 2018a) and has been adapted at NewFields Environmental Forensics for other damage assessment cases. The presence of particulate-, dissolved-, and mixed-phase samples from the DWH event was acknowledged and suggested as quantifiable by Boehm et al. (2016) but without further details. Beyond detecting the released oil, parsing sample components into particulate- and dissolved-phase components or, if mixed with another source, into estimated source and background contributions, the method permits more insightful interpretations.

Conceptually, the approach appropriately scales (normalizes) a reference oil profile to a common parameter (analyte) and then simply overlays the profile as a template (dotted line) atop the sample’s bar-chart profile (Figure S- 7). The reference analytes are typically rescaled to the biomarker, C-30 hopane, or if a better fit, sometimes to a conserved (non-degraded) PAH present in both profiles, preferably, C2-chrysene (C2) or C2-naphthobenozthiophene (NBT2). Scaled and overlaid on the sample (Figure S- 7), any graphic deficits or surpluses in the sample’s pattern (i.e., the unfilled spaces beneath

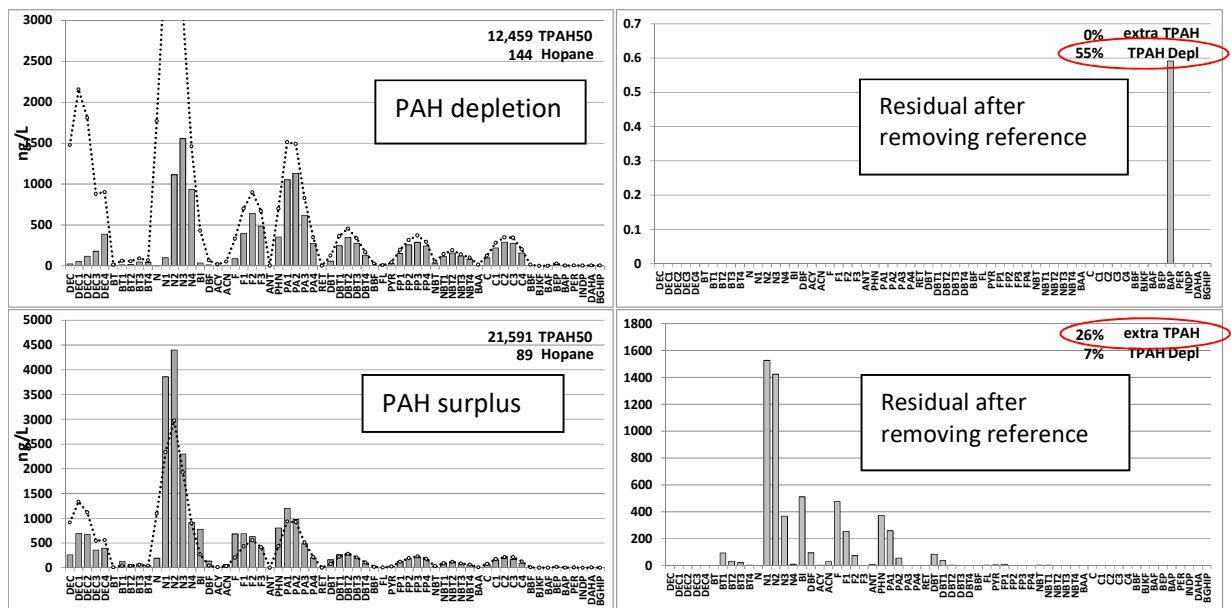


Figure S- 7. Example plots of scaling reference-source oil (dotted line) to fit sample's C2-NBT. Residual analytes (above the scaled-reference, dotted-line template) for these two samples appear in the plots at right along with calculated TPAH % depletion (upper plot) or % surplus (lower plot). Lower left plot shows a nearly-fresh source beneath an extra-dissolved component, which then appears "extracted" in lower-right residual plot (compare to filter-separated dissolved phase – third plot on left in Figure S- 3).

the dotted reference line or excess above the line, respectively) relative to the reference indicates either weathering losses or a mixture showing excess components. Often, the mixed components can be parsed into two-component phases or sources (discussed below).

If scaling with hopane is unsatisfactory (or not available), technically, the preferred C2-homologue scaling choices (C2-chrysene or C2-naphthobenzothiophene) reflect a more reliable integration comprising fewer isomer peaks in the chromatogram (versus ~30-40 for the more recalcitrant C3- or C4-homologues) and with an expected higher abundance than a parent or C1-homologue and therefore, a more accurate fit. If these analytes were unworkable (non-detects or flagged with interference), alternatives would be, in decreasing preference, a different homologue of the same PAH group or stepping left in the PAH sequence to a slightly less conservative PAH. An additional consideration is the effects of photooxidation in samples collected at or near the surface. Photooxidation can result in losses of higher-alkylated (C3- and C4-) chrysenes, fluoranthenes/pyrenes, benz(a)anthracene, and also, the triaromatic steranes (Andersson, 1993; Garrett et al., 1998; Prince et al., 2003; Plata et al., 2008; Aepli et al., 2014; Radovic et al., 2014; Bacossa et al., 2015; Stout et al., 2016a). In more severe cases, even the C2-homologues could be affected.

Hopane-confirmed assignments

Besides serving as a template-scaling parameter, the C30 hopane biomarker (T19) has additional utility for offshore water forensics. First, as a phase check, hopane has very low seawater solubility and can only occur in a sample's particulate phase; its presence confirms that oil droplets are present in a whole-water sample. Any anomalous hopane found in the dissolved portion of filtered samples (only 10 of 517 samples) suggests either trace amounts of colloidal-oil breakthrough during filtration or that sampling equipment/decontamination procedural failures have occurred. Furthermore, because the DWH event occurred in nearly pristine waters of the deep offshore environment where clean background water samples typically have only a trace to no PAH present (excepting the rare seep-).

focused samples or other obviously non-MC252-oil contaminants), any hopane in these deep water samples is expected to be predominantly, if not exclusively, from the MC252 source oil.

For water samples containing hopane, a novel “hopane balance” was developed to help validate weathering assignments and estimate proportions of dissolved- versus particulate-oil partitioning. Using an abbreviated total PAH value (TPAH42) comprising only the crude oil-relevant PAH (naphthalenes through chrysenes, not summing the more labile decalins and benzothiophenes, redundant retene, background-confounded perylene, nor pyrogenic 6-ring PAH), in fresh oil, TPAH42 to hopane was ~192.5 (Table S- 2). The TPAH42/hopane ratio decreases as the droplet’s PAH weather away while the insoluble hopane is conserved. Therefore, as a confirming check when selecting a weathered reference to match and assess a sample profile, the TPAH42/hopane ratios should also agree—if a good fit, the scaled amount of hopane in the reference should be close to the measured amount of hopane in the field sample. And because all of the hopane will belong to particulate oil, the ratio can also be used for parsing phase mixtures and alerting to mismatched comparisons, examples of which appear below.

Table S- 2. TPAH42/hopane ratios for weathered reference series (see Figure S- 4). TPAH42 summed the crude-oil-relevant 42 analytes between naphthalene and chrysenes.

Ref Series stage	Fresh	2	3	4	5	6	7	8	9	10	11
TPAH42/hopane	192.5	101.4	86.3	64.1	56.9	38.5	39.2	39.5	27.3	7.8	9.1

For DWH samples, the hopane-balance method worked best with fresher weathering stages but was consistent through at least the late-mid weathering series. Later-stage weathered references incorporated unknown variation, e.g., from variable natural exposure processes, but still agreed with the overall trend. Note the large interval in ratios between stages 9 and 10 (Table S- 2) where there were no representative filtered field samples to expand the series.

As noted in the previous section, at times, scaling a reference to hopane was unsatisfactory. The entire reference profile, when scaled to hopane, would “lift off” the naphthobenzothiophenes and chrysenes profiles. Clearly, there was too much hopane relative to the PAH in the sample. This occurred most often in surface samples where presumably, two (or more) weathered sources were mixing, one being a very weathered oil (with a lower TPAH42/hopane ratio) contributing the high hopane. At times, another conservative analyte scalar could be selected to achieve a closer comparison while noting the compromised fit as a “best estimate using....” These perplexing samples often were tagged as Category 3 for irresolvable phase parsing but depending on biomarkers and other lines of evidence, they could still be attributable as MC252 oil.

When these extreme elevated hopane anomalies were encountered, contamination from ROV hydraulic oil also became suspect. Fortunately, hydraulic oil was easily detected and discriminated by their biomarker profiles. Comparing PAH and biomarker profiles for MC252 and a field-collected, ROV hydraulic oil (Figure S- 8), the elevated norhopane (T15) relative to hopane (T19) was diagnostic as was the high hopane to TPAH42 ratio. Using expected hopane/TPAH42 and T15/T19 ratios usually allowed us to back-calculate the PAH contribution from the hydraulic-oil contamination. Hydraulic oil’s inherently low PAH content often meant there was only trivial (and thus ignorable) hydraulic-oil contribution to the sample’s PAH profile. However, it was decided that a conservative rule would be that samples with $\leq 5\%$ hydraulic contaminants could be MC252 matched but not phase reported.

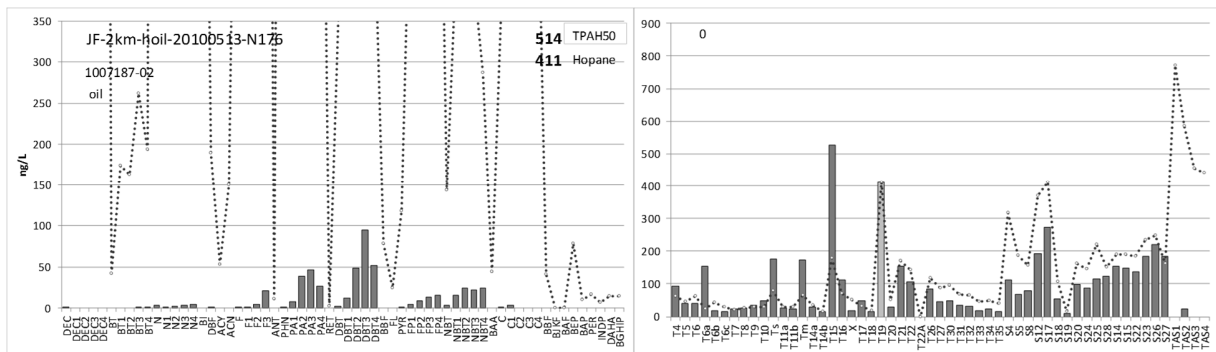


Figure S- 8. PAH and biomarker profile for ROV hydraulic oil overlaid with MC252 source oil (dotted line) scaled to sample hopane. Note diagnostic elevated norhopane (T15) relative to hopane (T19) in right biomarker plot. Also note modest levels of PAH relative to hopane-scaled MC252 source oil (dotted line in left PAH plot). TPAH42/hopane ratios are ~192 in fresh MC252 oil versus 1.3 in this hydraulic oil.

D/P Double Ratios

Another useful diagnostic for evaluating particulate-phase water samples was the use of traditional dibenzothiophene-to-phenanthrene (D/P) ratios (Douglas, et al., 1996). Water solubilities of phenanthrenes and dibenzothiophenes are similar and thus their weathering rates are nearly the same, but the sulfur-containing dibenzothiophenes are conserved slightly more in the oil phase than phenanthrenes. Using the respective C2- and C3-alkylated forms (D2/P2 and D3/P3) to create a double-ratio plot, other oils and weathering anomalies were easily spotted.

Compiling all DWH water samples containing these four PAH components, matched as MC252 particulate oil, and without any extra dissolved components, the D/P patterns fall along two general weathering paths, normal and dispersant-mediated (Figure S- 9). Note that the “normal,” non-dispersant-mediated samples tend to fit fairly tightly in the ascending linear trend. In contrast, for dispersant-mediated weathering, there appears to be a gradient response ranging from unaffected, where the ratios fall nearly amidst the grouping of the normally weathered samples, to completely affected, where the D3/P3 values have a general flat response at 0.4-0.6 and the DBT2/PA2 values range from 0.4 to 1.8. Examination of the dispersed-oil data suggest the D2/P2 ratio is changing rapidly while the D3/P3 is mostly unaffected, a pattern seen in phenanthrene and dibenzothiophene profiles in particulate oil samples with an accentuated, “left-notched” appearance and the presence of dispersant indicators. The most plausible explanation for this effect is accelerated dissolution loss of C2-phenanthrenes from the smaller dispersed oil droplets with higher surface area to volume ratios (see Part 2 of this manuscript series, Driskell and Payne, 2018b). The wider variance amongst dispersant-mediated samples (Figure S- 9) may reflect some unknown degree of dispersant interaction/concentrations, droplet-size distributions, weathering mixtures or a combination of factors beyond the resolution of our field data.

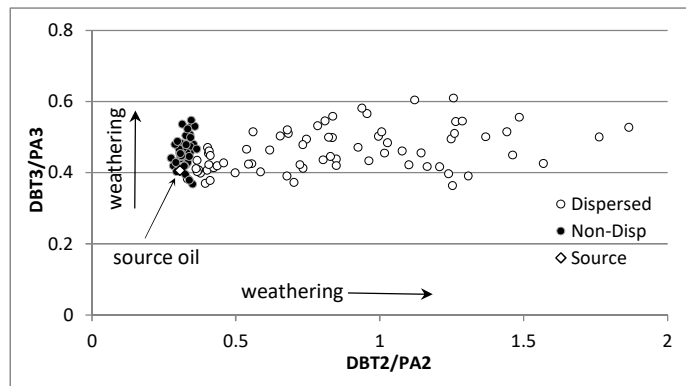


Figure S-9. Comparison of dispersed versus non-dispersed DWH water samples in double-ratio weathering plot of C2- and C3-alkylated dibenzothiophenes (DBT) and phenanthrene/anthracenes (PA). Lateral spread in dispersed samples is attributed primarily to accelerated loss of C2-phenanthrenes. Points represent filters and whole waters with only particulate profiles (whole oil only, no dissolved components) from the DWH NRDA data set (for further discussion, see Part 2 of this series, Driskell and Payne 2018b).

As noted above, biomarker anomalies revealed several compromised DWH samples due to an intermittent hydraulic-oil leak from the ROVs. These contaminated samples were readily identified with elevated D/P ratios appearing hyper-weathered, along the normal D/P path but far beyond any expected trend (weathered hydraulic oil plotted off-graph at 1.25, 2.05). Neat samples of the hydraulic oil (Figure S-8) confirmed a de-aromatized product with elevated hopane levels and norhopane-enriched biomarkers (variously abbreviated as T15, H29, S/T 30, or C29 $\alpha\beta$). Using the hopane balance and other mixing methods, the amount of hydraulic interference could often be calculated and used to estimate the hydraulic oil's contribution to TPAH (frequently trivial). If significantly compromised (>5% of TPAH), these samples were discarded from further interpretations.

Fingerprint Categories

The following section details examples of the profile types (Figure S-10) starting with fresh and depleted whole particulate oil and then the mixed, extra-dissolved-on-particulate profile, which was the breakthrough insight that led to developing the mixing-model and hopane-confirmation methods. The three initial matching-assignment categories (left side, Figure S-10) are typical for forensic assessments attempting to match a source oil. The additional subcategories and fingerprint classifications are unique to DWH water column methodology and the needs of NRDA modelers (French-McCay et al., 2015a, 2015b, 2016, and 2018; Spaulding et al., 2015).

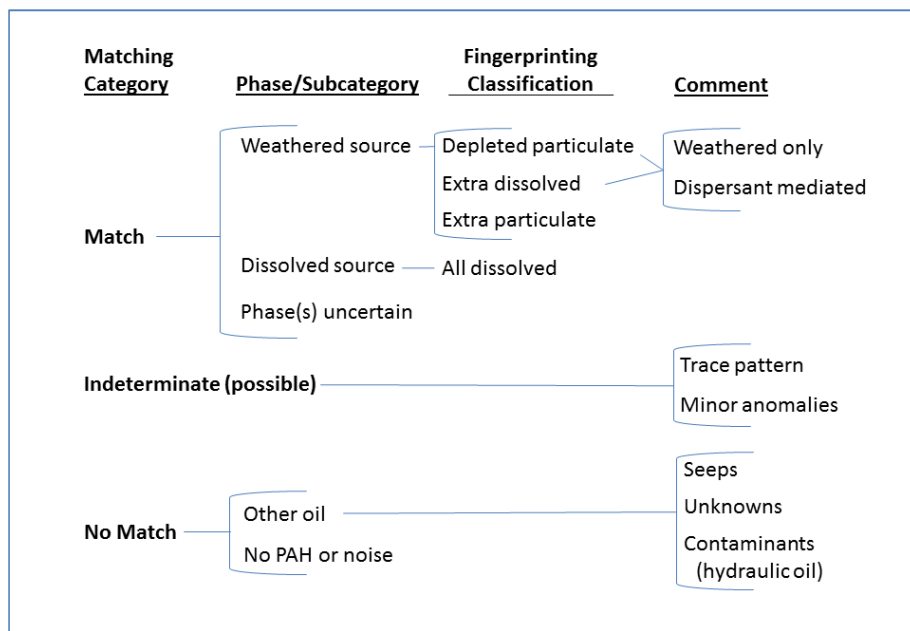


Figure S- 10. Scheme of categorizing water-column forensic assessments.

A whole oil profile would be, of course, nearly identical to the fresh reference where the sample is mostly unweathered or perhaps with a slight loss in the readily dissolvable/volatile components. Graphically, these samples appear as a near perfect fit with little or no residuals or deficits (similar to Figure S- 11). In the NRDA datasets, a scarcity of “fresh” field samples with high TPAH/hopane values suggested that the transition to subsequent weathering states occurred quickly as the oil droplets ascended in the water column or were advected horizontally (also see Stout et al., 2016a). Seemingly, these freshest of samples would only have been collected at depth and near the wellhead but for safety considerations, no NRDA sampling was allowed within 1 km of the wellhead during the event. There were, however, a handful of samples collected directly by the response-operations ROV just above the wellhead that showed roughly twice the TPAH42/hopane ratio as the NIST MC252 standard; however, these samples appear to contain extra dissolved components. Also, they were analyzed by another lab using different GC/MS response factors in quantifying the data and thus, could not be compared as fresh reference samples.

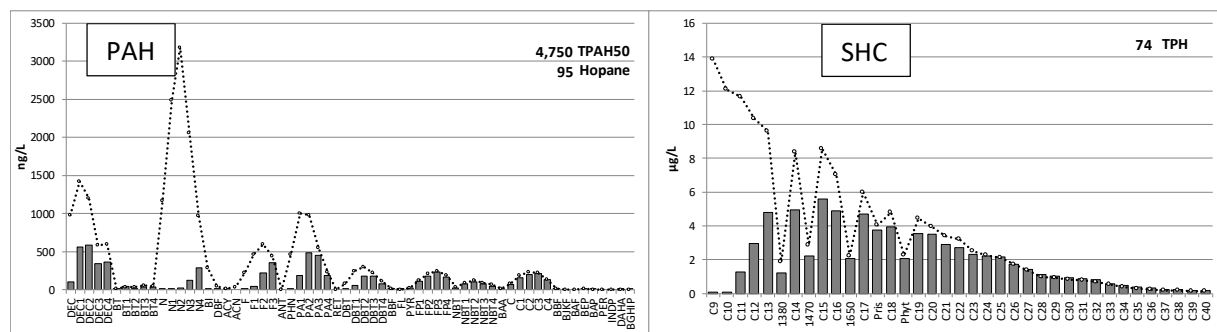


Figure S- 11. Example of an unfiltered (whole-water) sample with depleted particulate/oil relative to fresh source oil (dotted line) standardized to sample hopane.

The next category, a depleted-particulate profile, was simply a weathered version of whole oil missing more dissolved components (Figure S- 11). This sample would demonstrate a better fit to a more weathered reference sample and also a close, if not exact, match to expected hopane. TPAH depletion

is graphically represented by the empty spaces under fresh oil's hopane-scaled dotted reference line, which, after summing, calculates into % TPAH depletion. While the TPAH depletion from fresh oil was routinely calculated and reported, for DWH modeling needs, the sample was subsequently fitted to its closest weathered reference to detail individual analyte depletions.

The next phase category, extra-dissolved-on-particulate samples can present as two forms, either as a dissolved pattern with unexpected hopane (i.e., a predominantly dissolved sample with a bit of particulate oil) or as a mostly particulate sample with more TPAH and lower hopane than expected (i.e., predominantly particulate sample with additional dissolved components). For both cases, after selecting an appropriate weathered particulate reference from the series, the upper residual, the portion of the sample appearing above the scaled reference line, represents the "excess" dissolved components (Figure S- 12, left). Samples of this "extra dissolved" category were regularly seen near the wellhead in the area of rising droplets, where conceptually, buoyant droplets were transiting through a water parcel that still contained dissolved-phase PAH shed from passing droplets released earlier in the event. In the example, selecting a particulate reference to try to match the conserved naphthobenzothiophenes or chrysenes showed a significant excess in the measured naphthalenes with slightly smaller excesses in the mid-molecular-weight compounds, the fluorenes, phenanthrenes and dibenzothiophenes. Here it is obviously critical to overlay an appropriately weathered reference.

The solution to parsing these extra-dissolved samples was to fit a weathered reference to the higher-molecular-weight (upper-end) PAH profile, conserved components (NBT2 or C2) and then attributing the excess (residuals) as dissolved (Figure S- 12, center). Confirmation of a proper fit was closure in the hopane-matching between reference and sample whereby all hopane was attributable to just the particulate portion (or conversely, no contribution from the dissolved phase). A third, equally important constraint in assigning this category was that the residual, the above-the-reference portions (shown simultaneously in a smaller secondary plot, (Figure S- 12, center top), had to have an acceptable dissolved-signal profile. Specifically, the residual profile, if dissolved, should appear similar to the generic dissolved patterns observed in the dissolved-phase (filtered) water samples collected early in the spill event (e.g., Figure S- 3, middle left), i.e., reflecting a dissolution profile trending from high on the light ends to low or absent in the heavy ends and typically with descending patterns of alkylation in the homologues. Note that the presence of any significant hopane or SHC alerts to misclassifying the sample as an all-dissolved profile. The other fingerprinting modes and their hopane-matching characteristics became obvious after sorting out the above examples.

For the next category, particulate-on-particulate, the profile looks like a weathered particulate oil but actually is a mixture of two or more weathering states. In attempting to match these samples to a weathered reference (initially scaled to the sample's hopane), there was always more PAH than expected but the residual was not a dissolved profile. Instead, another weathered particulate oil mixed into the sample had added its own blend of hopane plus mid-molecular-weight components. The particulate-on-particulate concept was initially validated by applying a linear optimization model to demonstrate convergence of two parameters, the sample's TPAH and hopane values, via an optimized mix of two weathered references. Numerous samples and blends were tested to confirm the concept was valid. This exercise was not intended to derive definitive mixtures of the field sample but rather to simply demonstrate that there was at least one credible solution from mixing two weathered source samples that could closely match the observed PAH profile, TPAH, and hopane content. The particulate-on-particulate model was only necessary for 6% of the matches with most being dispersant-mediated (see Driskell and Payne, 2018b).

For demonstration purposes, in the example (Figure S- 13), the sample's hopane is only a modest 9% lower than expected from the reference fit to hopane (21.3 vs 23.4 ng/L) but note in the residual plot (right side) the surplus mid-range PAH components through the chrysenes. The patterns are anomalous

yet suggestive of a weathered oil pattern, i.e., an unknown contribution from another weathered source. By manually adjusting the reference contribution, a realistic solution can be found reflecting a combination of two particulate profiles (one a dispersant-mediated oil with significantly water-washed chrysenes – top right, see Driskell and Payne, 2018b) with a combined TPAH/hopane ratio that is similar to the observed value. Note that solution is merely “realistic” rather than “confirmed accurate.”

Without context, we acknowledge that this particulate-on-particulate deconvolution parsing may appear as a “quest for matching” that borders on over-interpreting data. We posit that the primary objective here is to confidently attribute a field sample to the source whereby assurance in confirming a match is based not solely on the profile-matching task but on multiple lines of evidence. We also feel that the omission of attributing sample matches simply due to an inconveniently difficult-to-match mixture profile represents a false negative with potential consequences to exposure modelling. Due to the uncertainties in the parsing this profile category, only the match assignment and TPAH values were reported to modelers, not the individual analyte portions.

The last phase-identifiable profile, all dissolved, is simply a dissolved-patterned profile (Figure S- 14) for a whole-water grab sample with higher-molecular-weight analytes absent, and almost universally, no hopane. Note that without its associated particulate compliment, dissolved PAH patterns alone in unfiltered whole-water samples are not directly traceable to a source oil; however, other lines of evidence including a concurrent DO sag and fluorescence spike in the CTD data, high concentrations, date, depth and location relative to the wellhead, presence of BTEX and dispersant indicators are used to attribute purely dissolved signals to MC252 source oil. Note in the all-dissolved profile example (Figure S- 14), an unfiltered, whole-water grab, that the appearance of SHC constituents below the laboratory reporting limit represents an ignorable trace-level colloidal fraction (note the graph scale) with n-C₂₅ and n-C₂₈ flagged by the laboratory as procedural artifacts.

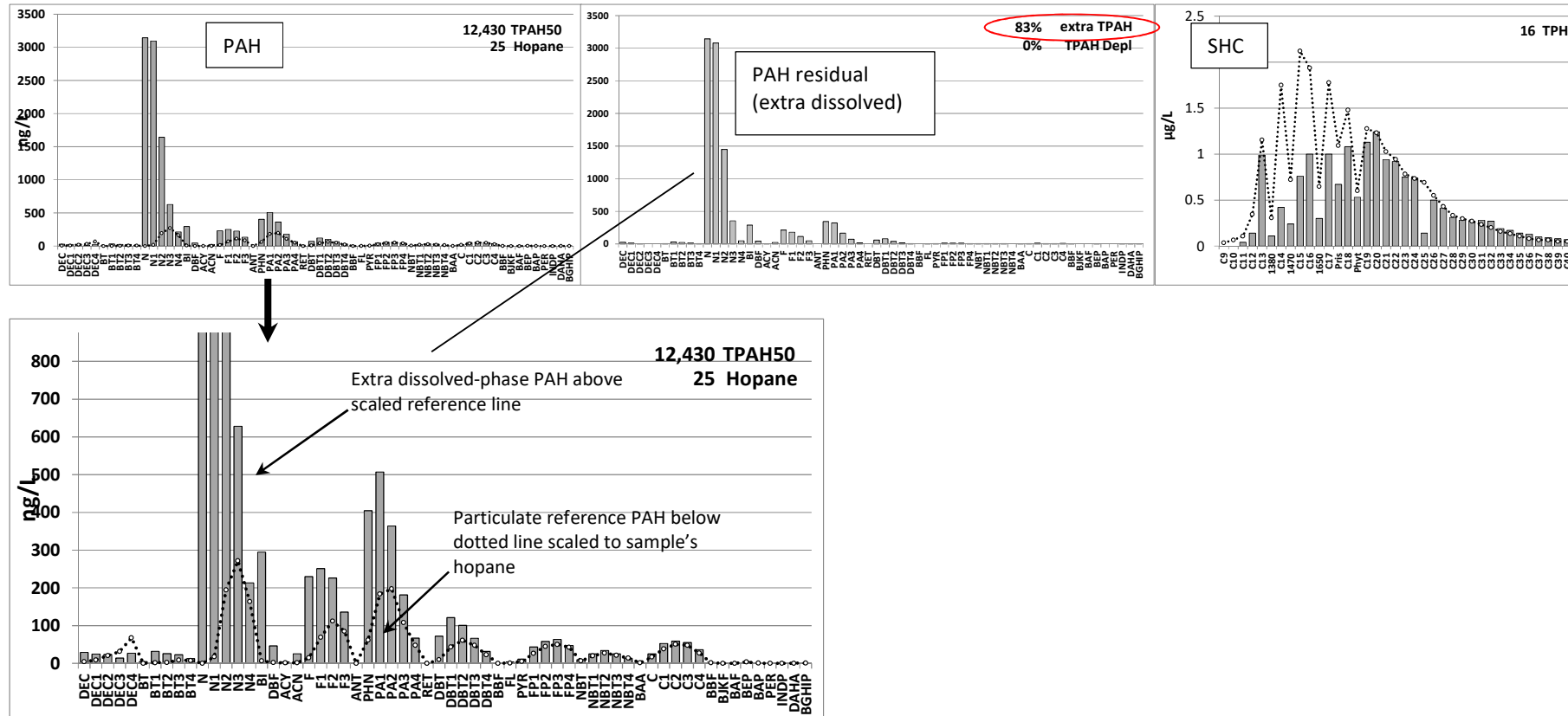


Figure S-12. Example profiles from parsing extra dissolved-on-particulate PAH in a whole (unfiltered) water sample. Left upper plot, full PAH profile with Weathered Source Reference 3 overlaid; center, the 83% extra-dissolved-residual profile after hopane-based parsing (note similarity to filtered-dissolved pattern in Figure S-3); right, weathered SHC from the particulate portion. Presence of hopane, higher-molecular-weight PAH, and SHC precludes this being a purely dissolved-phase sample. Lower plot zoomed in to show weathered particulate portion (beneath dotted reference line, here using Weathered Reference 3 scaled to sample's hopane) where the expected reference hopane (defined by scaling) was 25 ng/L versus reported 25ng/L in field sample; i.e., parsing confirmation by both pattern matching and hopane mass balance.

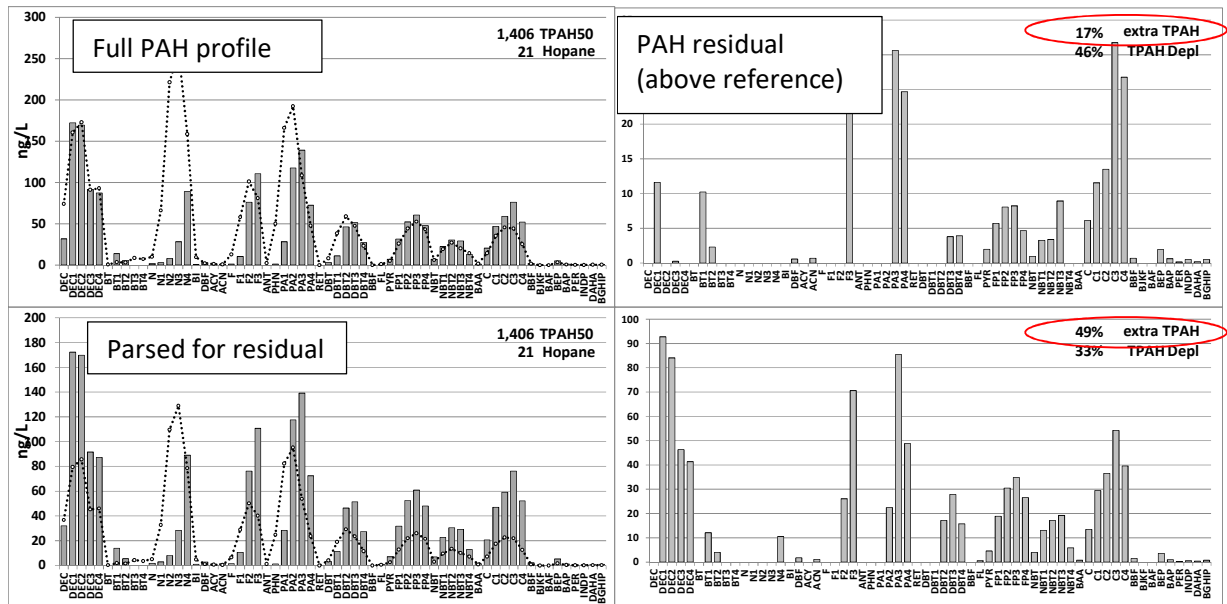


Figure S- 13. Example of parsing particulate-on-particulate PAH profile. Upper sample scaled to hopane and showing sketchy secondary dispersed-particulate profile with highly water-washed chrysenes – see Part 2, Driskell and Payne, 2018b) in the residual plot on the right. Lower plot shows same sample manually rescaled to demonstrate contribution from an additional oil profile with realistic MC252 D/P ratios. Note dispersant-mediated particulate profile in upper right residual represents 17% of sample's TPAH.

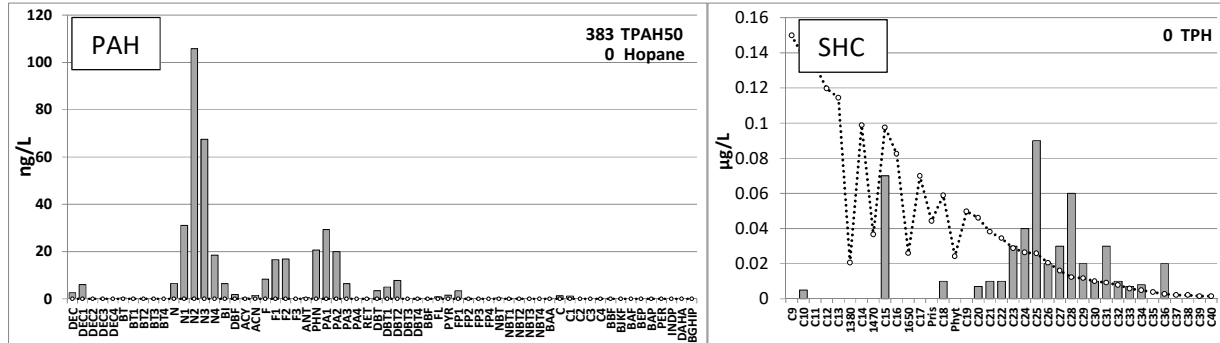


Figure S- 14. Example of a whole-water (unfiltered) all-dissolved PAH profile with no hopane and typical trace levels of SHC (presumably colloidal) that were below the laboratory reporting limit (TPH = 0.49 μ g/L). In this sample, the laboratory flagged n-C₂₅ and n-C₂₈ as trace-level procedural artifacts.

Finally, there were the “phase-uncertain” profiles that defied all efforts to parse or confirm to a matching reference. If there were strong corroborating evidence (e.g. CTD, fluorescence, DO sags, or dispersant indicators), the sample would be called a match but no phase assignment was made. Such mixtures were usually encountered in near surface water samples where, for example, a particulate sample had too much hopane for the TPAH, suggesting particulate oil mixed from different weathering states. With corroborating evidence, we speculate that these samples likely contained weathered-dissolved components (near-surface dissolved patterns subject to evaporative loss of naphthalenes and other lower-molecular-weight components through the air-sea interface) combined with weathered particulate oil(s). Photooxidation effects were also commonly observed in near surface samples as

reflected by the losses of higher-alkylated (C3- and C4-) chrysenes, fluoranthenes/pyrenes, benz(a)anthracene, and also, the triaromatic steranes (Andersson, 1993; Garrett et al., 1998; Prince et al., 2003; Plata et al., 2008; Aeppli et al., 2014; Radovic et al., 2014; Bacossa et al., 2015; Stout et al., 2016a).

Other than the matched samples, there were the categories of “indeterminate,” “other oil,” and “trace or no PAH” (Figure S- 10). Samples classified as indeterminate showed a solid oil-like pattern but were sketchy or sparse on corroborating evidence or too distant from the spill basin to be reliably classified as MC252 source oil; these were “possible” matches. “Other oils” meant known (e.g., hydraulic oil) or unknown non-MC252 oil patterns, especially those with elevated dibenzothiophenes. These were obviously other oils from distal locations and other sources, occasionally including surface samples. Finally, “Trace or no PAH” samples are self-descriptive affirmations of the essentially pristine nature of the Gulf outside of seeps and spills regions. During follow-up water and sediment sampling cruises in 2011, the upper and mid-water column turnover seemed complete; there were no extensive MC252 surface slicks like those observed in May-July 2010, no DO anomalies, and no fluorescence spikes in the mid-water-column profiles.

Reviewer Comments

One reviewer faults the reference weathering series, the “standards,” for lacking quantitative validation presumably expecting analyte variances among available samples for each weathering stage. The concern was that there were many sources of variance, both environmental and analytic, when reporting low concentration values and perhaps the selection process was too subjective. While the goal may have been desirable, we did not expect to establish a “gold standard” for each weathering stage in compiling the reference series. Knowing that each sample had been exposed to various manners and degrees of sub-surface biotic and abiotic environmental degradation, variance was expected. Indeed, a few replicate samples from the field were collected and analyzed, and there was considerable total PAH (TPAH) variability due to the patchy nature of particulate oil droplets in the water column (Payne and Driskell, 2015b). The weathering patterns, however, were less affected, and this TPAH heterogeneity did not reduce our ability to track the PAH pattern changes shown in our reference series (Figure S- 4). Reliance then fell to the robustness of the mixing-model assessment process whereby a multi-variate-driven assessment of reasonable and logical fit to PAH and biomarker profile expectations, DBT/PA double ratios, hopane-balance, dispersant indicators, BTEX and other non-analytic data determined the final confirmation. For most samples, the process seemed sufficient in that reasonably close fits were achieved. For the anomalous outliers, it was then a judgment call based on the nature and degree of anomalies that would determine their MC252 confirmation. As previously noted, there were additions and deletions to the reference series during the multi-year process as insights grew. From another perspective, the forensic process apparently was not overly flawed since forensic hydrocarbon distributions generally agreed with independent hydrodynamic/component modelling results (French-McCay et al., 2018).

Another review suggested that this method couldn’t work because the oil spill samples would likely comprise more than a single state of weathering. We agree, if a sample is not dominated by a single state of oil weathering, the pre-requisite matching to a reference source will result in a poor fit and hopane balance validation would be unreasonable—but that was not often the case during the DWH. At times, if the residual parsed profile suggested another identifiable particulate source, the sample would be categorized as particulate-on-particulate. In this instance, we would acknowledge the irresolvable phase parsing but check the other lines of evidence to see if it still supported a match, e.g., a near

surface sample with a poorly matching PAH profile but with appropriate biomarkers and dispersant indicators and in proximity to other confirmed samples would still be a confirmed match. Using this mixing-model approach for near-surface samples (from diverse mixed sources) was less effective relative to the mid-water samples, which were only affected by dissolution and microbial weathering. We also acknowledge that the parsed results were just best estimates, which at times fit the sources incredibly well and, at other times, were loose confirmations only modestly validated. But there's also an inherent robustness in working with 1,766 confirmed matches. In practice, we strongly suggest working closely with end data users, to point out the strong and weak results in the assessments. Also recall, prior to this approach, the modelers and toxicologists would be working only from a table of TPAH values.

Another reviewer was dismissive of these methods as merely expert judgment, apparently expecting a new statistical model to ease the oil forensics task. From the previous two paragraphs, our method obviously is not a simple solution. The approach requires significant expert knowledge of oil weathering processes but also helps resolve the dilemma of phase discrimination in unfiltered samples—a massive task during the DWH event. Subsequently, it also provides a wealth of new data for transport-and-fates modeling and toxicology, which are perhaps the pinnacle tasks for damage assessments.

References

Aeppli, C., R.K. Nelson, J.R. Radovic, C.A. Carmichael, D.L. Valentine, and C.M. Reddy. 2014. Recalcitrance and degradation of petroleum biomarkers upon abiotic and biotic natural weathering of *Deepwater Horizon* oil. *Environ Sci & Tech.* 48: 6726-6734.

Andersson, J.T. 1993. Polycyclic aromatic sulfur heterocycles III. Photochemical stability of the potential oil pollution markers phenanthrenes and dibenzothiophenes. *Chemosphere* 27: 2097-2102.

Bacosa, H.P., D.L. Erdner, Z. Liu. 2015 Differentiating the roles of photooxidation and biodegradation in the weathering of Light Louisiana Sweet crude oil in surface water from the *Deepwater Horizon* site. *Mar. Pollut. Bull.* 95 (1):265-272.

Bagby, S.C., C.M. Reddy, C. Aeppli, G.B. Fisher, and D.L. Valentine. 2016. Persistence and biodegradation of oil at the ocean floor following *Deepwater Horizon*. *Proc Natl Acad Sci U S A.* 2017 Jan 3;114(1):E9-E18. doi: 10.1073/pnas.1610110114. Epub 2016 Dec 19.

Boehm, P.D., K.J. Murray, and L.L. Cook. 2016. Distribution and attenuation of polycyclic aromatic hydrocarbons in Gulf of Mexico seawater from the *Deepwater Horizon* oil accident. *Environ Sci & Tech.* 50: 584-592. DOI: 10.1021/acs.est.5b03616.

Douglas, G.S., A.E. Bence, R.C. Prince, S.J. McMillen, and E.L. Butler. 1996. Environmental stability of selected petroleum hydrocarbon source and weathering ratios. *Environ Sci & Tech.* 30(7): 2332-2339.

Driskell, W.B., J.R. Payne and G.S. Douglas. 2010. Forensic fingerprinting of *Cosco Busan* samples containing mixed-oil sources. Presentation at the Society of Environmental Toxicology and Chemistry, Special session on the *Cosco Busan* Spill. SEATAC 31st Annual Meeting, November 7-10, 2010. Portland, OR.

Driskell, W.B. and J.R. Payne. 2018a. Development and application of phase-specific methods in oiled-water forensic studies. Oil Spill Environmental Forensics – Case Studies, S.A. Stout and Z. Wang (eds.), Elsevier/Academic Press. Pp. 289-321.

Driskell, W.B. and J.R. Payne, 2018b submitted. Macondo oil in northern Gulf of Mexico waters – Part 2: Dispersant-accelerated PAH dissolution in the *Deepwater Horizon* plume. *Mar. Pollut. Bull.*

French-McCay, D., J. Rowe, R. Balouskus, A. Morandi, and M.C. McManus. 2015a. Technical Reports for *Deepwater Horizon* Water Column Injury Assessment. WC-TR.28: Injury quantification for planktonic fish and invertebrates in estuarine, shelf and offshore waters. U.S. Dept. of Interior, *Deepwater Horizon* Response & Restoration, Admin. Record, www.doi.gov/deepwaterhorizon/adminrecord. DWH-AR0172019. 41 p. DWH NRDA Water Column Technical Working Group Report, September 30, 2015.

French-McCay, D.P, K. Jayko, Z. Li, M. Horn, Y. Kim, T. Isaji, D. Crowley, M. Spaulding, S. Zamorski, J. Fontenault, R. Shmookler, and J.J. Rowe. 2015b. Technical Reports for *Deepwater Horizon* Water Column Injury Assessment – WC_TR.14: Modeling oil fate and exposure concentrations in the deepwater plume and rising oil resulting from the *Deepwater Horizon* oil spill. RPS ASA, South Kingstown, RI, USA, August 2015.

French-McCay, D., M. Horn, Z. Li, D. Crowley, M. Spaulding, D. Mendelsohn, K. Jayko, Y. Kim, T. Isaji, J. Fontenault, R. Shmookler, and J. Rowe. 2016. Simulation modeling of ocean circulation and oil spills in the Gulf of Mexico – Appendix VI data collection, analysis and model validation. Prepared by RPS ASA for the US Department of the Interior, Bureau of Ocean Energy Management, Gulf of Mexico OCS Region, New Orleans, LA.

French-McCay, D., M. Horn, Z. Li, K. Jayko, M. Spaulding, D. Crowley, D. Mendelsohn. 2018. Modeling distribution, fate, and concentrations of *Deepwater Horizon* oil in subsurface waters of the Gulf of Mexico. In Case Studies in Oil Spill Environmental Forensics, S.A. Stout and Z. Wang (eds.), Elsevier/Academic Press.

Garrett, R.M., I.J. Pickering, C.E. Haith, and R.C. Prince. 1998. Photooxidation of crude oils. *Environ. Sci Technol.* 32(23): 3719-3723.

NOAA. 2014. Analytical quality assurance plan, Mississippi Canyon 252 (*Deepwater Horizon*) natural resource damage assessment, Version 4.0. May 30, 2014.

Payne, J.R., T.J. Reilly, and D.P. French. 1999. Fabrication of a portable large-volume water sampling system to support oil spill NRDA efforts. *Proceedings of the 1999 Oil Spill Conference*, American Petroleum Institute, Washington, D.C., 1179-1184.

Payne, J.R. and W.B. Driskell. 2015a. 2010 DWH offshore water column samples—Forensic assessments and oil exposures. U.S. Dept. of Interior, *Deepwater Horizon* Response & Restoration, Admin. Record, www.doi.gov/deepwaterhorizon/adminrecord. DWH-AR0039118, 37 p. DWH NRDA Chemistry Technical Working Group Report, September 1, 2015.

Payne, J.R. and W.B. Driskell. 2015b. Offshore adaptive sampling strategies. U.S. Dept. of Interior, *Deepwater Horizon* Response & Restoration, Admin. Record,

www.doi.gov/deepwaterhorizon/adminrecord. DWH-AR0023786, 75 p. DWH NRDA Chemistry Technical Working Group Report, August 30, 2015.

Payne, J.R. and W.B. Driskell. 2015c. Forensic fingerprinting methods and classification of *Deepwater Horizon* oil spill offshore water samples. U.S. Dept. of Interior, *Deepwater Horizon Response & Restoration*, Admin. Record, www.doi.gov/deepwaterhorizon/adminrecord. DWH-AR0039170, 31 p. DWH NRDA Chemistry Technical Working Group Report, September 1, 2015.

Payne, J.R. and W.B. Driskell. 2015d. Dispersant effects on waterborne oil profiles and behavior during the *Deepwater Horizon* Oil Spill. U.S. Dept. of Interior, *Deepwater Horizon Response & Restoration*, Admin. Record, www.doi.gov/deepwaterhorizon/adminrecord. DWH-AR0039201, 22 p. DWH NRDA Chemistry Technical Working Group Report, August 30, 2015.

Payne, J.R. and W.B. Driskell. 2016. Water column sampling for forensics. In Standard Handbook Oil Spill Environmental Forensics – Fingerprinting and Source Identification (2nd Edition), S. Stout and Z. Wang (eds.) Elsevier/Academic Press, 2016: 983-1014.

Payne, J.R. and W.B. Driskell. 2017. Water-column measurements and observations from the *Deepwater Horizon* oil spill Natural Resource Damage Assessment. *Proceedings of the 2017 International Oil Spill Conference*, American Petroleum Institute, Washington, D.C.

Plata, D.L., C. Sharpless, C.M. Reddy. 2008. Photochemical degradation of polycyclic aromatic hydrocarbons in oil films. *Environ. Sci. Technol.* 24: 2432-2438.

Prince, R.C., D.L. Elmendorf, J.R. Lute, C.S. Hsu, C.E. Haith, J.D. Senius, G.J. Dechert, G.S. Douglas, E.L. Butler. 1994. 17 α (H)-21 β (H)-hopane as a conserved internal marker for estimating the biodegradation of crude oil. *Environ. Sci. Technol.* 1994, 28 (1), 142–145.

Prince, R.C., R.M. Garrett, R.E. Bare, M.J. Grossman, T. Townsend, J.M. Suflita, K. Lees, E.H. Owens, G.A. Sergy, J.F. Braddock, J.E. Lindstrom, R.R. Lessard. 2003. The roles of photooxidation and biodegradation in long-term weathering of crude and heavy fuel oils. *Spill Sci. Technol. Bull.* 8(2): 145-156

Radović, J.R., C. Aeppli, R.K. Nelson, N. Jimenez, C.M. Reddy, J.M. Bayona, and J. Albaigés. 2014. Assessment of photochemical processes in marine oil spill fingerprinting. *Mar. Pollut. Bull.* 79(1–2): 268–277, <http://dx.doi.org/10.1016/j.marpolbul.2013.11.029>.

Spaulding, M.S., D. Mendelsohn D. Crowley, Z. Li and A. Bird. 2015. Technical Reports for *Deepwater Horizon* Water Column Injury Assessment—WC_TR 13. Application of OILMAP DEEP to the *Deepwater Horizon* blowout. RPS ASA, 55 Village Square Drive, South Kingstown, RI 02879. August 2015.

Stout, S.A. and J.R. Payne. 2016. Macondo Oil in deep-sea sediments: Part 1 Sub-sea weathering on oil deposited on the seafloor. *Mar. Pollut. Bull.* 111: 365-380.

Stout, S.A., J.R. Payne, S. Emsbo-Mattingly, and G. Baker. 2016a. Weathering of field-collected floating and stranded Macondo oils during and shortly after the *Deepwater Horizon* oil spill. *Mar. Pollut. Bull.* 105: 7-22.

Stout, S.A., J.R. Payne, R.W. Ricker, G. Baker, and C. Lewis. 2016b. Macondo oil in deep-sea sediments: Part 2 – Distribution and distinction from background and natural oil seeps. *Mar. Pollut. Bull.* 111: 381-401.

Valentine, D.L., I. Mezic, S. Macesic, N. Crnjarc-Zic, S. Ivic, P.J. Hogan, V.A. Fonoberov, and S. Loire. 2012. Dynamic autoinoculation and the microbial ecology of a deepwater hydrocarbon irruption. *PNAS* 2012 109:20286-20291; doi:10.1073/pnas.1108820109